



**CHALMERS**  
UNIVERSITY OF TECHNOLOGY



# **Electrified semitrailer longitudinal wheel-torque control within safe operation and how the communication between vehicle units affects the motion performance**

Master's thesis in Mobility Engineering

Harald Hermansson  
Joakim Tjärnlund Leppämäki

**DEPARTMENT OF MECHANICS AND MARITIME SCIENCES**

CHALMERS UNIVERSITY OF TECHNOLOGY  
Gothenburg, Sweden 2024  
[www.chalmers.se](http://www.chalmers.se)



MASTER'S THESIS IN MOBILITY ENGINEERING

**Electrified semitrailer longitudinal wheel-torque  
control within safe operation and how the  
communication between vehicle units affects the  
motion performance**

HARALD HERMANSSON  
JOAKIM TJÄRNLUND LEPPÄMÄKI



**CHALMERS**  
UNIVERSITY OF TECHNOLOGY

Department of Mechanics and Maritime Sciences  
Division of Vehicle Engineering and Autonomous Systems  
CHALMERS UNIVERSITY OF TECHNOLOGY  
Gothenburg, Sweden 2024

Electrified semitrailer longitudinal wheel-torque control within safe operation and how the communication between vehicle units affects the motion performance

HARALD HERMANSSON

JOAKIM TJÄRNLUND LEPPÄMÄKI

© HARALD HERMANSSON, 2024.

© JOAKIM TJÄRNLUND LEPPÄMÄKI, 2024.

Supervisors:

Christian Oscarsson, Volvo Group Trucks Technology

Bengt J H Jacobson, Mechanics and Maritime Sciences, Chalmers

Umur Erdiņ, Mechanics and Maritime Sciences, Chalmers

Mukesh Choudhary, Volvo Group Trucks Technology

Examiner:

Bengt J H Jacobson, Mechanics and Maritime Sciences, Chalmers

Master's Thesis 2024

Department of Mechanics and Maritime Sciences

Chalmers University of Technology

SE-412 96 Gothenburg

Sweden

Telephone +46 31 772 1000

Cover: Volvo tractor with semitrailer and VTM model of the investigated vehicle combination side by side.

Typeset in L<sup>A</sup>T<sub>E</sub>X

Gothenburg, Sweden 2024

Electrified semitrailer longitudinal wheel-torque control within safe operation and how the communication between vehicle units affects the motion performance

HARALD HERMANSSON

JOAKIM TJÄRNLUND LEPPÄMÄKI

Department of Mechanics and Maritime Sciences

Division of Vehicle Engineering and Autonomous Systems

Chalmers University of Technology

## Abstract

In the electrification of the heavy duty fleet, electrified semitrailers are a big talking point and a lot of work is being put into researching how they could work and how they should be controlled.

This thesis focuses on how two different levels of communication will affect the performance, stability and drive-ability of an electric semitrailer. The first level of communication follows the ISO 11992-2:2014 standard, which mainly allows for only brake-torque requests from the tractor to the trailer (called type 3 communication in this thesis). This will be compared to a new communication interface that allows more request signals from the tractor to the semitrailer and more data in both directions (called type 4 communication). This means all wheel speeds, axle loads and torque requests can be communicated back and forth at all times.

Four different controller algorithms were created. One for the type 4 level communication, and three for the type 3 level, where two are equipped with two extra sensors, a coupling force sensor and an articulation angle sensor. The last one only relies on the sensors available in a standard semitrailer according to ISO 11992-2:2014.

The controllers were tested in a high-fidelity simulation environment in four different use cases, where their motion performance was measured and compared to a tractor with a non-driven semitrailer. All vehicle combinations performed better than the normal tractor and semitrailer combination, although they were more prone to failures such as jackknives and rollovers due to the added powertrain on the electrified semitrailers.

In conclusion, having an electrified semitrailer can improve the performance of the vehicle, but the level of communication did not have a big impact on the results from the simulated use cases investigated in this thesis.

Keywords: Heavy duty vehicle, Electric semitrailer, Torque distribution, Vehicle dynamics



# Preface

This report presents the outcome of our master's thesis project carried out at the Department of Mechanics and Maritime Sciences at Chalmers University of Technology during the spring of 2024.

# Acknowledgements

We would like to thank Volvo GTT and our main supervisor Christian Oscarsson for the opportunity to work on this project. It has been really interesting and insightful. We would also like to thank our second supervisor Mukesh Choudhary who has been great at guiding us whenever we needed help. Finally, we would like to express our heartfelt gratitude to our examiner Bengt Jacobson and our supervisor Umur Erding from Chalmers University of Technology. Their invaluable guidance, support, and encouragement have been instrumental in keeping us on track to make this thesis as good as possible.

Harald Hermansson, Gothenburg, June 2024

Joakim Tjärnlund Leppämäki, Gothenburg, June 2024



# List of Acronyms

Below is the list of acronyms that have been used throughout this thesis listed in alphabetical order:

**BEV** Battery electric vehicle  
**E-semitrailer** Electric Semitrailer  
**ICE** Internal combustion engine  
**LPT** Longitudinal Performance Test  
**RWA** Road wheel angle  
**SWA** Steering wheel angle  
**VTM** Volvo Transport Models



# Nomenclature

Below is the nomenclature of indices, parameters, and variables that have been used throughout this thesis.

## Indices

$i$	Index for vehicle unit
$j$	Index for axle on vehicle unit $i$
$s$	Index for the left or right side of axle $j$ on vehicle unit $i$
$calc$	Calculated value
$init$	Initial
$max$	Max possible value
$out$	Signal exiting a block
$powertrain$	Index for the powertrain (engine to drive axle)
$prop$	Propulsion
$ref$	Reference
$req$	Request
$tot$	Total

## Parameters

$m_i$	Mass of unit $i$
$m_{ij}$	Mass of axle $j$ on vehicle unit $i$
$g$	Gravitational acceleration
$r_i$	Wheel radius on unit $i$
$\mu_{road}$	The road's coefficient of friction
$\mu_{tyre}$	The coefficient of friction that the tyres utilise

---

# Variables

## Forces & torques

$F_{x,i}$	Sum of longitudinal forces on all wheels of vehicle unit $i$
$F_{y,i}$	Sum of lateral forces on all wheels of vehicle unit $i$
$F_{z,i}$	Sum of normal forces forces on all wheels of vehicle unit $i$
$F_{x,ij}$	Sum of longitudinal forces on all wheels of axle $j$ on vehicle unit $i$
$F_{y,ij}$	Sum of lateral forces on all wheels of axle $j$ on vehicle unit $i$
$F_{z,ij}$	Sum of normal forces on all wheels of axle $j$ on vehicle unit $i$
$F_{x,ij_s}$	Longitudinal force on wheel on side $s$ of axle $j$ on vehicle unit $i$
$F_{y,ij_s}$	Lateral force on wheel on side $s$ of axle $j$ on vehicle unit $i$
$F_{z,ij_s}$	Normal force on wheel on side $s$ of axle $j$ on vehicle unit $i$
$F_{cx}$	Sum of longitudinal forces in the coupling between the vehicle units
$F_{cy}$	Sum of lateral forces in the coupling between the vehicle units
$F_{cz}$	Sum of vertical forces in the coupling between the vehicle units
$T_{ij}$	Sum of wheel-torques on all wheels of axle $j$ on vehicle unit $i$
$T_{ij_s}$	Wheel-torque on wheel on side $s$ of axle $j$ on vehicle unit $i$

## States

$s_{x,i}$	Traveled distance of vehicle unit $i$ in longitudinal direction
$s_{y,i}$	Traveled distance of vehicle unit $i$ in lateral direction
$v_{x,i}$	Longitudinal velocity of vehicle unit $i$
$v_{y,i}$	Lateral velocity of vehicle unit $i$
$a_{x,i}$	Longitudinal acceleration of vehicle unit $i$
$a_{y,i}$	Lateral acceleration of vehicle unit $i$
$v_{x,ij}$	Longitudinal velocity of axle $j$ on vehicle unit $i$
$a_{x,ij}$	Longitudinal acceleration of axle $j$ on vehicle unit $i$
$\alpha_i$	Road gradient for vehicle unit $i$
$\theta$	Articulation angle between tractor and semitrailer
$\omega_{w,ij}$	Average wheel rotational velocity for axle $j$ on vehicle unit $i$
$\omega_{w,ij_s}$	Rotational velocity of wheel on side $s$ of axle $j$ on vehicle unit $i$

---

$S_{x,ij}$	Average longitudinal slip of axle $j$ on vehicle unit $i$
$S_{y,ij}$	Average side (lateral) slip of axle $j$ on vehicle unit $i$
$S_{x,ij_s}$	Longitudinal slip of wheel on side $s$ of axle $j$ on vehicle unit $i$
$S_{y,ij_s}$	Side (lateral) slip of wheel on side $s$ of axle $j$ on vehicle unit $i$

SI units are used when else is not given



# Contents

<b>List of Acronyms</b>	<b>ix</b>
<b>Nomenclature</b>	<b>xi</b>
<b>1 Introduction</b>	<b>1</b>
1.1 Background . . . . .	1
1.2 Purpose . . . . .	1
1.3 Objectives . . . . .	2
1.4 Limitations . . . . .	2
<b>2 Theory and definitions</b>	<b>3</b>
2.1 Levels of communication between tractor and E-semitrailer . . . . .	3
2.2 Propulsion strategies . . . . .	5
2.3 Use cases . . . . .	7
2.4 Volvo Transport Models . . . . .	8
2.5 Defining safe motion . . . . .	9
2.6 Performance metrics . . . . .	11
2.7 Vehicle setup . . . . .	11
<b>3 Controller modelling</b>	<b>13</b>
3.1 Controller modelling process . . . . .	13
3.1.1 General controller design . . . . .	13
3.1.2 Torque distribution tests during the controller development phase . . . . .	15
3.1.2.1 Constant speed circle driving . . . . .	15
3.1.2.2 Acceleration in a turn . . . . .	18
3.1.2.3 Fail statistics in downhill turn . . . . .	20
3.1.3 Determining applied propulsive torque reduction for the E- semitrailer when cornering . . . . .	21
3.2 Final Controllers . . . . .	23
3.2.1 Speed controller . . . . .	23
3.2.2 Type 4 torque allocation . . . . .	24
3.2.3 Traction controller, torque limiter and power limiter . . . . .	29
3.2.4 Type 3 torque controllers . . . . .	33
3.2.4.1 Type 3 tractor torque allocation . . . . .	33
3.2.4.2 Type 3.1 semitrailer torque allocation . . . . .	35
3.2.4.3 Type 3.2 semitrailer torque allocation . . . . .	38

3.2.4.4	Type 3 light semitrailer torque allocation . . . . .	39
3.2.4.4.1	Type 3 light instability testing . . . . .	41
<b>4</b>	<b>Final comparison of E-semitrailer controller algorithms</b>	<b>47</b>
4.1	Simulation setup - tested controllers . . . . .	47
4.2	Sim 1: Longitudinal performance test . . . . .	49
4.2.1	Sim 1 - Setup . . . . .	49
4.2.2	Sim 1 - Results . . . . .	49
4.3	Sim 2: Flat intersection . . . . .	54
4.3.1	Sim 2 - Setup . . . . .	54
4.3.2	Sim 2 - Results . . . . .	55
4.4	Sim 3: Downhill intersection . . . . .	59
4.4.1	Sim 3 - Setup . . . . .	59
4.4.2	Sim 3 - Results . . . . .	60
4.5	Sim 4: Uphill intersection . . . . .	65
4.5.1	Sim 4 - Setup . . . . .	65
4.5.2	Sim 4 - Results . . . . .	66
<b>5</b>	<b>Discussion</b>	<b>69</b>
5.1	Type 3 coupling force sensor . . . . .	69
5.2	Type 3.1 vs type 4 . . . . .	69
5.3	Traction control and fail statistics . . . . .	70
5.4	Type 3 light speed sensor . . . . .	70
5.5	Result discussion . . . . .	70
5.5.1	Uphill intersection test on low $\mu$ . . . . .	70
5.6	Torque factor . . . . .	71
5.7	Speed controller . . . . .	71
<b>6</b>	<b>Conclusion</b>	<b>73</b>
<b>7</b>	<b>Future work</b>	<b>75</b>
7.1	Traction control and tyre model . . . . .	75
7.2	Torque vectoring . . . . .	75
7.3	Jack-knife avoidance . . . . .	76
7.4	Energy optimisation . . . . .	76
<b>A</b>	<b>Matlab function scripts</b>	<b>I</b>
A.1	Type 4 Fz proportional distribution torque allocation . . . . .	I
A.2	Type 3 tractor torque allocator . . . . .	III
A.3	Type 3.1 semitrailer torque allocator . . . . .	IV
A.4	Type 3.2 semitrailer torque allocator . . . . .	V
A.5	Type 3 light semitrailer torque allocator . . . . .	VI
<b>B</b>	<b>Simulation Results</b>	<b>IX</b>
B.1	Longitudinal Performance Test . . . . .	IX
B.1.1	Flat . . . . .	IX
B.1.2	Uphill . . . . .	XII

# 1

## Introduction

### 1.1 Background

The automotive industry is moving towards a more electrified fleet. A part of this transition is the electrification and hybridisation of heavy commercial tractors. Another step within the electrification of heavy duty vehicles is for the trailers to have their own propulsion and regenerative braking. This allows a higher efficiency of the vehicle, and a hybridisation of a truck even if the tractor is not a hybrid or Battery electric vehicle (BEV).

But this is a complex solution. The trailer can have limited data on the current operation and applying the incorrect torque on the wheels can lead to instability and eventually to events like jackknifing, trailer-sway or rollovers, if not controlled correctly [1]. Therefore, this thesis aims to contribute to the electrification of heavy commercial vehicle transports, by developing a torque allocation strategy that can efficiently allocate propulsion and brake requests between the tractor and the Electric Semitrailer (E-semitrailer). The combination should be able to operate both energy efficiently and safely. Safe means that the vehicle remains stable, and no combination of forces should result in any of the previously mentioned detrimental situations. The vehicle combination that will be studied in this thesis is a 4x2 tractor with a semitrailer with 3 axles, where the first axle is driven. The communication between the tractor and semitrailer is not obvious, and thus the torque allocation strategy needs to be developed for two different types of communication between the units. Type 3 will have limited communication between the tractor and the semitrailer while type 4 will have full communication between the units.

### 1.2 Purpose

The purpose of the thesis work is to compare how the performance, stability and driveability depend on the type of communication between a tractor and an E-semitrailer. To do the comparison, controllers for longitudinal wheel-torque distribution need to be developed for each communication type.

### 1.3 Objectives

- Investigate existing research on the safe operating envelope of a tractor and E-semitrailer combination, proposing controllers for type 4 and type 3 E-semitrailers.
- Develop torque allocation algorithms to distribute torque on both units to ensure the overall safety of the vehicle combination. One algorithm for each type of E-semitrailer communication.
- Test the algorithm for various scenarios, including different speeds and varying friction coefficients.
- Compare the E-semitrailer types with the developed controllers with respect to motion (safety and performance).

### 1.4 Limitations

This project can have a wide variety of tests, parameters, and variables to create the two controllers and compare their performance. To limit the project in a reasonable scope a number of limitations have been defined.

- The tests will only be evaluated on the road, no off-road testing will be done.
- The vehicle setup is limited to a 4x2 tractor with rear-wheel drive, and an attached 6x2 semitrailer with front wheel drive. No axles will be steerable except for the tractor's front axle.
- There will be no cases involving reversing or parking.
- The performance evaluation will not involve any energy optimisation and will only look at motion dynamics such as stability, accelerations and driveability.
- The thesis will not look into optimisation algorithms such as "control allocation" or "predictive control" for reducing energy consumption.
- Use cases involving heavy braking will not be studied, because all levels of communication will have the same standard interface for braking.
- The thesis assumes that the road friction coefficient is known at all times and that it is equal for all of the wheels' contact patches at the same moment in time. In reality, it is not known but it may be estimated.
- The thesis assumes that the current road gradient for each unit is known at all times. In reality, it is not known but it can be estimated with high precision.

# 2

## Theory and definitions

This chapter explains the theory and definitions that are fundamental to understanding the material within this thesis. Section 2.1 defines the different levels of tractor-semitrailer communication that have been studied. Section 2.2 describes different propulsion strategies. Section 2.3 describes the selection of use cases for the controller comparison. The simulation environment is described in chapter 2.4. Section 2.5 defines safe motion for a tractor and semitrailer combination. Section 2.6 describes the performance metrics for the controller comparison. Finally, section 2.7 explains the vehicle setup for this thesis.

### 2.1 Levels of communication between tractor and E-semitrailer

To safely drive a multi-unit vehicle of the size of tractors and semitrailers, communication is needed between the units. This is especially important when you want to electrify a unit that is normally towed, which for this thesis means giving a semitrailer the opportunity of helping the tractor in propulsion. The more information that can be transferred between the units, the higher the possibility of safely controlling the vehicle combination. Increasing the amount of transferred data, however, is not free. Added information likely implies adding new sensors, new software and a completely new signal interface within the vehicle in some scenarios.

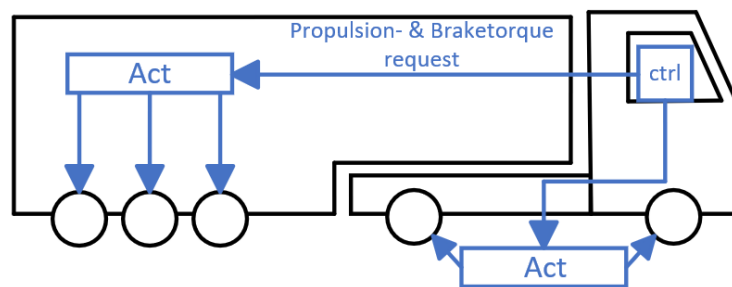
As this thesis wants to compare how different levels of communication between a tractor and a semitrailer impact the motion performance of the vehicle combination, three different "types" of E-semitrailers have been defined, with inspiration from an ongoing standardisation work in EU:

- **Type 4:** Type 4 E-semitrailer is a vehicle combination with full communication between the tractor and the E-semitrailer. All the information in the semitrailer is known by the tractor. It uses a centralised controller located in the tractor which controls the propulsion and brake torques on both the tractor and the semitrailer.
- **Type 3:** The type 3 E-semitrailer is restricted to the ISO-11992-2:2014 standard for its communication between the tractor and the semitrailer. In terms

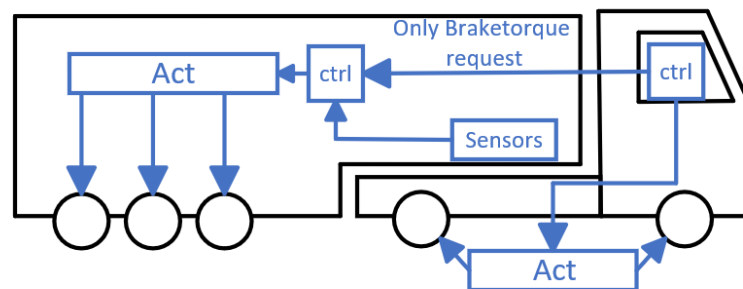
of controller signals, the only request signal that can be sent from the tractor to the semitrailer is a brake pressure request. In this thesis, it is assumed that the semitrailer can decide from the brake pressure request whether it should brake by retardation with its electric motor or by friction brakes. No signal is going from the semitrailer to the tractor, which results in the tractor not knowing it has a propelled semitrailer. The advantage of this is that this type of E-semitrailer is planned to work with any tractor, no matter the brand or communication interface, as long as it has the ISO-11992-2 2014 standard.

In addition to the ISO standard communication, it is equipped with a coupling force sensor, which allows it to sense the coupling force in the x, y and z-direction. It is also equipped with an articulation angle sensor.

- **Type 3 Light:** Type 3 light is also restricted to the ISO-11992-2 2014 standard. It is, however, not equipped with any additional equipment. The only sensors and signals available are the ones included in the ISO standard.



(a) Type 4



(b) Type 3

**Figure 2.1:** General controller principle difference between the type 4 and type 3 E-semitrailer

Figure 2.1 shows a visual overview of type 3 and type 4 communication concepts. See tables 2.1 and 2.2 for complete tables explaining the differences in signals available for the tractor and semitrailer in this thesis, respectively.

**Table 2.1:** Available signals for the tractor depending on the type of controller. X = Signal is available at all times, Static = Signal is only measured at standstill, Parameter = Used as a parameter, signal is not dynamically measured.

Signal	Unit	Type 3 light	Type 3	Type 4
Tractor individual wheel speeds	rad/s	X	X	X
Semitrailer individual wheel speeds	rad/s			X
Tractor IMU information	rad/s and m/s <sup>2</sup>	X	X	X
Semitrailer IMU information	rad/s and m/s <sup>2</sup>			X
Tractor axle loads	kg	X	X	X
Semitrailer axle loads	kg	Static	Static	X
Semitrailer available torque	Nm			X
Semitrailer articulation information	rad			X
Coupling force information	N			Can be estimated
Steering wheel angle	rad	X	X	X
Driver's force request	N	X	X	X
Road friction coefficient		X	X	X
Tractor tyre radius	m	Parameter	Parameter	X
Semitrailer tyre radius	m			X

**Table 2.2:** Available signals for the semitrailer depending on the type of controller. X = Signal is available at all times, Static = Signal is only measured at standstill, Parameter = Used as a parameter, signal is not dynamically measured.

Signal	Unit	Type 3 light	Type 3	Type 4
Tractor individual wheel speed	rad/s			X
Semitrailer individual wheel speed	rad/s	X	X	X
IMU tractor information	rad/s and m/s <sup>2</sup>			X
IMU semitrailer informationr	rad/s and m/s <sup>2</sup>	lateral accelerometer and slope sensor	X	X
Tractor axle loads	kg			X
Semitrailer axle loads	kg	X	X	X
Tractor available torque	Nm			X
Semitrailer available torque	Nm	X	X	X
Tractor pneumatic brake request	Pa	X	X	X
Tractor retardation request	m/s <sup>2</sup>	X	X	X
Semitrailer articulation information	rad		X	X
Coupling force information	N		X	Can be estimated
Steering wheel angle	rad			X
Driver's force request	N			X
Road friction coefficient		X	X	X
Tractor tyre radius	m			X
Semitrailer tyre radius	m	Parameter	Parameter	X

## 2.2 Propulsion strategies

The strategy used to distribute propulsion force is not trivial, and it can be altered between the different types of E-semitrailers. From a brainstorming session, together with a study of previous projects about E-semitrailers, a few propulsion strategy concepts were constructed.

The type 3 E-semitrailer was divided into two groups, type 3 and type 3 light. Type 3 is equipped with 2 extra sensors, a coupling force sensor and an articulation angle sensor, whilst type 3 light only relies on the sensors available in a standard semitrailer according to ISO 11992-2:2014.

- **Manually set distribution factor (type 4)**

For a requested acceleration, the required total force is calculated, then distributed between the tractor and the semitrailer based on a pre-set factor. If the factor is set to 0.6, it will propel with 60% of the force on the tractor and 40% on the semitrailer.
- **Longitudinal coupling force proportional (type 3)**

By measuring the coupling force with a sensor, the current force times a factor could be used to propel the semitrailer to achieve a specific wanted coupling force.
- **Longitudinal force distribution proportional to vertical axle loads (type 4)**

From the paper [2] "*Validation of high-fidelity simulation-based safe operating envelopes for articulated heavy vehicles using real test data*" it can be motivated that the most optimal distribution for a vehicle combination with both truck and semitrailer propelled is to stay close to the same friction utilisation on both units. This can be achieved by distributing torque with respect to the dynamic axle loads on the truck axles in relation to the loads on the semitrailer axles. If the semitrailer's axles carry 70% of the weight, it should output 70% of the propulsion force.
- **Vertical coupling force proportional to longitudinal coupling force (type 3)**

By measuring the coupling force in both the longitudinal and vertical direction, as well as the vertical load on the semitrailer's axles, the proportion between the longitudinal and vertical force can be calculated in the coupling and thereby the force to propel in proportion to the axle load can be calculated. This will ensure unit-wise equal friction utilisation on both the tractor and the E-semitrailer.
- **Longitudinal acceleration dependent (type 3 light)**

With the help of the wheel speed sensor in the brake system on the semitrailer and the axle load sensor, both the current acceleration and the axle load mass can be calculated. This can be used to find the force required to propel the weight carried by the semitrailer's axles, resulting in unit-wise equal friction utilisation.

## 2.3 Use cases

During the initial research period, no standardised test manoeuvres for E-semitrailers were found. To test and evaluate the performance of the controllers, several use cases needed to be defined and simulated. Brainstorming sessions were conducted to identify potential use cases and determine their relevance. The project focuses on short intense sequences, like crossing an intersection or driving up a steep hill while turning, rather than longer distances like driving through a city.

The full list of use cases discussed in the brainstorming session can be seen in table 2.3. The use cases with a red background colour are the ones that were determined as not interesting for this thesis.

**Table 2.3:** Use cases from brainstorming

Use Cases
Start in intersection
Sharp turn immediately after downhill
High acceleration start on flat road
Acceleration in long and wide turn
Roundabout
Hard regeneration without using service brakes
Stand still to start in a sharp turn immediately after uphill
Overtake or lane change
Sharp turn uphill (low friction)
Sharp turn downhill (low friction)
Uphill with decreasing friction
Going uphill with increasing slope gradient with constant speed
Start on very low friction uphill
Accelerating with different friction coefficients on each wheel
Braking with different friction coefficients on each wheel
Reversing/parking
Hard braking
Hard braking while turning
Start in uphill
Start in downhill
180-degree turn high speed
Highway at constant speed
Gravel or country road (uneven road)

## 2.4 Volvo Transport Models

Volvo Transport Models (VTM) is Volvo GTT's library of high-fidelity simulation and vehicle models implemented in Simulink. It is an in-house developed simulation tool and can be used to test anything from vehicle setups to controller design.

The VTM model library contains different templates depending on the desired tractor-trailer combination. A template consists only of the vehicle plant model specific to the chosen combination. The vehicle plant uses inputs from road steering wheel angles, wheel-torques and vertical wheel positions to simulate the vehicle movement on a defined road. It outputs forces and states for both bodies, axles and wheels.

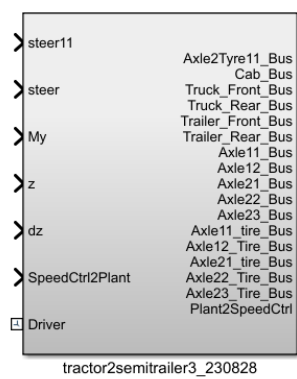


**Figure 2.2:** VTM template for a tractor with 2 axles and semitrailer with 3 axles

Figure 2.2 shows the vehicle plant block in Simulink. The working area of this thesis was outside of the block, creating logic that determined the wheel-torque input into the vehicle plant model. For the template plant model, the wheel-torques were input as one torque per wheel, formatted as a column vector with the same length as the number of wheels. The input "SpeedCtrl2Plant" should be connected to a speed controller that calculates the wheel-torques. If additional wheel-torques were to be added separately from the speed controller, they should be input through the "My" input port.

The steering inputs will be determined by a path follower taken from Volvo's VTM library. It is a model that is trying to keep the vehicle on the predefined road that has been chosen, by looking at a line created in the middle of the lane. It can be defined how "skilled" the driver model is, by altering parameters like reaction time and correction speed. The parameters were set to simulate a realistic driver according to Volvo GTT's standard values.

"z" and "dz" are inputs that define where the vehicle is on the road, or more precisely the height of the road on the current location, as well as the current change in height of the road.

## 2.5 Defining safe motion

Safe travel has been defined with definitions taken from the master thesis "Safe operating envelope for electric semi-trailer" [1]:

There are 4 scenarios that need to be avoided: jackknifing, trailer-sway, rollover and off-tracking. Each of these needs to be defined in a way that they can be detected in Simulink during simulation.

### Jackknifing:

Jackknifing occurs when the tractor loses traction, primarily on the rear wheels, whilst the trailer keeps its traction, making the trailer push the tractor sideways in front of it. From the master's thesis "Safe operating envelope for electric semi-trailer", jackknifing has been defined by equations 2.1-2.3.

$$S_{y,12} = \frac{|v_{y,12}|}{|v_{x,12}|} > 0.8 \quad (2.1)$$

$$S_{y,22} = \frac{|v_{y,22}|}{|v_{x,22}|} < 0.4 \quad (2.2)$$

$$|\theta| \geq 90^\circ \quad (2.3)$$

where  $S_{y,12}$  and  $S_{y,22}$  are the sideslips of the second axle on the tractor and trailer respectively.  $\theta$  is the articulation angle between the tractor and the trailer. According to A. Hansson and E. Andersson, the threshold values are chosen from experience in their simulation where they let a tractor with an E-semitrailer drive through a  $180^\circ$  turn with varying turn radius and longitudinal velocity.

Since jackknifing only will occur when the tractor and trailer turn into each other by having a too high articulation angle, the threshold for  $\theta$  is intuitively 90 degrees. As stated in [1], "When all thresholds are fulfilled, jackknifing is considered to occur".

### Trailer-sway:

The second unsafe scenario is trailer-sway. Trailer-sway occurs when the trailer loses traction, whilst the tractor keeps its traction, making the trailer slide out in one direction. Essentially the opposite of a jackknife situation. This makes the slip part of the threshold definition reversed. See equations 2.4-2.6 for all the thresholds that need to be fulfilled to consider it as a trailer-sway incident.

$$S_{y,12} = \frac{|v_{y,12}|}{|v_{x,12}|} < 0.4 \quad (2.4)$$

$$S_{y,22} = \frac{|v_{y,22}|}{|v_{x,22}|} > 0.8 \quad (2.5)$$

$$|\theta| \geq 30^\circ \quad (2.6)$$

**Rollover:**

A rollover is a scenario when the tractor or the trailer has rolled over and the threshold for this is a roll angle of  $90^\circ$ .

**Off-tracking:**

The last unsafe scenario according to [1] is off-tracking. It occurs when the front-most axle of the tractor deviates from the desired path and the threshold is half the width of a single lane from the centre of the lane. The value is set to 1.75m.

## 2.6 Performance metrics

This thesis has compared the vehicle combination's motion performance depending on the different levels of communication. Methods to measure motion performance needed to be defined. First and foremost the vehicle needed to avoid all of the unsafe scenarios described in section 2.5. For the cases when unsafe driving was not reached, the following performance metrics have been defined to reveal the best-performing controller:

- ***Completion Time:***

The total time it takes for the combination to finish the track or scenario. A shorter time means that the vehicle has travelled faster through the track, meaning improved motion performance.

- ***Mean Acceleration:***

For scenarios including an acceleration, the mean acceleration of the combinations through the track or scenario. A higher value means that the vehicle has on average managed to accelerate at a higher rate.

- ***Deviation from track:***

For a certain axle, the deviation from the track is the lateral offset from the intended path generated by the path follower. It is measured from the centre of the axle to the path. Usually measured as the maximum value during the event. A low value is desired.

- ***Cumulative steering:***

For scenarios that involve cornering, the cumulative steering value is the total amount of Steering wheel angle (SWA) changes during a defined time. For example, if a driver would steer 40 degrees left of neutral steering and then 30 degrees right of neutral steering then the cumulative steering value would be:  $40^\circ + (40^\circ + 30^\circ) = 110^\circ$ .

## 2.7 Vehicle setup

The vehicle combination in this thesis consists of a 4x2 (4 wheels, 2 driven) tractor and a 6x2 (6 wheels, 2 driven) semitrailer.

The tractor is rear wheel driven and has a powertrain similar to a typical diesel truck engine, with a maximum power of 450 kW and a peak wheel-torque output of 56 000 Nm. The semitrailer is front wheel driven and has an electric motor that can deliver a power of 580 kW and a peak wheel-torque of 25 000 Nm. This is a pretty big powertrain for a semitrailer, but since this thesis is researching the potential of the E-semitrailer, a big powertrain is needed to not immediately be torque or power limited on the tested use cases.

Both the tractor and the semitrailer are able to retard or engine brake. The tractor can be seen as an Internal combustion engine (ICE) or as a BEV, either way, it can

## 2. Theory and definitions

---

engine brake up to  $-2.5 \text{ m/s}^2$  and the semitrailer can retard up to its torque limit of 25 000 Nm.

The E-semitrailer and tractor carries 21.3 and 18.5 tonnes of weight respectively, resulting in a gross weight of 39.8 tonnes. The vehicle combination's weights and dimensions can be seen in figure 2.3 (figure is drawn in scale).

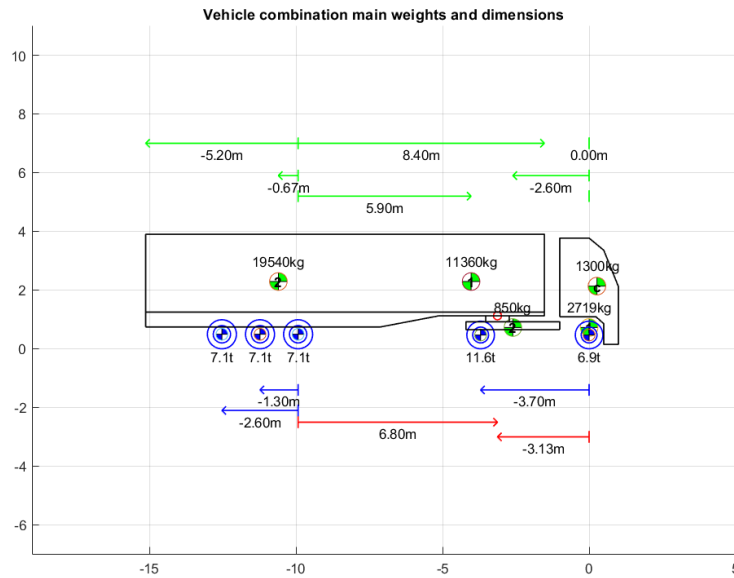


**Figure 2.3:** Vehicle combination main weights and dimensions

# 3

## Controller modelling

Controllers and roads had to be modelled in Matlab and Simulink to compare the different levels of communication. This chapter first explains the process of how the controllers were made in section 3.1. Section 3.2 describes the architecture and logic of the final controllers used in the comparison.

### 3.1 Controller modelling process

Before the modelling work started, an idea of the difference between the type 3 and type 4 E-semitrailers was established. See figure 2.1 for a sketch showing the difference in interface between the types. These simple sketches proved to be very useful to create the foundational controller logic within Simulink.

The process of creating the controllers in Simulink was iterative. Basic logic was designed and tested in different scenarios to ensure it functioned as expected. This process often led to updates and improvements. Hence, all the changes made to the controllers can not be shown in this report and neither all of the simulation results from intermediate tests made to improve the controllers. The following subsections will describe the most important milestones and findings during the process of developing the controllers. The first subsection explains the most general design differences between the types of communication. The rest of the subsections describe the tests that were done to understand how different torque distributions affect the movement of the vehicle combination.

#### 3.1.1 General controller design

First, the Simulink template for a 4x2 tractor and a 3-axle semitrailer was chosen. From existing example projects within VTM, a driver model block called "path follower" could be used (mentioned in 2.4), meaning it was not necessary to create a driver model from scratch.

A sketch of how the outermost layer of the type 4 controller was designed can be seen in figure 3.1

### 3. Controller modelling

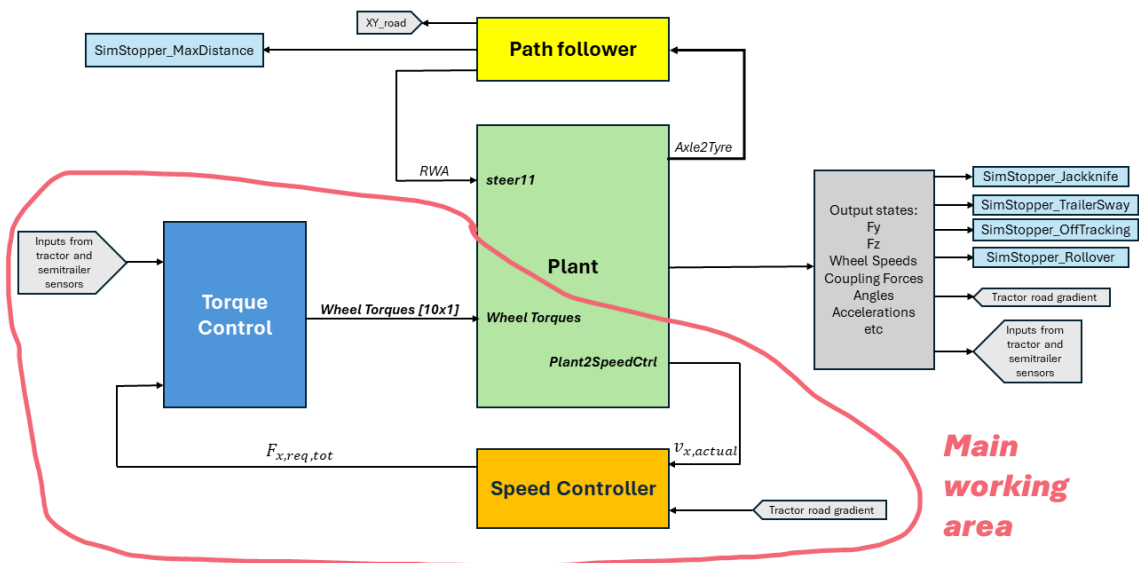


**Figure 3.1:** Type 4 general architecture of the Simulink controller model

The figure shows the main working area of this thesis. A speed controller was created, that compared the actual velocity to the requested velocity and output a total longitudinal force request for the entire vehicle. This force request along with data from sensors was used in a torque control block, that determined the wheel-torques for the plant in each time step of the simulation. The speed controller should act as close as possible to a real driver, and therefore the same logic was used for all models. The complete logic of the speed controller is described later in subsection 3.2.1. The blocks called "SimStopper" in figure 3.1 were used to calculate whether any of the unsafe scenarios described in section 2.5 had occurred. The simulation was stopped if an unsafe scenario was detected. The simulation was also stopped if the maximum distance of the current road had been reached.

The main difference between the different types of communication for the Simulink models was the torque control block. The type 4 communication models only needed one torque control block, that determined the wheel-torques for every single wheel of the vehicle combination, as shown in figure 3.1. The torque control block for the type 3 level communication, however, needed to be split into two torque control blocks, representing the tractor and semitrailer controlling their own axles in terms of torque. See figure 3.2.

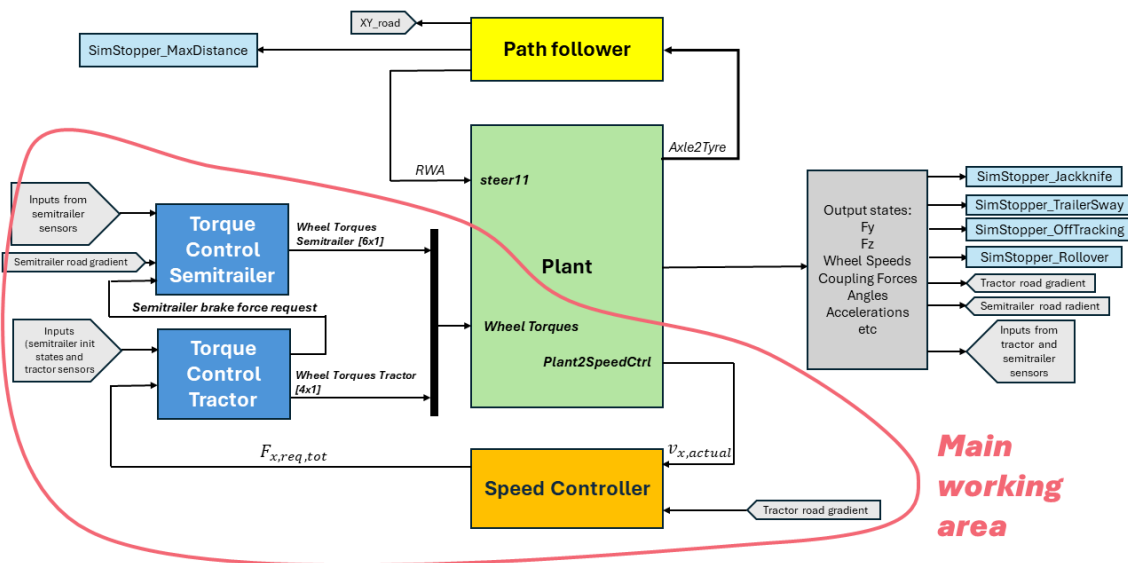


**Figure 3.2:** Type 3 general architecture of the Simulink model

The only signal that could be communicated between the tractor and the semitrailer torque control blocks was the brake force request. The semitrailer had to use its available sensors to determine when and how much it should propel.

### 3.1.2 Torque distribution tests during the controller development phase

Multiple tests were done during the controller development, mainly to investigate the difference in torque distributions and how they affected the dynamics and driveability of the vehicle, as well as the failure points and outcome of extreme situations. If a truck is in a position where it is unable to avoid a single accident, the way it fails can have a big impact on the harm it does to the driver and the vehicle. This makes failure investigation dependent on distribution an interesting topic.

#### 3.1.2.1 Constant speed circle driving

To check whether the distribution of torque between the tractor and the semitrailer had any effect on the minimum turning radius the vehicle combination could handle, a test was set up that allowed the vehicle to drive in a circle with a decreasing radius while driving at a constant speed. The track decreased to a minimum radius of 12 meters, which was approximately the smallest possible turning radius for the vehicle combination. See figure 3.3

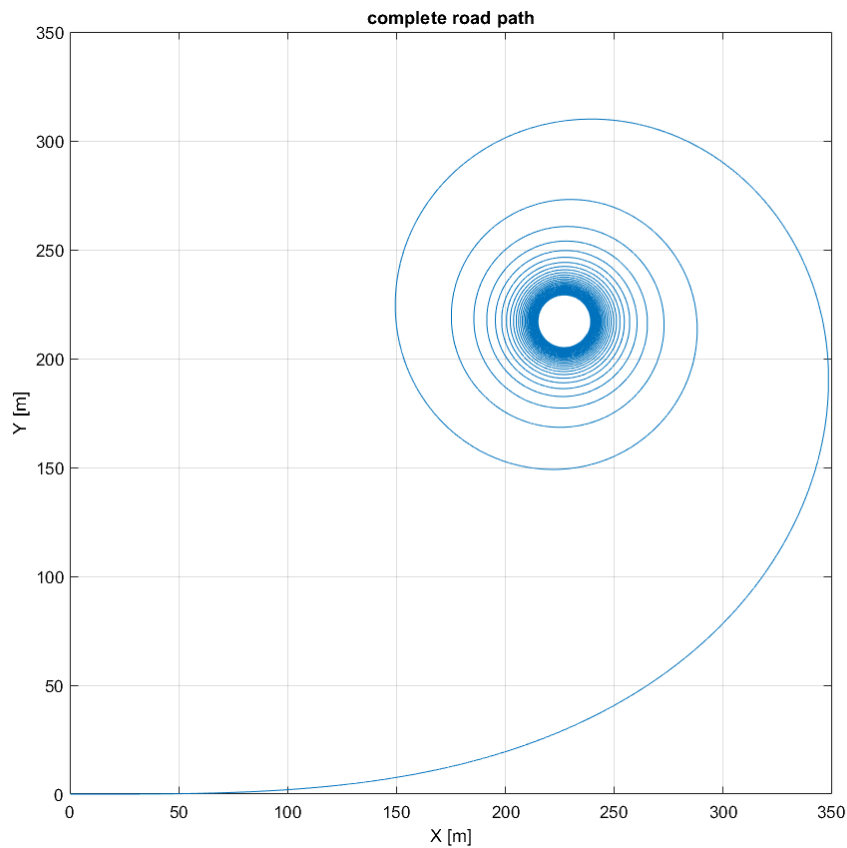
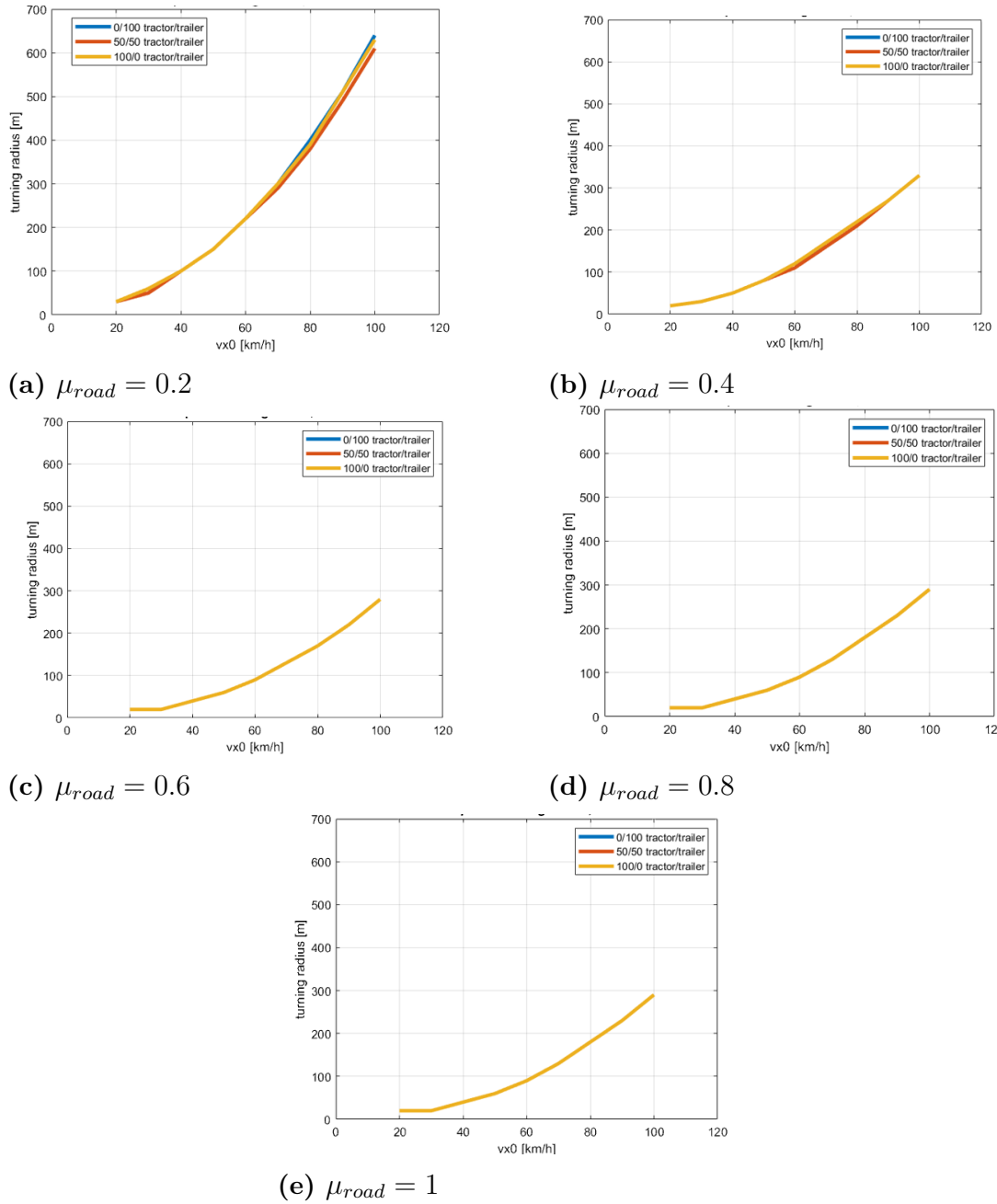


**Figure 3.3:** Maximum speed per turning radius test track

The vehicle combination travelled at a constant speed through the course and the simulation ended when the vehicle either jackknifed, rolled over, trailer-swayed, off-tracked or completed the track. The road friction coefficient,  $\mu_{road}$ , was varied from 0.2 to 1 with 0.2 intervals, and velocities were varied from 20 to 100 km/h with 10 km/h intervals.

Three different torque distributions were tested:

- **100/0 tractor/semitrailer** - Only tractor propelling
- **50/50 tractor/semitrailer** - Force request is split equally between tractor and semitrailer
- **0/100 tractor/semitrailer** - Only semitrailer propelling



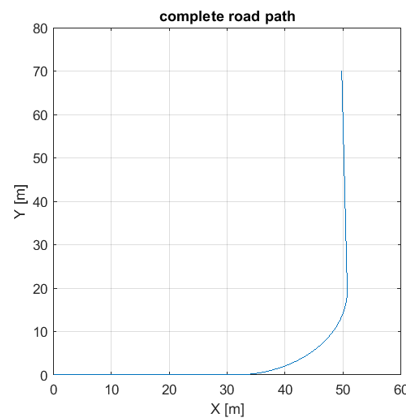
**Figure 3.4:** Constant speed decreasing turning radius results, distribution refers to "Tractor/Semitrailer". The figures are plotted as minimum turning radius versus constant velocity.

Figure 3.4 shows the test results. The minimum turning radius increased for increased velocities. The vehicle combinations are not able to drive in the area below their plotted lines, without failure. The difference between the different distributions was very small, making no difference at all for most cases. For higher  $\mu_{road}$  (0.6 and above) the most common failure scenario was a rollover, which is almost guaranteed when reaching a lateral acceleration above  $3 \text{ m/s}^2$ . For lower  $\mu_{road}$  it was not able to reach lateral accelerations above  $3 \text{ m/s}^2$ , and problems like jackknife, trailer-sway

or off-tracking were more common, which explains the small differences that can be seen in figure 3.4a and 3.4b as this is more affected by the type of distribution.

#### 3.1.2.2 Acceleration in a turn

Different torque distributions between the tractor and the semitrailer were also tested while accelerating in a turn, as constant speed driving while turning did not reveal any significant effects of the torque distribution used. See figure 3.5 for the shape of the corner created in Matlab. The same corner and manoeuvre were used for one of the final tests between the controllers in section 4.3, where the reason for its shape is explained.



**Figure 3.5:** Intersection created in Matlab with approximately 19.55 m radius

The vehicle combination first drove at 5 km/h until the start of the turn, and then it was given an acceleration request. If the vehicle completed the corner, meaning that it did not fail by any of the unsafe scenarios mentioned in section 2.5, a higher acceleration request was given for the next simulation. This process continued until the vehicle either failed or could no longer increase its speed despite further acceleration requests, indicating it would not fail regardless of how much the request was increased.

This was done for several different torque distributions between the tractor and the semitrailer. Numerical results of completion time and mean acceleration through the turn were retrieved for all of the simulations and plotted against the requested acceleration. See figure 3.6. This meant that it was possible to see how different torque distributions would react in terms of increasing its acceleration through a turn.

For this test, the torque distributions were named after the fraction of the longitudinal force request that was given to the tractor. For example, "1.0" meant that only the tractor propelled and "0.4" meant that the tractor propelled with 40% of the total longitudinal force request while the semitrailer propelled with 60% of the total longitudinal force request.

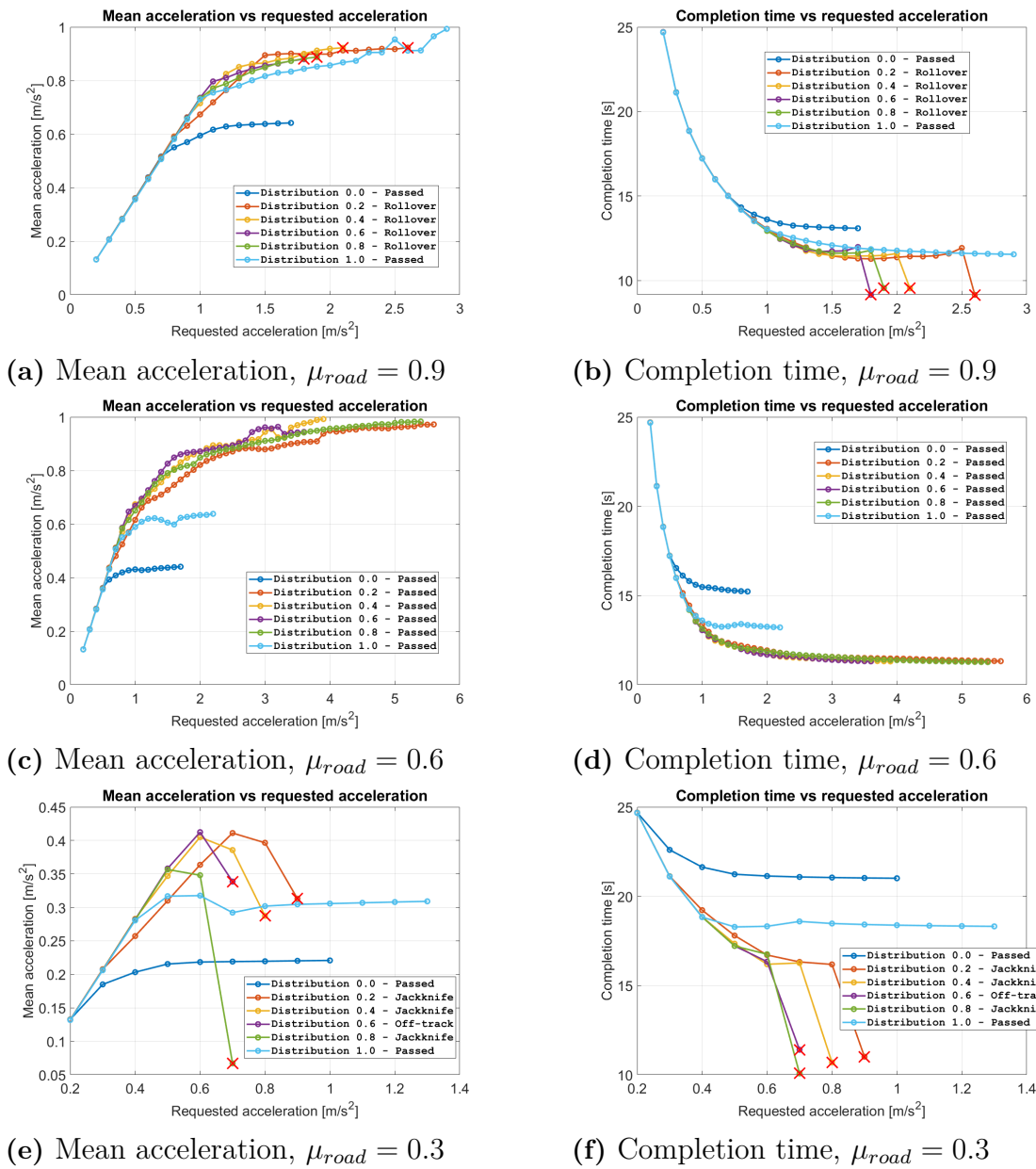


**Figure 3.6:** Torque distribution comparison while accelerating in a turn. The red crosses indicate the simulations that ended in a failure. The type of failure is mentioned in the legends.

Each point in the plots represents a single simulation. The most notable results from the tests relevant to controller modelling were that propelling only with the tractor or only with the semitrailer (distributions "0.0" and "1.0") never ended in failure. They were, however, completing the turn at a much slower time, where only semitrailer propulsion was the slowest. This showed that any combination of torque distributed between the vehicle units resulted in a faster completion time through the corner. It also demonstrated that a function that would redistribute the torque towards a tractor-driven distribution through the turn could increase safety.

### 3.1.2.3 Fail statistics in downhill turn

A test was set up where the truck drives at various initial speeds into a downhill turn. As it entered the curve, it started to accelerate. The parameters for the test can be seen below.

**Table 3.1:** Parameters for low-mid mu, downhill turning test

ax request [ $m/s^2$ ]	Initial speed [km/h]	Distributions	Friction coefficient
0.5	5	0	0.1
1	10	0.1	0.2
1.5	15	0.2	0.3
2	20	0.3	0.4
	25	0.4	0.5
		0.5	0.6
		0.6	
		0.7	
		0.8	
		0.9	
		1	
		Fz proportional	

These parameters were tested in all possible combinations. Every acceleration request together with every initial speed, distribution and friction coefficient. This made a total of 1440 simulations. The distributions tested were again named after the fraction of the total longitudinal force request that the tractor used (e.g. "0.8" is 80% tractor, 20% semitrailer). The captured results focused on whether it passed or failed to go through the curve. If it failed, the fail scenario was documented. The results can be seen below in two parts. The first figure (3.7a) shows the most number of fails per scenario for every distribution, as well as the number of successfully passed simulations, with mu varying from 0.1 to 0.6. The second figure (3.7b) shows the results from the simulations with respect to the friction coefficient.

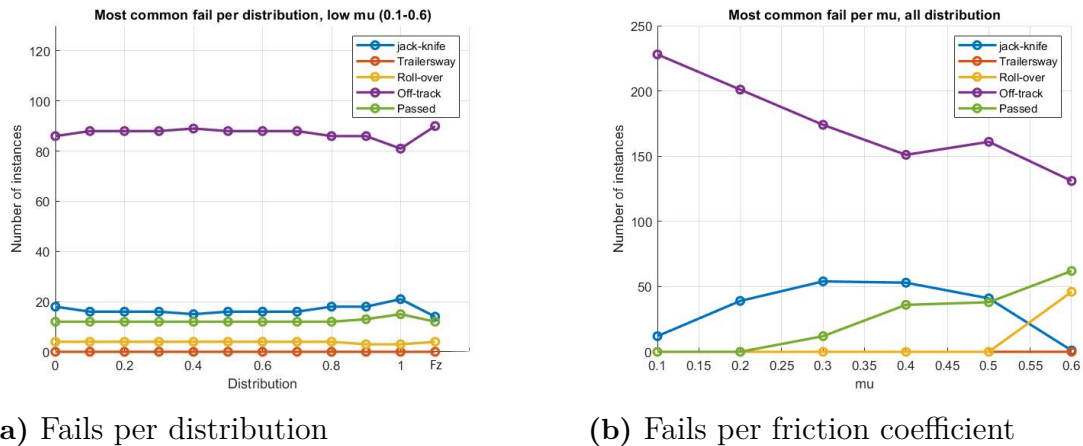


**Figure 3.7:** Most common fail dependent on torque distribution and friction coefficient

The main takeaway from these results was that the number of failures and the specific failure scenarios were not significantly influenced by the distribution, but

showed a strong correlation with the friction coefficient. There was a slight decrease in off-tracking and an increase in jackknives occurring at distribution 1 (tractor-only propulsion), but also an increase in passed tests.

Jackknife, which is seen as a severe incident, only occurred at friction coefficients up to 0.5, after this point, rollovers seem to be increasing as "traction sensitive" fails (jackknife, trailer-sway and off-tracking) are decreasing.

### **3.1.3 Determining applied propulsive torque reduction for the E-semitrailer when cornering**

A hypothesis when modelling the controller was that to increase the safety of the vehicle combination while turning, the torque applied on the semitrailer's driven axle should be reduced to some extent, and at an articulation angle of  $90^\circ$ , all the semitrailer's propulsion torque should be 0 Nm (although it is allowed to break).

To model this phenomenon, a function called "Torque factor" was created. It was a factor that could reduce the calculated output torque depending on the articulation angle. It was constructed in 2 parts. First, a value of an "accepted articulation angle" was defined. Up to this articulation angle, the output torque was not reduced. If the articulation angle exceeded this angle, a scaling factor was applied to the output torque to decrease it. This could be a linear scaling from the accepted articulation angle down towards 0 at  $90^\circ$  or an exponential downward scaling.

To test which angle and scaling method was the most optimal, a test in an intersection was performed where the truck accelerated as it turned on low friction. The accepted theta and scaling factor were iterated and the strategy with the best performance was chosen as the factor for the final controllers. Figure 3.8 shows an example of the accepted articulation angle ( $15^\circ$  in this case) and multiple scaling factors that were tested.

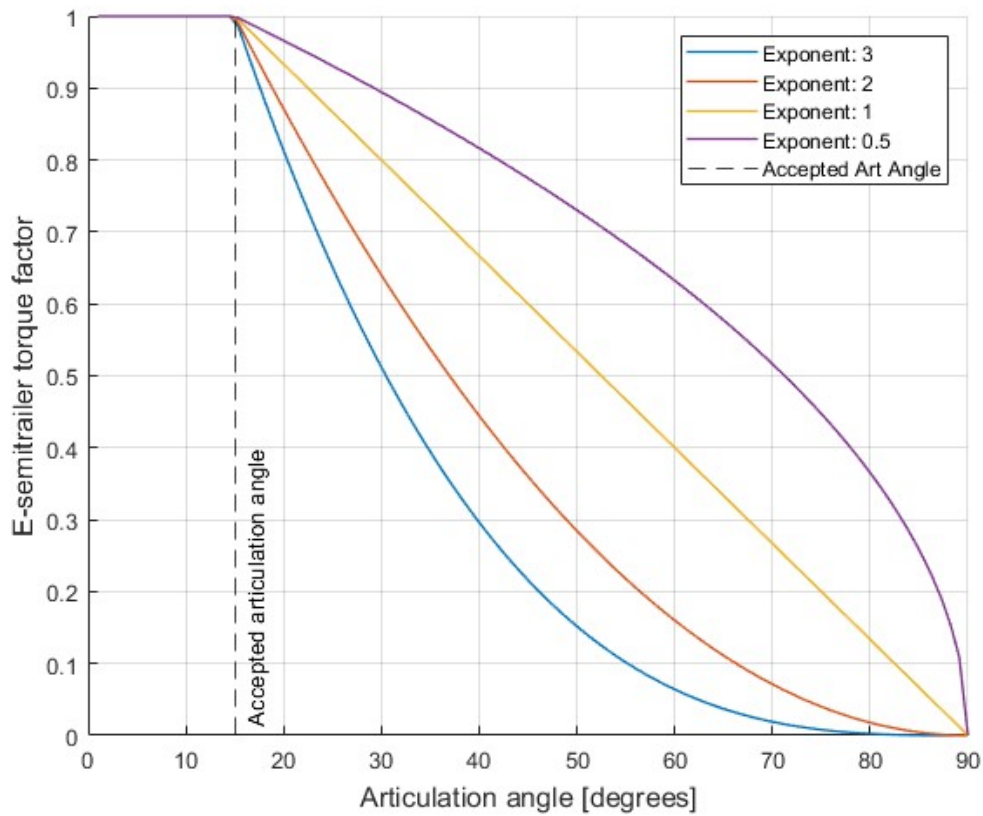


**Figure 3.8:** Visualisation of the "Torque Factor" function.

Tests were done on controllers of both type 4 and type 3 level communication controllers, which both showed the same trend. They all improved by just adding any form of torque factor, but the exact angle and scaling factor had lower impacts. After the data had been analysed, an accepted articulation angle of  $15^\circ$  and a scaling exponent of 3 were chosen, as these were the most common parameters for the simulations that had successfully made it through the turn in the shortest amount of time. However, varying these values in a close realm did not impact the results a lot.

## 3.2 Final Controllers

This section aims to describe the logic for the controllers used in the final comparison in chapter 4, as detailed as necessary to understand how the torque is allocated for different levels of tractor and semitrailer communication. The controllers will be explained in the most chronological way possible in terms of requests and outputs, starting with the speed controller in subsection 3.2.1. The torque allocation strategy of the type 4 communication level will be explained in subsection 3.2.2. Subsection 3.2.3 will explain how the allocated torque is limited due to traction and the power-trains' maximum usable torque and power, for the type 4 controllers. However, the later explained type 3 controllers use many of the same principles when limiting the allocated torques. The torque allocation strategy for the type 3 level communication will finally be explained in subsection 3.2.4.

### 3.2.1 Speed controller

A speed controller was developed from scratch. It had to be developed within this work because the existing speed controller in the VTM library converted a velocity request to a wheel-torque input for the vehicle plant directly. Since the wheel-torques should be distributed between the tractor and the semitrailer with different logic depending on the communication level, the torque distribution logic was split from the speed controller logic in this work. All of the controllers used the same speed controller. The speed controller's purpose was to act like a real-life driver and the most fair comparison was achieved when the same driver was used for the different types of E-semitrailers. The logic of the speed controller is visually explained in figure 3.9.

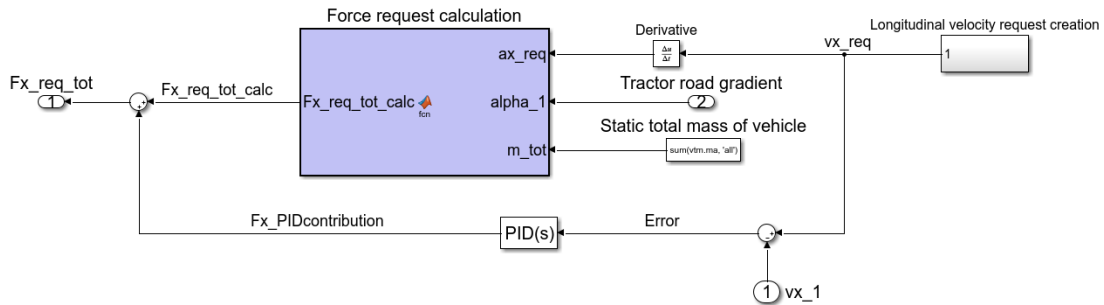


**Figure 3.9:** Speed controller in Simulink

Starting from the right side of the figure 3.9, a longitudinal velocity request,  $v_{x,req}$ , was created depending on the scenario and manoeuvre. The request was derivated to retrieve a longitudinal acceleration request  $a_{x,req}$ . The function "Force request calculation" calculated the total longitudinal force request according to equation 3.1

$$F_{x,req,tot,calc} = m_{tot}(a_{x,req} + g \cdot \sin(\alpha_1) + RRC) \quad (3.1)$$

where  $m_{tot}$  is the total mass of both tractor and semitrailer,  $g = 9.82 \text{ m/s}^2$  is the gravitational constant,  $\alpha_1$  is the current road gradient for the tractor and  $RRC = 0.008$  is the rolling resistance coefficient. The known disturbances have been modelled into the calculation, but a PID controller was also used to act on the error between the requested longitudinal velocity and the actual longitudinal velocity, to remove the remaining unknown disturbances. The PID controller is described by equation 3.2.

$$F_{x,PIDcontribution} = e \left( K_p + K_i \frac{1}{s} + K_d \frac{N}{1 + N \frac{1}{s}} \right) \quad (3.2)$$

where  $K_p = 1 \cdot 10^5 \frac{N}{m/s}$ ,  $K_i = 1 \cdot 10^4 \frac{N}{m}$ ,  $K_d = 5 \cdot 10^4 \frac{N}{m/s^2}$ ,  $N = 100$  and  $e$  is the velocity error. This contribution was summed with the calculated total longitudinal force request to retrieve the total longitudinal force request for the vehicle combination ( $F_{x,req,tot}$ ). This value was used in the torque controller blocks of the models to calculate torque requests for the wheels. Note that the total longitudinal force requested could be both positive and negative, where a positive value indicated that the vehicle should propel and a negative value indicated that the vehicle should brake.

#### 3.2.2 Type 4 torque allocation

The type 4 controller consisted of 2 parallel torque distribution methods for propulsion (see figure 3.10). The first one, "Fz proportional distribution", used the total vertical force on the units' axles and distributed torque proportionally. By studying the results from the paper *Validation of high-fidelity simulation-based safe operating envelopes for articulated heavy vehicles using real test data* [2] it can be motivated that the most optimal torque distribution is in most cases to distribute the torque proportional to the vertical load on the axles for each unit. The paper is focused on braking, but this theory assumed that the same results were true for acceleration. This resulted in both vehicle units having equal friction utilisation at all times. See equations 3.3-3.5 for how the torques were distributed in propulsion.

$$T_{12,req} = F_{x,req,tot} \cdot r_1 \cdot \frac{F_{z,1}}{F_{z,1} + F_{z,2}} \quad (3.3)$$

$$T_{21,req} = F_{x,req,tot} \cdot r_2 \cdot \frac{F_{z,2}}{F_{z,1} + F_{z,2}} \quad (3.4)$$

$$T_{11,req} = T_{22,req} = T_{23,req} = 0 \quad (3.5)$$

where  $T_{ij,req}$  is the requested wheel-torque for axle  $j$  on vehicle unit  $i$ .  $r_i$  is the wheel radius for vehicle unit  $i$ .  $F_{z,i}$  is the sum of the vertical forces on all of the wheels on vehicle unit  $i$ .

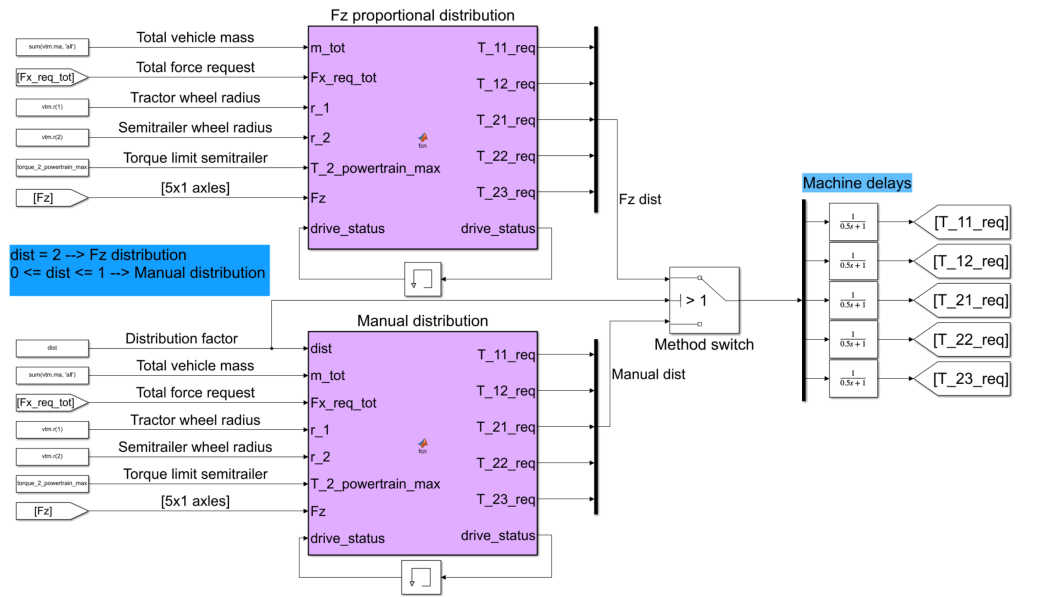


**Figure 3.10:** Type 4 controller torque allocation methods in Simulink

The second torque distribution strategy was to manually set the torque distribution as a percentage between the two units. The distribution was determined by a set distribution factor from 0 to 1 (0-100%), where 1 was only tractor propelling, and 0 was only semitrailer propelling. The torque request for the tractor's driven axle was determined by multiplying the total longitudinal force request by the distribution factor. The remaining force from the request was directed to the semitrailer's driven axle. See equations 3.6-3.8

$$T_{12,req} = F_{x,req,tot} \cdot r_1 \cdot dist \quad (3.6)$$

$$T_{21,req} = F_{x,req,tot} \cdot r_2 \cdot (1 - dist) \quad (3.7)$$

$$T_{11,req} = T_{22,req} = T_{23,req} = 0 \quad (3.8)$$

This method served two purposes. One was to test how the performance changed depending on the torque distribution to find the most optimal distribution method in different situations (see section 3.1.2). Another reason was to mimic a "turning knob" for the choice of torque distribution. This would allow the driver to adjust the torque distribution. For instance, they could prioritise depleting the battery on the semitrailer more quickly than on the tractor, or vice versa. This thesis will not go further in-depth into the controller strategy for the manual distribution and how it should cooperate with the "Fz proportional distribution". The value of the distribution variable ("dist") decides what method will be used.

Torque distribution for braking has also been modelled. However, as no heavy braking scenarios were analysed in the final comparison, different strategies for braking have not been studied in detail. As mentioned before, optimal braking is achieved when the brake force is distributed proportional to the vertical axle loads of each vehicle unit, according to [2]. Therefore, the total longitudinal force request was first split into a longitudinal force request for each unit according to equations 3.9 and 3.10. Note that the total longitudinal force request was negative for braking.

$$F_{x,1,req} = F_{x,req,tot} \cdot \frac{F_{z,1}}{F_{z,1} + F_{z,2}} \quad (3.9)$$

$$F_{x,2,req} = F_{x,req,tot} \cdot \frac{F_{z,2}}{F_{z,1} + F_{z,2}} \quad (3.10)$$

where  $F_{x,1,req}$  and  $F_{x,2,req}$  were the requested longitudinal forces for each unit.

A drive status variable (see figure 3.10) was used to define what driving mode the tractor currently was in and to add hysteresis when switching between the modes. The possible modes were "Propulsion", "Retardation" and "Braking". "Propulsion" meant that propulsive torques were applied to the driven axles. "Retardation" meant that the driven axles were braking by retarding with their motors. "Braking" meant that the brake force request for the tractor would not be achieved by only retardation, meaning that frictional service brakes had to be initiated in this mode.

The drive status variable worked both as an input and output to the functions, as it should stay in its current driving mode if nothing triggered it to switch to another mode. The drive status variable changed depending on the value of the longitudinal force request for the tractor ( $F_{x,1,req}$ ) and the thresholds are described in the following list:

- If  $F_{x,1,req} > 1000$  N  
→ **Enter mode: "Propulsion"**
- If  $F_{x,1,req} \leq -2000$  N and  $F_{x,1,req} \geq F_{x,1,ret,max} + 1000$  N  
→ **Enter mode: "Retardation"**
- If  $F_{x,1,req} \leq F_{x,1,ret,max}$   
→ **Enter mode: "Braking"**

where  $F_{x,1,ret,max} = m_{tot} \cdot a_{x,1,ret,max}$  was the maximum retardation force for the tractor, calculated from the maximum tractor retardation  $a_{x,1,ret,max} = -2.5m/s^2$ .

If the tractor was in the "Propulsion" mode, the torque request formulas from equations 3.3-3.5 or equations 3.6-3.8 were used, depending on the chosen distribution method. With the added hysteresis, there was a chance that the total longitudinal force request was negative, while the tractor still was considered to be in the "Propulsion" mode. Therefore the requested torques were set to 0 Nm for all of the axles if  $F_{x,req,tot} < 0$  N in the "Propulsion" mode. The requested torques were also set to 0 Nm if the total longitudinal force request was above 0 N while the tractor was in the "Retardation" mode.

The "Retardation" and "Braking" modes have been modelled the same for both of the type 4 distribution methods seen in figure 3.10. If the tractor was in the "Retardation" mode, the braking torques for each unit was only put on the driven axles, see equations 3.11-3.13.

$$T_{12,req} = F_{x,1,req} \cdot r_1 \quad (3.11)$$

$$T_{21,req} = F_{x,2,req} \cdot r_2 \quad (3.12)$$

$$T_{11,req} = T_{22,req} = T_{23,req} = 0 \quad (3.13)$$

For the type 4 communication level, the tractor was able to know when the semitrailer becomes torque-limited. Therefore, if the tractor still was in the "Retardation" mode when the brake torque request for the semitrailer became a larger negative value than the negative torque available in the semitrailer's electric engine ( $F_{x,2,req} \cdot r_2 < -T_{2,powertrain,max}$ ), the driven axle of the semitrailer would retard at its maximum rate, while the remaining force request was distributed equally to the service brakes on the second and the third axle of the semitrailer. See equations 3.14-3.17.

$$T_{11,req} = 0 \quad (3.14)$$

$$T_{12,req} = F_{x,1,req} \cdot r_1 \quad (3.15)$$

$$T_{21,req} = -T_{2,powertrain,max} \quad (3.16)$$

$$T_{22,req} = T_{23,req} = \frac{F_{x,2,req} \cdot r_2 - (-T_{2,powertrain,max})}{2} \quad (3.17)$$

For the "Braking" mode, the tractor's brake force request had surpassed the tractor's retardation threshold. In this case, the driven axle of the tractor would continue to

retard at its maximum capacity, while the remainder of the brake force request was fulfilled by the service brakes on the tractor's front axle. The semitrailer braked in the same manner as explained for the "Retardation" mode. It prioritised only retarding on its driven axle until it was limited by its max possible retardation torque, and then the semitrailer's two undriven axles braked with their service brakes to fulfil the brake force request. See equations 3.18-3.21 for the case when the brake force request for both units exceeds each unit's possible retardation torque.

$$T_{11,req} = (F_{x,1,req} - F_{x,1,ret,max}) \cdot r_1 \quad (3.18)$$

$$T_{12,req} = T_{1,powertrain,max} = F_{x,1,ret,max} \cdot r_1 = m_{tot} \cdot a_{x,1,ret,max} \cdot r_1 \quad (3.19)$$

$$T_{21,req} = -T_{2,powertrain,max} \quad (3.20)$$

$$T_{22,req} = T_{23,req} = \frac{F_{x,2,req} \cdot r_2 - (-T_{2,powertrain,max})}{2} \quad (3.21)$$

where  $T_{2,powertrain,max}$  is the torque limit of the E-semitrailer's electric motor, defined as a positive torque. The motor can retard with the same torque magnitude.

To summarize, the braking strategy started with allocating the requested braking force for each unit proportional to the vertical loads that they were carrying. Each unit then prioritised to brake by retarding with their driven axles. If the brake force request for each unit surpassed its retardation force limit, the service brakes on the non-driven wheels fulfilled the total brake force request. At some point, the driven axles would also have to start braking with their service brakes given a very high brake force request. But as heavy braking manoeuvres were not to be regarded in this thesis, the brake blending between engine retardation and service brakes was not modelled. This meant that the driven axles only braked with their maximum retardation capability at most.

The Matlab function script used for the type 4 controller's "Fz proportional distribution" method can be seen in appendix A.1.

Delays were added to the requested torques, by using the low pass filter in equation 3.22. It has a time constant of 0.5 seconds. The transfer function was supposed to model the real-life delay from requested torque to actual torque output due to machine delays. For simplicity, it was assumed to be the same value for both propulsion and braking, no matter the machinery being used. In reality, the time constant for an electric machine is different to the time constant for mechanical service brakes.

$$G_{torquedelay}(s) = \frac{1}{0.5s + 1} \quad (3.22)$$

### 3.2.3 Traction controller, torque limiter and power limiter

Regarding longitudinal vehicle manoeuvres, the plant model only required torque input values for all of the wheels in the vehicle combination to be simulateable. This meant that it did not consist of any kind of traction controller or powertrain limitations that would further limit the inputted wheel-torques. These kinds of functions therefore had to be created in the torque controller Simulink block before the torques were transmitted to the plant model.

Figure 3.11 shows the subsystem in Simulink that consists of traction controllers for all of the axles and torque limiters due to the powertrains' torque and power limits for the driven axles. Note that it was modelled per axle and not per wheel.

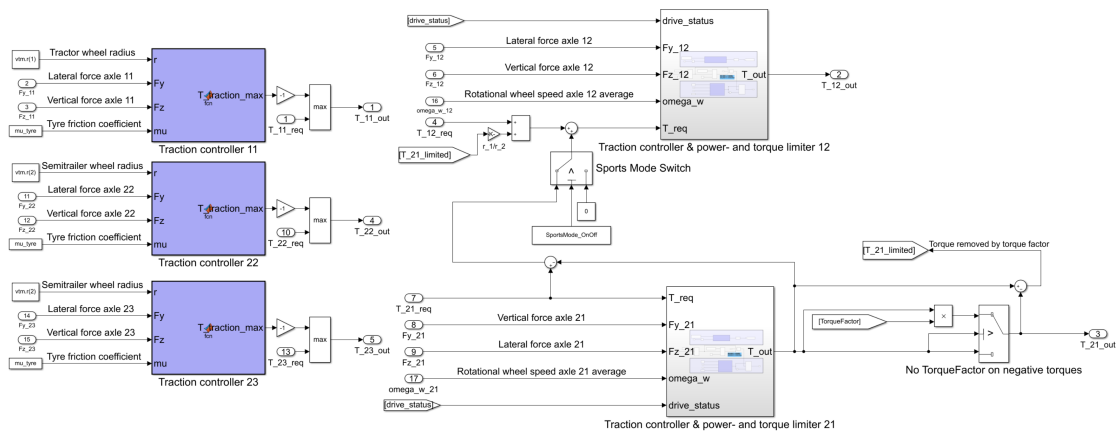


**Figure 3.11:** Type 4 traction control, power limitation and torque limitation

Traction controllers existed to make sure the force did not exceed the traction limit depending on the normal load and the friction coefficient. In this thesis, they were modelled as ideal traction controllers. As all of the models were using the same traction controller logic, it was at this stage assumed that the realism of the traction controller would not impact the results in a major way and make a fair comparison.

The ideal traction controllers assumed that the friction coefficient is known and could therefore use the friction circle to make sure the output torque never exceeded the maximum available torque due to friction, according to equation 3.23 (from equation 2.41 in Bengt Jacobson's compendium [3], rewritten to maximum torque instead of maximum longitudinal force).

$$T_{ij,traction,max} = \sqrt{(\mu_{tyre} \cdot F_{z,ij})^2 \cdot r_i^2 - F_{y,ij}^2 \cdot r_i^2} \quad (3.23)$$

where  $T_{ij,traction,max}$  is the maximum torque that can currently be applied to axle  $j$  on vehicle unit  $i$  to avoid wheel slipping.  $\mu_{tyre} = 0.9 \cdot \mu_{road}$ , is the friction coefficient that the tyres utilise.  $F_{z,ij}$  and  $F_{y,ij}$  are the sum of the vertical forces and the sum of the lateral forces on the wheels for axle  $j$  on vehicle unit  $i$ , respectively.  $r_i$  is the wheel radius on vehicle unit  $i$ .

### 3. Controller modelling

The traction controller was used for all the axles as it was used for both propulsion and braking. Equation 3.24 describes how the traction limit value was used to limit the torque both positively and negatively.

$$T_{ij,out} = \max(\min(T_{ij,req}, T_{ij,traction,max}), -T_{ij,traction,max}) \quad (3.24)$$

where  $T_{ij,out}$  is the output torque for axle  $j$  on vehicle unit  $i$ .

The driven axles needed to be limited by their respective powertrain's available torque and available power. Each driven axle required a separate Simulink subsystem to account for this. Figure 3.12 shows the subsystem in Simulink that limited the torque of the tractor's driven axle. The subsystem for the semitrailer's driven axle was modelled the same except for using the relevant powertrain parameters.

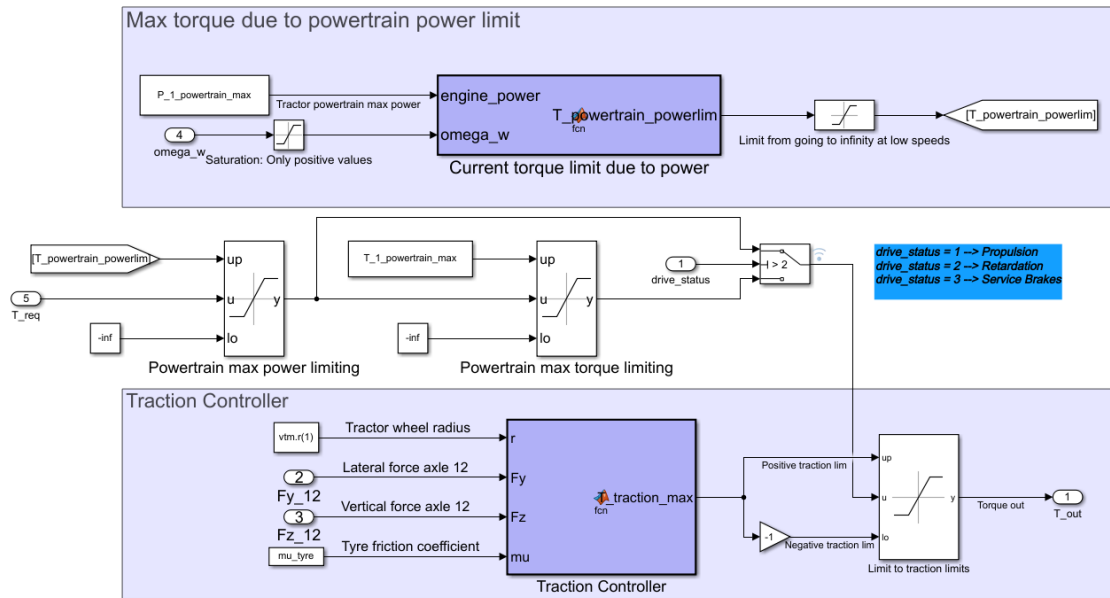


**Figure 3.12:** Type 4 Simulink subsystem: Traction controller & power- and torque-limiter 12

First the maximum available torque due to power was calculated according to equation 3.25.

$$T_{powertrain,powerlim} = \frac{P_{i,powertrain,max}}{\omega_{w,ij}} \quad (3.25)$$

where  $P_{i,powertrain,max}$  is the power of the engine for vehicle unit  $i$  and  $\omega_{w,ij}$  is the average rotational velocity of the wheels on axle  $j$  on vehicle unit  $i$ . The torque request for the driven axle was only limited by the value of  $T_{powertrain,powerlim}$  for positive torque request values.

Then, the drive status variable (explained in section 3.2.2) was used to decide whether the axle torque request should be limited by the powertrain's torque limit or not. If the tractor was in either the "Propulsion" or the "Retardation" mode, the tractor's torque was only positively limited by the available torque in its powertrain. The tractor's torque was not negatively limited by the powertrain's available torque, because that was accounted for in the torque allocation blocks earlier. However, the semitrailer's torque was limited both positively and negatively by the powertrain's maximum torque (not seen in the figure), because the semitrailer's driven axle can not retard with a larger value than the electric motor's maximum torque value. If the tractor was in the "Braking" mode, the torque request signal bypassed the torque limiter because the service brakes were assumed to have infinite negative torque.

The already power and sometimes torque-limited signal was then passed through the traction controller, which worked exactly like the traction controllers already described by equations 3.23 and 3.24.

The subsystems for torque limiting of the driven axles were modelled in a very general manner. In this thesis, the braking for all controllers was designed to avoid using the service brakes on the driven axles, meaning some of the logic to limit the negative torque had no effect.

In figure 3.11, two other functions that redistribute propulsive torque between the tractor and semitrailer can be seen. The first one was a switch which allowed the user to activate a "sport mode". The sport mode checked whether the output torque matched the requested input torque on the semitrailer. If it did not have enough output torque due to traction or powertrain limits, it sent the remaining torque as an addition to the torque request to the tractor. The reason for this was that the E-semitrailer would always reach its traction limit before the tractor. Since the driven axle for the tractor carried 11.6 tonnes of load, whilst the semitrailer's driven axle only carried 7.1 tonnes, the semitrailer usually reached the traction limit before the tractor.

This resulted in there being no reason to make a function to transfer torque from the tractor to the semitrailer. The use of this function made the vehicle's distribution strategy differentiate from the more optimal vertical force proportional distribution in exchange for more longitudinal force. This gave the vehicle a higher longitudinal acceleration if possible, at the cost of stability.

The second function reduced the semitrailer's torque depending on the "Torque Factor" that was explained in section 3.1.3. For positive torque (propulsion), the semitrailer's torque was reduced depending on the articulation angle. The reduced torque was redistributed to the tractor's torque request on its driven axle.

### 3. Controller modelling

In the end, the actual torques for each wheel were determined by dividing the limited requested axle torques by two. This can be seen in figure 3.13. This meant that the models in this thesis always output equal torque for both wheels on the same axle.

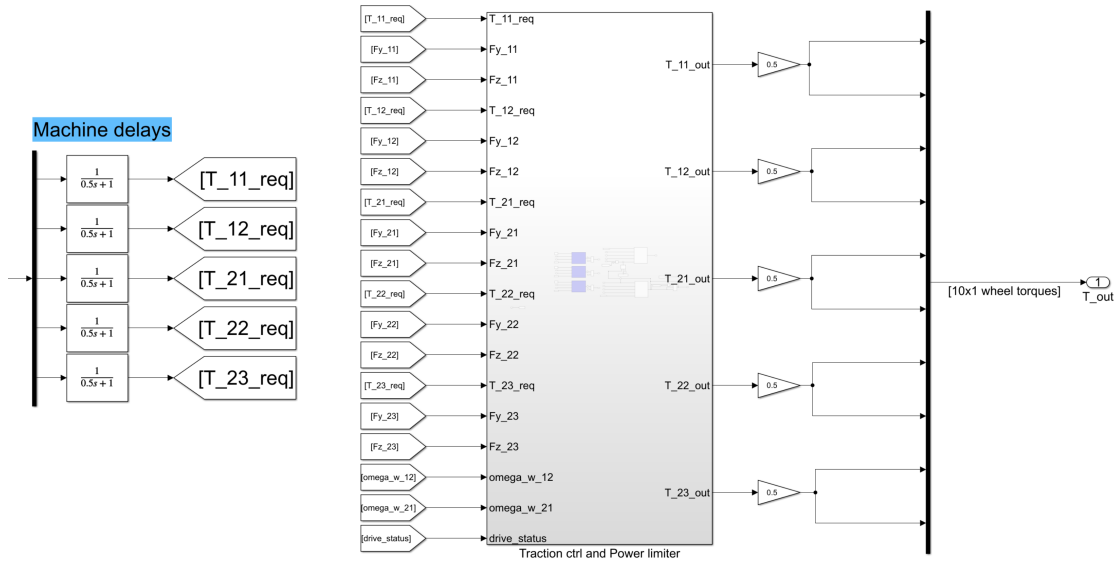


**Figure 3.13:** Type 4 Simulink architecture: Subsystem for limiting allocated torque and output of actual wheel-torques to the plant model

### 3.2.4 Type 3 torque controllers

This subsection will describe the logic of how torque is distributed between a tractor and E-semitrailer for the type 3 level communication. As mentioned in section 2.1, the type 3 communication was divided into "Type 3" and "Type 3 Light", where the first one had a coupling force sensor and an articulation angle sensor, whereas the second one did not have these sensors. Two methods of propulsion were generated for the "Type 3", and thus it was also divided into the controllers "Type 3.1" and "Type 3.2". Consequently, there are 3 different controllers explained in this section: "Type 3.1", "Type 3.2" and "Type 3 Light".

In the Simulink model for the type 3 level communication controllers, there was one torque control block for the tractor, and one torque control block for the semitrailer, see figure 3.2. A type 3 level communication E-semitrailer should be compatible with standard tractors, meaning the tractor does not need to be aware that it is connected to an E-semitrailer. The logic for the tractor torque control Simulink block therefore remained the same for all type 3 controllers. This subsection will first describe the tractor torque controller, followed by explanations of the E-semitrailer torque controllers for each of the defined type 3 controllers.

#### 3.2.4.1 Type 3 tractor torque allocation

Figure 3.14 shows the torque allocation part of the type 3 tractor's torque controller subsystem in Simulink. Its inputs were the total longitudinal force request created by the speed controller, the mass of the total vehicle combination (assumed to be measurable at a standstill), the tractor wheel radius and the dynamic vertical axle loads of all of the vehicle's axles. In reality, the tractor will not have any dynamic information about the axle loads of the semitrailer, but it was only used to calculate the braking forces proportional to the axle loads. This is done pneumatically in real life, and therefore it was simplified in the model by assuming that the tractor could dynamically read the semitrailer's axle loads for braking calculations.

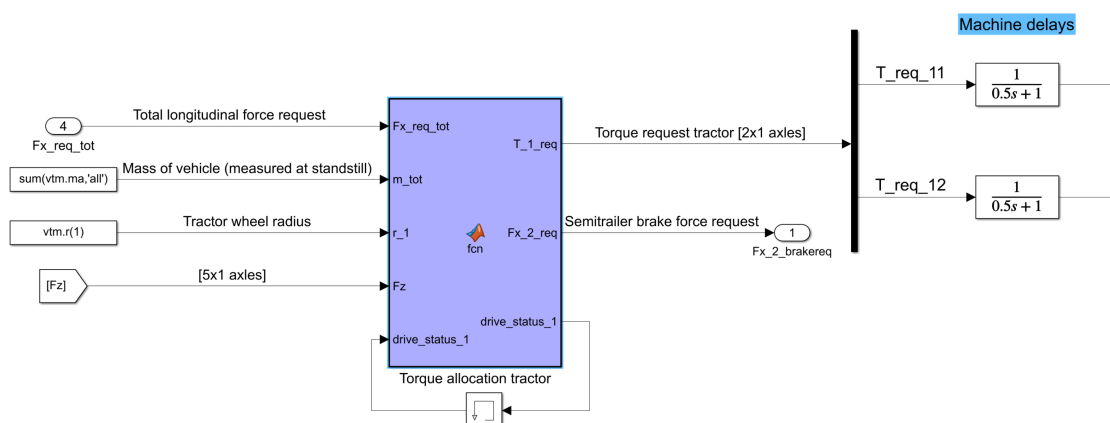


**Figure 3.14:** Matlab function in Simulink: Type 3 tractor torque allocation

The first thing the function did was to distribute the total longitudinal force request proportional to the axle loads of each unit [2], according to previously mentioned equations 3.9 and 3.10. Exactly as for the type 4 controllers, a drive status variable specific to the tractor ("drive\_status\_1" in figure 3.14) was defined. It had the same three modes "Propulsion", "Retardation" and "Braking", but the thresholds were different compared to the thresholds that the drive status variable for the type 4 controllers used. The thresholds are described in the following list:

- If  $F_{x,req,tot} > 1000$  N  
→ **Enter mode: "Propulsion"**
- If  $F_{x,1,req} \leq -10000$  N and  $F_{x,1,req} \geq F_{x,1,ret,max} + 1000$  N  
→ **Enter mode: "Retardation"**
- If  $F_{x,1,req} < F_{x,1,ret,max}$   
→ **Enter mode: "Braking"**

where  $F_{x,1,ret,max} = m_{tot} \cdot a_{x,1,ret,max}$  is the maximum retardation force for the tractor, calculated from the maximum tractor retardation  $a_{x,1,ret,max} = -2.5$  m/s<sup>2</sup>. The main difference for the new thresholds was the larger negative force required to enter the "Retardation" mode. This added hysteresis was needed for the stability of the controllers.

In each mode, a longitudinal force request was output to the semitrailer torque control block ( $F_{x,2,req}$  in figure 3.14). This force request was intended to emulate the brake request that the tractor could always transmit to semitrailer. In this model, it was assumed that the semitrailer torque controller would receive the brake force request signal from the tractor and independently determine how the torques should be distributed.

If the tractor was in the "Propulsion" mode and the total longitudinal force request was zero or a positive value ( $F_{x,req,tot} \geq 0$  Nm), the full request was applied on the tractor's driven axle, as the tractor always assumed it should propel the mass of the entire vehicle combination. The semitrailer longitudinal force request was put to 0 N as no brake request was transmitted to the semitrailer in the "Propulsion" mode. See equations 3.26-3.28.

$$T_{11,req} = 0 \tag{3.26}$$

$$T_{12,req} = F_{x,req,tot} \cdot r_1 \tag{3.27}$$

$$F_{x,2,req} = 0 \tag{3.28}$$

If the tractor was in the "Retardation" mode and the total longitudinal force request was a negative value ( $F_{x,req,tot} < 0$  Nm), the driven axle of the tractor retarded with

the tractor's current longitudinal force request while the semitrailer's longitudinal force request was transmitted to the semitrailer. See equations 3.29-3.31.

$$T_{11,req} = 0 \quad (3.29)$$

$$T_{12,req} = F_{x,1,req} \cdot r_1 = F_{x,req,tot} \cdot \frac{F_{z,1}}{F_{z,1} + F_{z,2}} \cdot r_1 \quad (3.30)$$

$$F_{x,2,req} = F_{x,req,tot} \cdot \frac{F_{z,2}}{F_{z,1} + F_{z,2}} \quad (3.31)$$

The torque requests for the tractor's axles and the brake force request for the semitrailer were put to 0 Nm and 0 N, respectively, if the total longitudinal force request was a positive value in the "Retardation" mode or a negative value in the "Propulsion" mode.

If the tractor was in the "Braking" mode, the driven axle of the tractor retarded with its maximum retardation force, while the remainder of the force request was fulfilled by the service brakes on its undriven axle. The semitrailer's longitudinal force request was transmitted to the semitrailer. See equations 3.32-3.34.

$$T_{11,req} = (F_{x,1,req} - F_{x,1,ret,max}) \cdot r_1 = ((F_{x,req,tot} \cdot \frac{F_{z,1}}{F_{z,1} + F_{z,2}}) - F_{x,1,ret,max}) \cdot r_1 \quad (3.32)$$

$$T_{12,req} = T_{1,powertrain,max} = F_{x,1,ret,max} \cdot r_1 = m_{tot} \cdot a_{x,1,ret,max} \cdot r_1 \quad (3.33)$$

$$F_{x,2,req} = F_{x,req,tot} \cdot \frac{F_{z,2}}{F_{z,1} + F_{z,2}} \quad (3.34)$$

The requested torques for the tractor's axles then followed the same Simulink chain as described for the type 4 controllers. They were delayed by a lowpass filter (equation 3.22), and then they were limited exactly as the torques were limited for the type 4 controller, described in subsection 3.2.3.

The Matlab function script used for the type 3 tractor torque allocation can be seen in appendix A.2.

### 3.2.4.2 Type 3.1 semitrailer torque allocation

By using the coupling force sensor to measure the vertical and longitudinal force in the coupling, the proportion between these two forces could be used to determine the optimal amount of propulsive force for the semitrailer. The formula to calculate the propelling force is seen in equation 3.35

$$F_{x,21,req} = \frac{F_{cx}}{F_{cz}} F_{z,2} \quad (3.35)$$

### 3. Controller modelling

where  $F_{cx}$  is the longitudinal coupling force,  $F_{cz}$  is the vertical coupling force,  $F_{z,2}$  is the total vertical force on the semitrailer's axles and  $F_{x,21,req}$  is the requested longitudinal force on the semitrailer's driven axle. This allowed the vehicle combination to have the same friction utilisation on the driven axles, without knowing the current propulsion force on the tractor.

Figure 3.15 shows how the type 3.1 semitrailer torque allocator was implemented in the subsystem "semitrailer torque controller" in Simulink. The longitudinal and vertical coupling force inputs were low pass filtered with a time constant of 1 second and then the signals were delayed by 0.3 seconds. This was done to model how a sensor would output a signal in real life. The longitudinal coupling force was also saturated to only positive values, as a positive coupling force implied tension in the coupling. The E-semitrailer should only propel when the tractor was "pulling" the E-semitrailer.

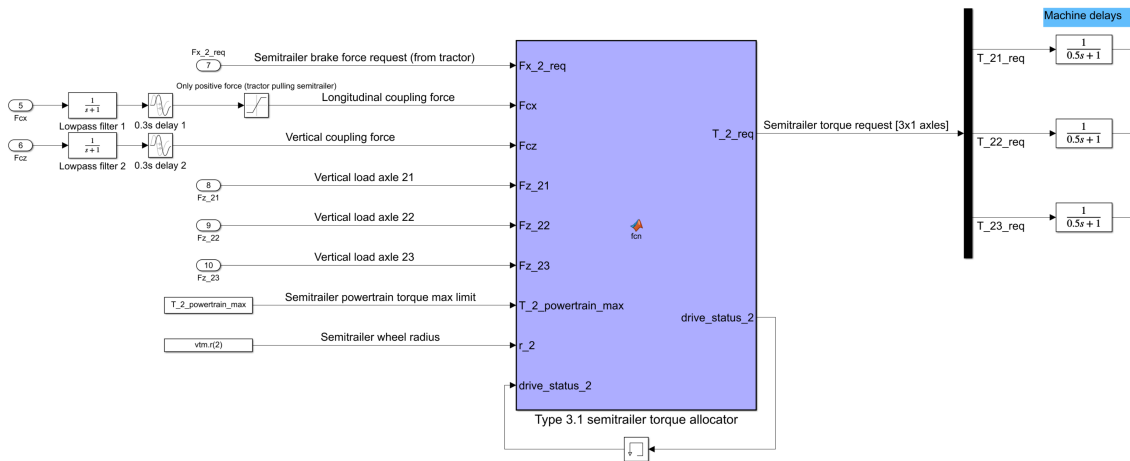


**Figure 3.15:** Matlab function in Simulink: Type 3.1 semitrailer torque allocator

The semitrailer torque allocator used another drive status variable that was separate from the tractor's drive status variable. It contained the same driving modes and their thresholds are described in the following list:

- If  $F_{x,2,req} \geq 0$  N and  $F_{x,prop,req} \geq 2000$  N  
→ **Enter mode: "Propulsion"**
- If  $F_{x,2,req} \leq -10000$  N and  $F_{x,2,req} \geq F_{x,2,ret,max} + 100$  N  
→ **Enter mode: "Retardation"**
- If  $F_{x,1,req} < F_{x,2,ret,max}$   
→ **Enter mode: "Braking"**

where  $F_{x,2,ret,max} = -T_{2,powertrain,max}/r_2$  is the maximum retardation force for the

semitrailer and  $F_{x,prop,req} = F_{z,2} \cdot (F_{cx}/F_{cz})$  is the calculated force the semitrailer should propel with according to equation 3.35.

If the semitrailer was in the "Propulsion" mode and  $F_{x,prop,req} > 0$ , the requested wheel-torques were set according to equations 3.36 and 3.37

$$T_{21,req} = F_{x,prop,req} \cdot r_2 = (F_{z,2} \cdot \frac{F_{cx}}{F_{cz}}) \cdot r_2 \quad (3.36)$$

$$T_{22,req} = T_{23,req} = 0 \quad (3.37)$$

If the semitrailer was in the "Retardation" mode and  $F_{x,2,req} < 0$ , the driven axle retarded with the semitrailer brake force request received from the tractor. See equations 3.38 and 3.39.

$$T_{21,req} = F_{x,2,req} \cdot r_2 \quad (3.38)$$

$$T_{22,req} = T_{23,req} = 0 \quad (3.39)$$

For the opposite cases, when the semitrailer was in the "Propulsion" mode and  $F_{x,prop,req} < 0$  or when the semitrailer was in "Retardation" mode and  $F_{x,2,req} > 0$ , all the axle torque requests were set to 0 Nm.

If the semitrailer was in the "Braking" mode, the brake force request received from the tractor was larger than the retarding capability of the semitrailer. The service brakes on the undriven axles of the semitrailer split equally on the remaining part of the brake force request that the driven axle could not fulfil. See equations 3.40 and 3.41.

$$T_{21,req} = F_{x,2,ret,max} \cdot r_2 = -T_{2,powertrain,max} \quad (3.40)$$

$$T_{22,req} = T_{23,req} = \left( \frac{F_{x,2,req} - F_{x,2,ret,max}}{2} \right) \cdot r_2 \quad (3.41)$$

The requested torques for the semitrailer's axles were delayed by the lowpass filter described by equation 3.22 and then they were limited in the same way as described in section 3.2.3. The limiting logic depended on whether the axle was driven or not. Finally, the "torque factor" function reduced the torque on the driven axle depending on the articulation angle. The difference to the type 4 controller's "torque factor" function, however, was that it could not redistribute the reduced torque to the tractor again. This meant that there was an overall torque reduction when cornering, which a real-life driver could manually account for by pressing the acceleration pedal more if necessary.

The Matlab function script for the type 3.1 semitrailer torque allocator can be seen in appendix A.3

### 3.2.4.3 Type 3.2 semitrailer torque allocation

The type 3.2 E-semitrailer was the same E-semitrailer as the type 3.1, but it used another formula to determine the propulsion force. The logic for the type 3.2 controller was to aim for 0 N longitudinal coupling force. See equation 3.42.

$$F_{x,21,req} = -F_{cx,error} = -(F_{cx,ref} - F_{cx}) = -(0 - F_{cx}) \quad (3.42)$$

where  $F_{cx,error}$  is the error between a reference value for the longitudinal coupling force ( $F_{cx,ref}$ ) and the current value of the longitudinal coupling force.

The hypothesis was that the E-semitrailer would propel in such a way that there would be no longitudinal force in the coupling. This was not the case for a dynamic system. Tests showed that the actual propulsion force became approximately half of what the coupling force would have been with a non-driven semitrailer, and the coupling force error did not reach 0 N.

Figure 3.16 shows a conceptual example where the semitrailer's propulsion was switched off until 0.5 seconds. Before 0.5 seconds, the longitudinal coupling force was 20 kN, but as the semitrailer propulsion was switched on, the forces met at half of the original coupling force. The propulsion force could not be increased infinitely fast and the error decreased during the propulsion increase. In the example figure, the coupling force stabilised at 10 kN, and the E-semitrailer propelled with the same force. The defined formula for propulsion held true, but it never reached zero longitudinal coupling force and could never do so, as the longitudinal coupling force and the E-semitrailer's propulsion force depended on each other.

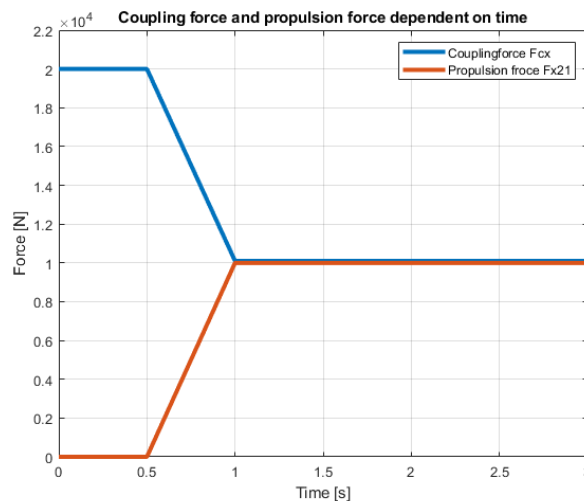


**Figure 3.16:** Visualisation of the type 3.2 e-trailers propulsion logic

Using a PID controller on the error between the longitudinal coupling force and the reference value 0 N could let the error go to zero. However, when experimenting with using a PID controller, the vehicle combination became extremely unstable. It was therefore decided to not use a PID-controller for this propulsion method, as it showed to be stable and propelled conservatively without it. Added hysteresis would likely have helped the PID-controller approach, as it was very hard to keep the longitudinal coupling force at exactly 0 N without creating an oscillatory behaviour.

Figure 3.17 shows how the type 3.2 semitrailer torque allocator was implemented in the subsystem "semitrailer torque controller" in Simulink. The longitudinal coupling force signal was filtered and delayed exactly as it was for the type 3.1 controller.

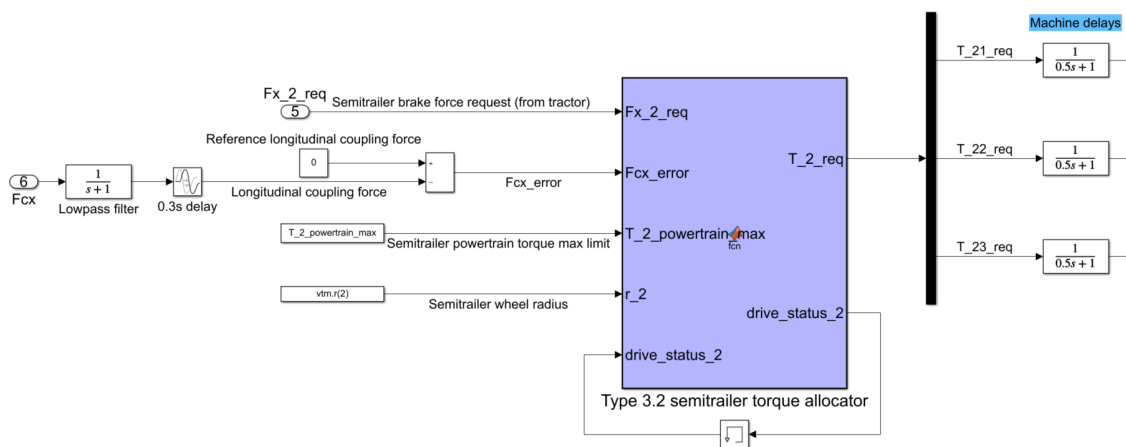


**Figure 3.17:** Matlab function in Simulink: Type 3.2 semitrailer torque allocator

The function also used a drive status variable with the same thresholds used for the type 3.1 controller. The only difference to the type 3.1 controller was the formula used to define the propulsive force put on the driven axle in the "Propulsion" mode. The Matlab function script for the type 3.2 torque allocator can be seen in appendix A.4

The requested torque outputs from the function were delayed due to machine delays and limited by traction and the E-semitrailer's powertrain's available power and torque, exactly as the type 3.1 controller was. The "Torque factor" function was also applied at the end of the chain in the same manner.

#### 3.2.4.4 Type 3 light semitrailer torque allocation

With the use of a wheel speed sensor, the longitudinal velocity could be found by multiplying the speed of a non-driven wheel on the semitrailer with the wheel radius (equation 3.43). The longitudinal wheel speed was assumed to be equal to the current longitudinal speed of the vehicle (equation 3.44). By calculating the derivative of the speed, the current acceleration was found (equation 3.45). Then the axle load sensors were used to find the axle forces, which were divided by the gravitational constant  $g$  to find the mass of the load on the semitrailer's axles



Figure 3.19 shows how the type 3 light semitrailer torque allocator was implemented in the subsystem "semitrailer torque controller" in Simulink. The sensor input was the average rotational velocity of the wheels on the undriven axle 22. It was converted to the longitudinal velocity of the axle by multiplication with the semitrailer's wheel radius. The signal was delayed by 0.3 seconds. Except for being an input to the function, it was also derivated to retrieve the longitudinal acceleration signal. The acceleration signal was processed by a lowpass filter with a time constant of 1 second, saturated to only positive values and finally put through a deadband that made the signal value 0 if it was of a smaller magnitude than  $0.01 \text{ m/s}^2$ .

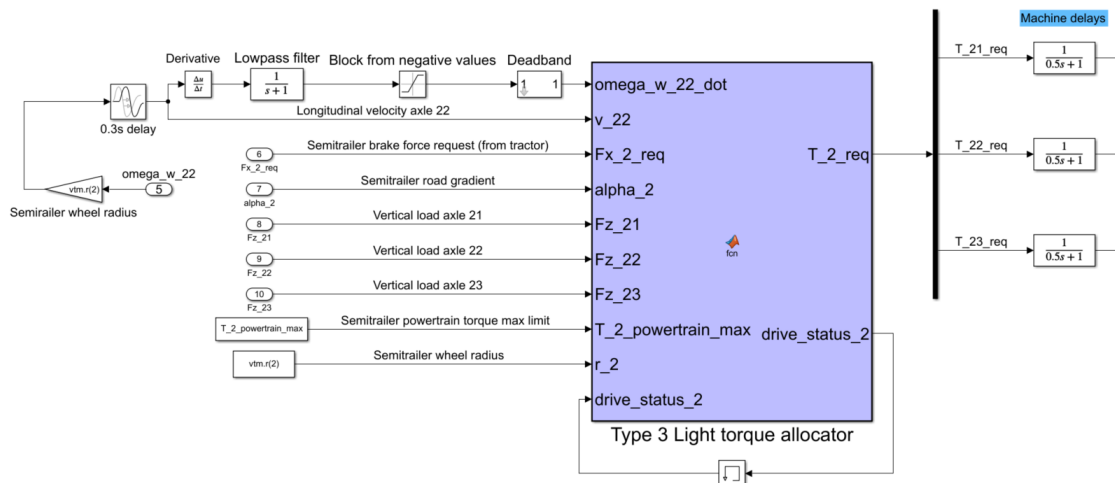


**Figure 3.19:** Matlab function in Simulink: Type 3.2 semitrailer torque allocator

The drive status variable was used with the same modes and thresholds as for the other type 3 controllers. The only difference was the formula used to calculate the requested propulsion force (equation 3.49). There was, however, no air resistance in VTM so that part was omitted in the Matlab function. For safety reasons, the rolling resistance compensation was only activated at speeds above 30 km/h, to not have a constant torque value applied at low speeds. The Matlab function script for the type 3 light torque allocator can be seen in appendix A.5

Exactly as for all of the other type 3 controllers, the requested axle torques were delayed and then limited due to available traction, power and powertrain torque. It also used the "Torque Factor" function to decrease the E-semitrailer's torque when cornering.

#### 3.2.4.4.1 Type 3 light instability testing

Since the type 3 light's torque output was based on the current acceleration and the semitrailer axle load, the system needed to be tested to ensure it would not create a self-induced acceleration and thereby keep increasing the torque request higher and higher. Especially in a potential situation where the sensor data from the axle load sensors could be false (due to a malfunction). To test what would

### 3. Controller modelling

happen if the torque controller senses a heavier axle load than in reality, the input for the vertical load was altered and simulated.

The test was done by removing the torque and power limit from the semitrailer (to ensure that these would not be the limiting factor). The tractor and semitrailer accelerated together for a certain time, and then all torque was cut off from the tractor, without sending any brake request to the semitrailer. See Figure 3.20.

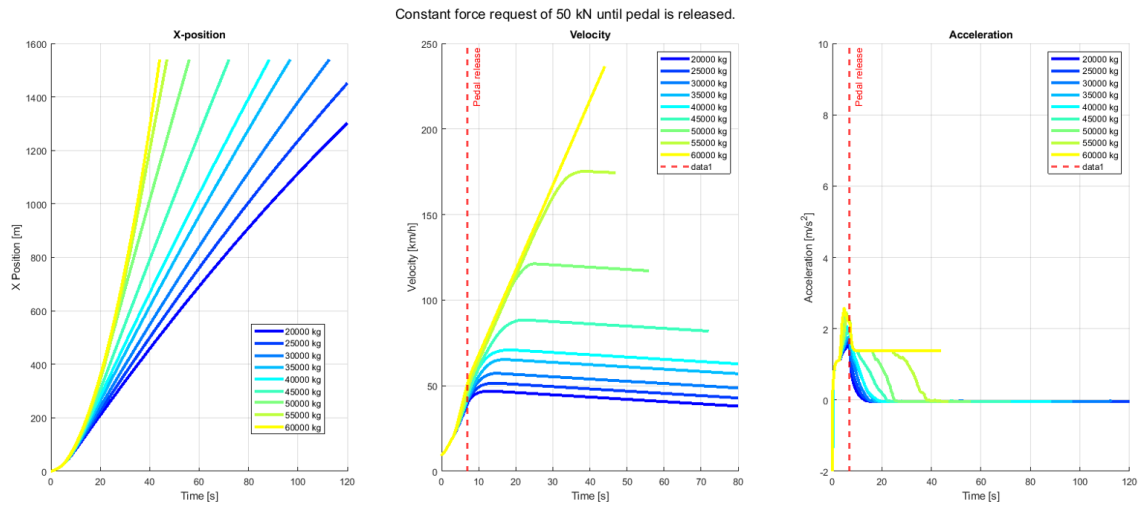


**Figure 3.20:** Type 3 light instability test - calculated acceleration signal. Plots of travelled distance, velocity and acceleration versus time.

This test used the calculated acceleration signal, from the derivative of the actual wheel speed signal (of the non-driven axle 22). It was then filtered to make the signal smoother. This resulted in a lower calculated acceleration than the real acceleration. It can be seen in figure 3.20 that the combination never stopped accelerating when  $m_{2,propelled}$  surpassed 60 000 kg, which was a larger value than the total vehicle combination's gross weight of roughly 40 000 kg.

A simplified free-body diagram was used to explain the behaviour of the system. See figure 3.21.

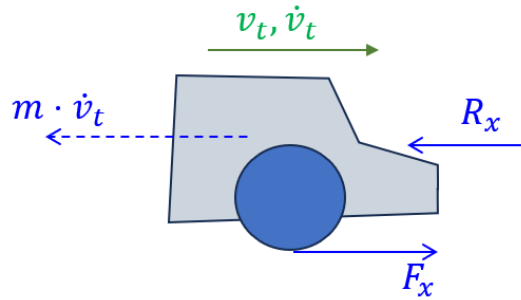


**Figure 3.21:** Type 3 light simplified free-body-diagram

The semitrailer was modelled as a vehicle with one wheel, a propulsion force  $F_x$  on the wheel and  $R_x$  were all the resistances acting on the semitrailer. The tractor pulling the semitrailer could also be seen as a resistance, but in the negative direction (to the right). Equations 3.50 and 3.51 describe the system.

$$m \cdot \dot{v}_t = F_x - R_x \quad (3.50)$$

$$F_x = k \cdot m \cdot \dot{v}_{t-1} \quad (3.51)$$

where  $m$  represents the gross weight of the entire vehicle combination and  $k$  serves as a scaling factor determining the force required based on the proportion of the vehicle combination's total weight that should be propelled.  $k = 0.5$  would mean that the semitrailer should propel for 50% of the vehicle combination's total weight.

The equations were solved for  $\dot{v}_t$ :

$$\dot{v}_t = k \cdot \dot{v}_{t-1} - \frac{R_x}{m} \quad (3.52)$$

From equation 3.52, it was seen that if  $k = 1$ , and resistances  $R_x = 0$  N, the acceleration request for the next timestep would be the same as the last. If there were any resistances, the acceleration would decrease and go towards zero.

As long as  $k < 1$ , the acceleration should decrease towards zero, if the resistance forces are not large enough. A steep downhill or the tractor pulling the semitrailer is seen as a resistance in the negative direction in this model, and will thereby increase the acceleration.

The controller in the type 3 light considered the slope, increasing (for uphill) or decreasing (for downhill) the torque request relative to the road gradient.

### 3. Controller modelling

To test if this model was correct, the actual acceleration was used as an input, instead of the derivated and filtered wheel speed that was used before to retrieve the acceleration for the propulsion formula.

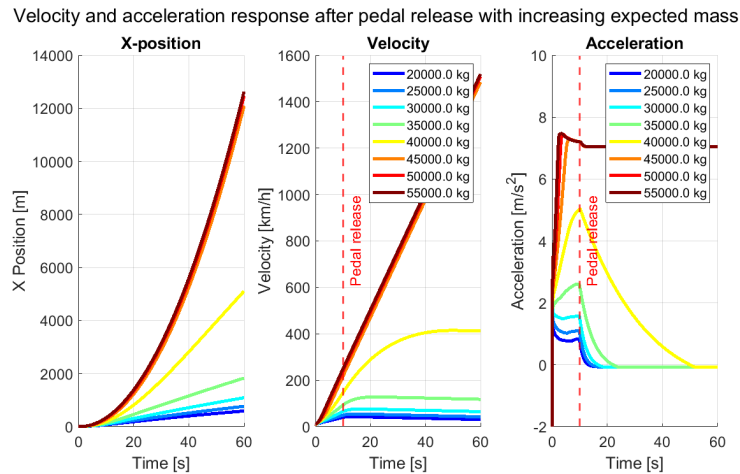


**Figure 3.22:** Type 3 light instability test - actual acceleration signal. Plots of travelled distance, velocity and acceleration versus time.

This test partially confirmed the hypothesis that propelling the semitrailer with a force greater than that required to accelerate the weight of the entire vehicle combination would result in the acceleration approaching infinity. The acceleration went towards zero for  $k < 1$ , but only stayed constant for  $k \geq 1$ . When  $k > 1$  it should have, according to the hypothesis, continued to increase its acceleration towards infinity (since the simulation environment did not have air resistance, which would have increased the resistances as the speed increased). The vehicle combination instead started to slip when the torque output increased. The torques can be seen in figure 3.23.

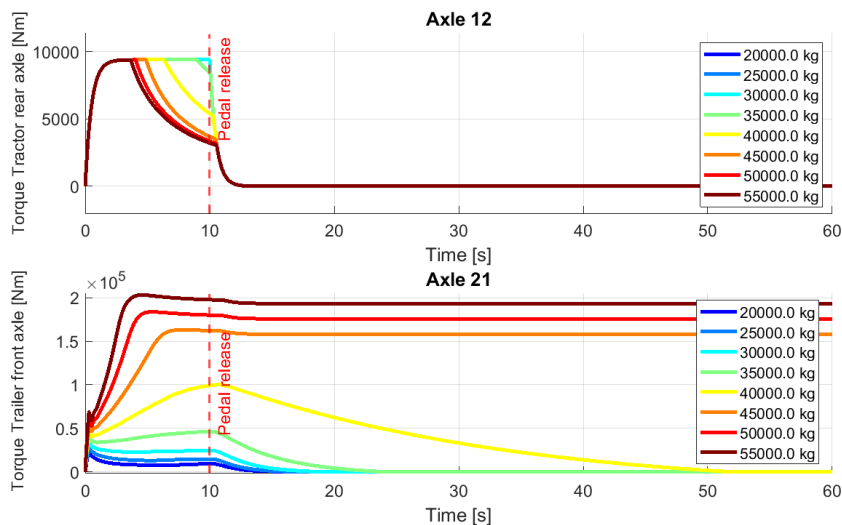


**Figure 3.23:** Type 3 light instability test. Plots of torque on driven axles

The torque output was higher for the simulations with higher  $k$ -value, but the acceleration did not increase. When the simulation was studied in detail, it was found that it started to slip instead of accelerating more, even though the ideal traction controller should not have allowed any slip.

Figure 3.24 shows a conceptual sketch of how the current time step's acceleration ( $\dot{v}_t$ ) depends on the resistance forces and the value of  $k$  based on equation 3.52. It shows different regions of how the system should react regarding the change in acceleration according to the equation. The sketch is specific to the when the last time step's acceleration  $\dot{v}_{t-1} = 1 \text{ m/s}^2$ . The sketch would look different for other values of  $\dot{v}_{t-1}$  as the value of the current timestep's acceleration depends on the last timestep's acceleration as well. The yellow line that splits the green and red region of the sketch should rotate around the point  $(k, R_x/m) = (1, 0)$  for different values of  $\dot{v}_{t-1}$ .

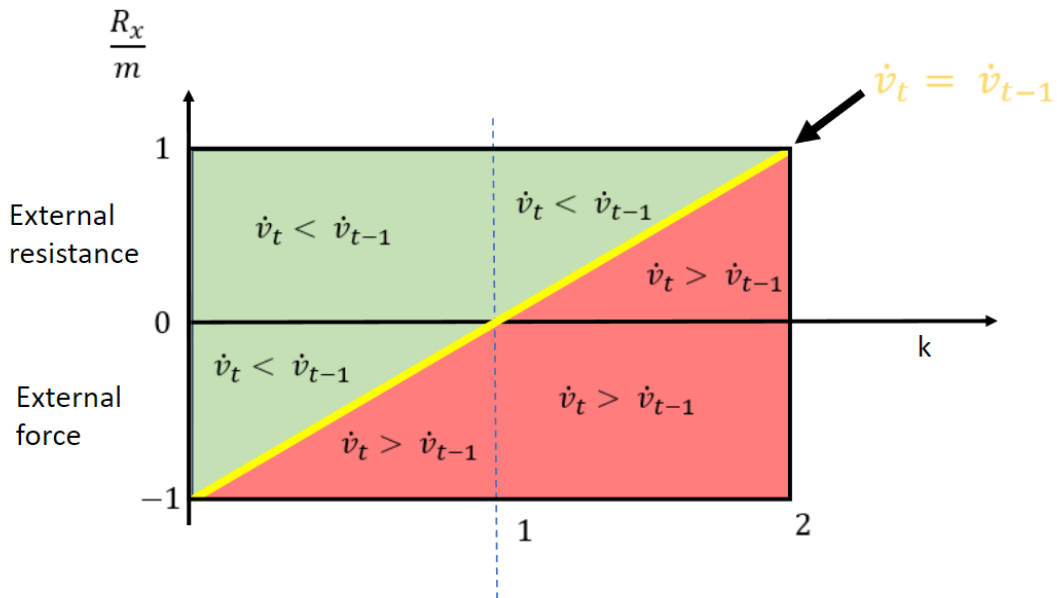


**Figure 3.24:** Type 3 light instability regions as a conceptual visualisation for  $\dot{v}_{t-1} = 1 \text{ m/s}^2$ . Red region: Acceleration approaches infinity. Green region: Acceleration decreases towards zero. Yellow line: Acceleration remains constant.

Due to time constraints in the project, this was not further studied. Since the type 3 light controller was based on the axle loads on the semitrailer,  $m_{2,propelled} = \frac{F_{z,2}}{g}$ , its propelled weight would always be lower than  $m$  (gross weight of entire vehicle combination). This resulted in a system where the acceleration always approached zero, as long as the resistances did not force it to accelerate.



# 4

## Final comparison of E-semitrailer controller algorithms

This chapter describes the simulations and simulation results from the tests considered to be the final comparison between the controllers. The final comparison consisted of 4 use cases that were either chosen directly from the list of use cases in table 2.3, or it was inspired by one of them.

1. Longitudinal performance test
2. Acceleration in intersection
3. Acceleration in intersection immediately after uphill
4. Acceleration in intersection immediately after downhill

These were the use cases that were believed to reveal the biggest differences between the controllers in terms of motion performance.

Subsection 4.1 describes the 6 different variants of controllers that were used in the simulations. The following subsections in this chapter detail the simulation setup for each test and present the corresponding results.

### 4.1 Simulation setup - tested controllers

This thesis compares 2 types of communication, but the modelling process resulted in 4 different variants of control methods. All of the simulations included all of the controllers, as well as a type 4 controller with the "sport mode" turned on and a "benchmark" truck which only has a propelled tractor that pulls a non-driven semitrailer. All controller variations and their communication type can be seen below:

- **Benchmark:**

A tractor and semitrailer where only the tractor is propelled with the same powertrain as the rest of the tractors, a 450 kW engine with a maximum torque of 56 000 Nm (transmission gear ratio included). This resulted in a weaker

vehicle combination, but it was used to compare the controllers developed in this thesis to a "standard" tractor and semitrailer combination.

- **Type 4:**

The type 4 has full communication to and from the semitrailer at all times. This allows it to know the state of the tractor at all times, as well as receiving a direct torque request from the driver. The torque distribution between the tractor and the semitrailer is based on the vertical load on the axles on the tractor and the semitrailer. The two units will propel with a force proportional to its axle load.

- **Type 4 sport:**

The type 4 sport has the same communication and torque distribution method as the type 4 with one added feature. When it reaches its torque limit on the semitrailer, it sends the request forward to the tractor, increasing the request on the tractors powertrain. From testing in simulation, its been confirmed that the semitrailer always reaches its limit first, and therefore this feature only needs to send torque request from the semitrailer to the tractor.

- **Type 3.1:**

The type 3.1 semitrailer has communication limited to the ISO 11992-2:2014 standard and is equipped with a coupling force sensor and an articulation angle sensor. The torque applied on the semitrailer is based on the vertical force compared to the longitudinal force in the coupling to achieve a vertical load proportional propulsion, as in the type 4 setup.

- **Type 3.2:**

The type 3.1 semitrailer has communication limited to the ISO 11992-2:2014 standard and is equipped with a coupling force sensor and an articulation angle sensor. The force applied on the semitrailers driven axle is equal to the longitudinal coupling force.

- **Type 3 light:**

The type 3 light semitrailer has communication limited to the ISO 11992-2:2014 standard and has no extra sensor equipped. The semitrailer is dependent only on the signals available in the ISO standard to decide the amount of torque it should apply. It applies torque based on the current velocity measurements as well as compensating for resisting forces, such as road gradient, air resistance and rolling resistance.

## 4.2 Sim 1: Longitudinal performance test

A Longitudinal Performance Test (LPT) was setup to see if there were any differences between the controllers in their traction capability and to compare how torque was applied on the driven axles when requesting a high acceleration. The test was done both for a flat and an uphill road, to reveal the influence of load transfer and grade resistance.

### 4.2.1 Sim 1 - Setup

Two models of a straight road were used for the tests. One was completely flat and the other was an uphill slope with a constant grade of 10%. For each road, the controllers were tested with a high, medium and low road friction coefficient. The truck was asked to drive at a slow constant speed, and then at a certain point, a very large acceleration request was demanded. The main performance metrics for the test were the time taken to reach a certain distance, and the time taken to reach a certain velocity. The distance and velocity depended on whether it was the flat or the uphill test. See table 4.1 for the complete test setup data. The total amount of simulations for this test was 36 (6 scenarios · 6 controllers).

**Table 4.1:** Setup for the longitudinal performance test

Test number	Road name	$\mu_{road}$ [-]	Initial requested velocity [km/h]	Race distance [m]	Race velocity [km/h]
1.1	Flat	0.9	1	400	80
1.2	Flat	0.6	1	400	80
1.3	Flat	0.3	1	400	80
1.4	Uphill	0.9	5	300	50
1.5	Uphill	0.6	5	300	50
1.6	Uphill	0.3	5	300	50

### 4.2.2 Sim 1 - Results

Tables 4.2-4.7 shows the numerical results from the LPT. The tables are sorted from the fastest to the slowest controller to finish the race distance.

It can be seen that the type 4 and the type 4 sport controllers were the fastest in all scenarios except for a low road friction coefficient in uphill driving. The benchmark truck was by far the slowest controller, due to it being the only combination propelling only on the tractor. In uphill driving, the benchmark did not manage to reach 50 km/h before the end of the track. In low road friction and uphill driving, none of the controllers managed to reach 50 km/h before the end of the track. Here, the benchmark did not even manage to start the race, as it could not drive in the 10% sloped uphill at such low road friction. According to the result, the general order of fastest to slowest controller seems to be:

#### 4. Final comparison of E-semitrailer controller algorithms

---

1. Type 4 Sport
2. Type 4
3. Type 3.1
4. Type 3.2/Type 3 Light
5. Benchmark

The difference between the type 4 and the type 4 sport, however, was insignificant. This happened because the tractor was already traction limited at the time when the semitrailer became limited and requested more torque from the tractor.

**Table 4.2:** LPT Result  
Flat road,  $\mu_{road} = 0.9$

Controller	400 m [s]	80 km/h [s]
Type 4 Sport	20.808	11.730
Type 4	20.811	11.729
Type 3.1	21.012	11.920
Type 3.2	22.326	14.516
Type 3 Light	22.433	15.051
Benchmark	26.939	26.071

**Table 4.3:** LPT Result  
Uphill road,  $\mu_{road} = 0.9$

Controller	300 m [s]	50 km/h [s]
Type 4 Sport	21.687	8.575
Type 4	21.688	8.576
Type 3.1	21.759	8.658
Type 3 Light	21.984	8.760
Type 3.2	24.368	12.765
Benchmark	34.513	N/A

**Table 4.4:** LPT Result  
Flat road,  $\mu_{road} = 0.6$

Controller	400 m [s]	80 km/h [s]
Type 4 Sport	21.312	12.300
Type 4	21.314	12.302
Type 3.1	21.676	12.655
Type 3 Light	23.033	15.219
Type 3.2	23.322	15.711
Benchmark	28.004	27.305

**Table 4.5:** LPT Result  
Uphill road,  $\mu_{road} = 0.6$

Controller	300 m [s]	50 km/h [s]
Type 4 Sport	22.528	9.631
Type 4	22.528	9.631
Type 3.1	22.710	9.834
Type 3 Light	23.164	10.179
Type 3.2	25.840	14.903
Benchmark	37.345	N/A

**Table 4.6:** LPT Result  
Flat road,  $\mu_{road} = 0.3$

Controller	400 m [s]	80 km/h [s]
Type 4	26.170	19.186
Type 4 Sport	26.172	19.184
Type 3.1	26.535	19.554
Type 3.2	27.546	21.275
Type 3 Light	27.566	21.527
Benchmark	33.957	35.290

**Table 4.7:** LPT Result  
Uphill road,  $\mu_{road} = 0.3$

Controller	300 m [s]	50 km/h [s]
Type 3.1	45.224	N/A
Type 3 Light	45.264	N/A
Type 4 Sport	45.556	N/A
Type 4	45.664	N/A
Type 3.2	50.991	N/A
Benchmark	N/A	N/A

Figures 4.1 and 4.2 show plots of the vehicle combinations' longitudinal states for the flat and uphill scenarios with  $\mu_{road} = 0.9$ . The graphs of type 4, type 4 sport and type 3.1 are on top of each other. It can be seen from both the numerical results and the graphs that the type 3 light controller narrowed the gap to the fastest controllers on the uphill road compared to the flat road. This is due to that it only accelerates with its estimated acceleration on a flat road, but on a slope, it gets a correct amount of slope compensation that will make it keep up with the others better.

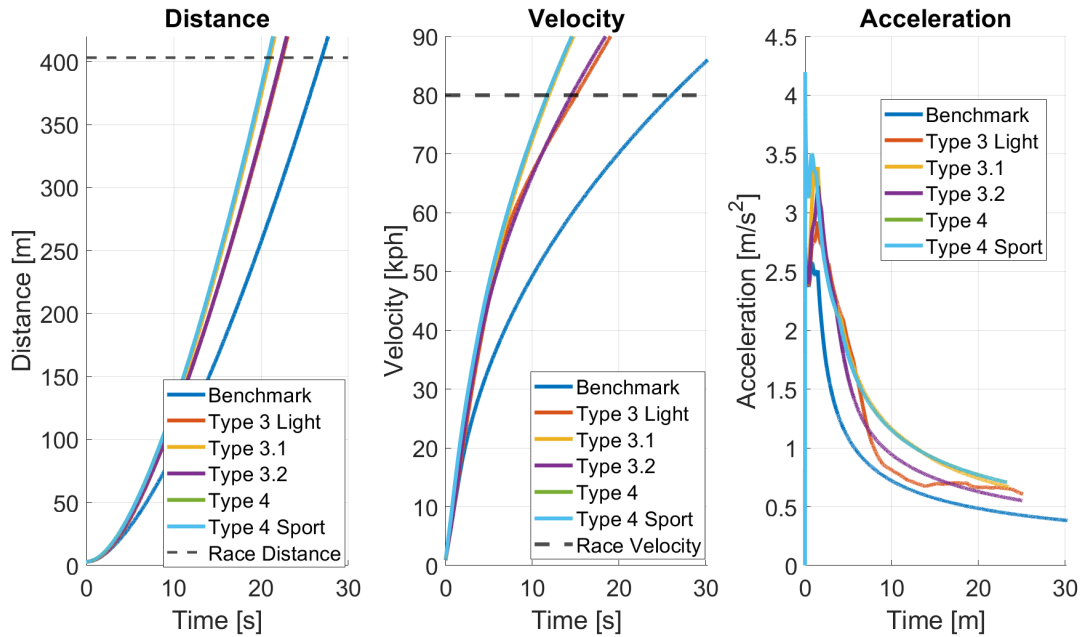


Figure 4.1: LPT - Longitudinal states, Flat road,  $\mu_{road} = 0.9$

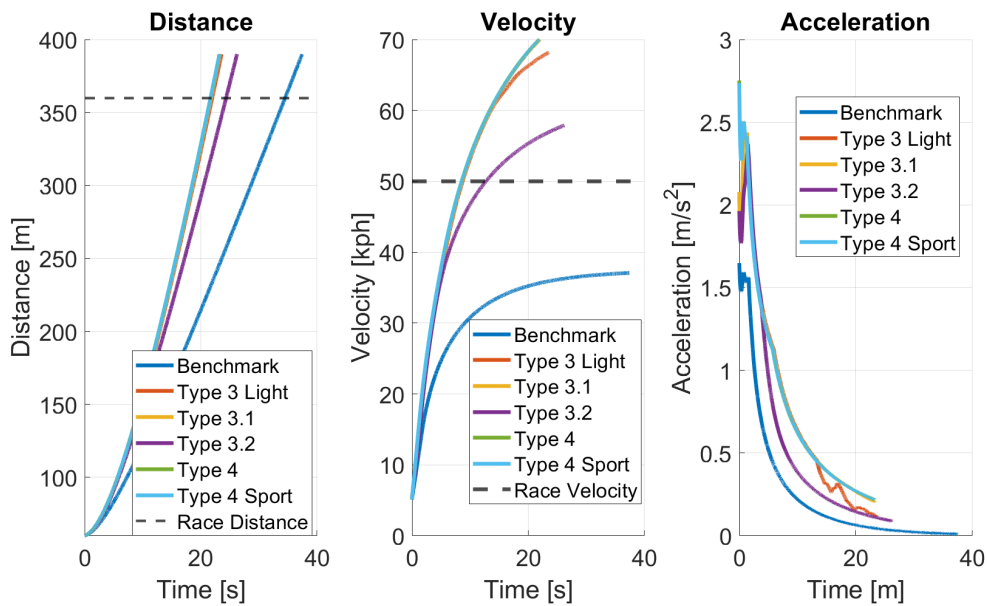
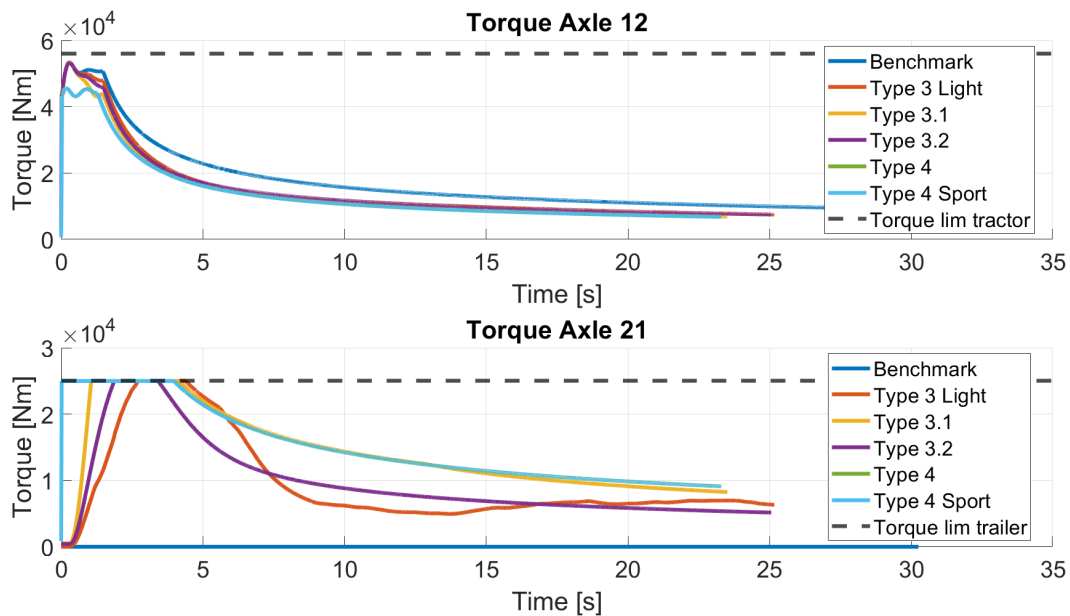


Figure 4.2: LPT - LPT - Longitudinal states, Uphill road,  $\mu_{road} = 0.9$

#### 4. Final comparison of E-semitrailer controller algorithms

Figures 4.3-4.6 shows plots of torque and power on the driven axles of each controller during the same event as in figures 4.1 and 4.2. The tractor became traction-limited in the beginning (the plateau in the torque graphs) and then became power-limited. There was a slight torque delay on the semitrailer on all of the type 3 controllers compared to the type 4 controllers. After the delay, the type 3.1 controller was able to output a similar torque as the type 4 controllers on the semitrailer



**Figure 4.3:** LPT - Torque on driven axles, Flat road,  $\mu_{road} = 0.9$

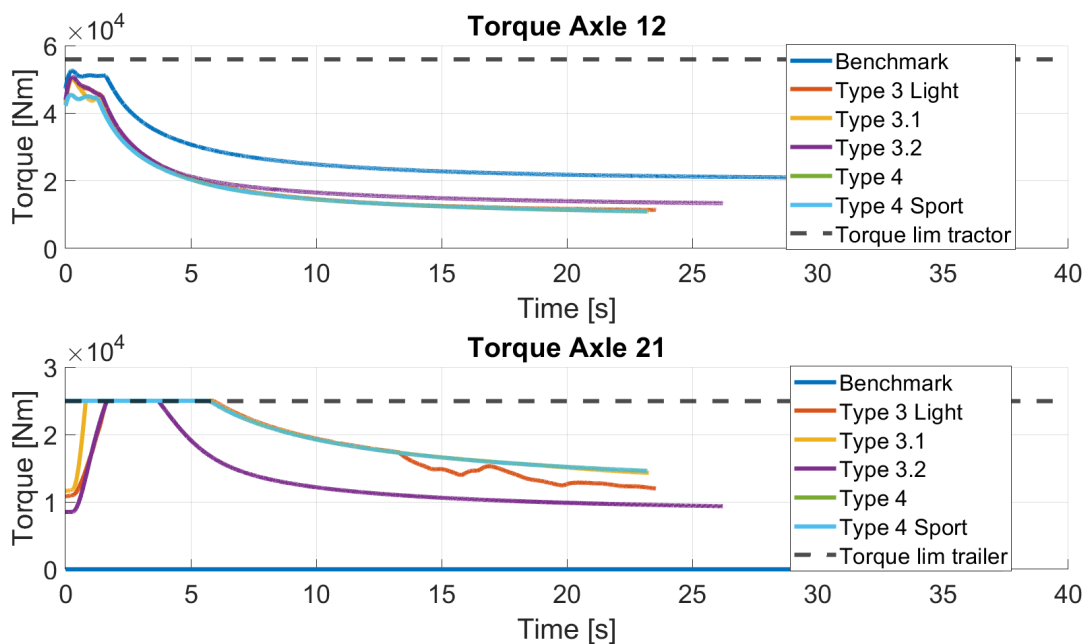


**Figure 4.4:** LPT - Torque on driven axles, Uphill road,  $\mu_{road} = 0.9$

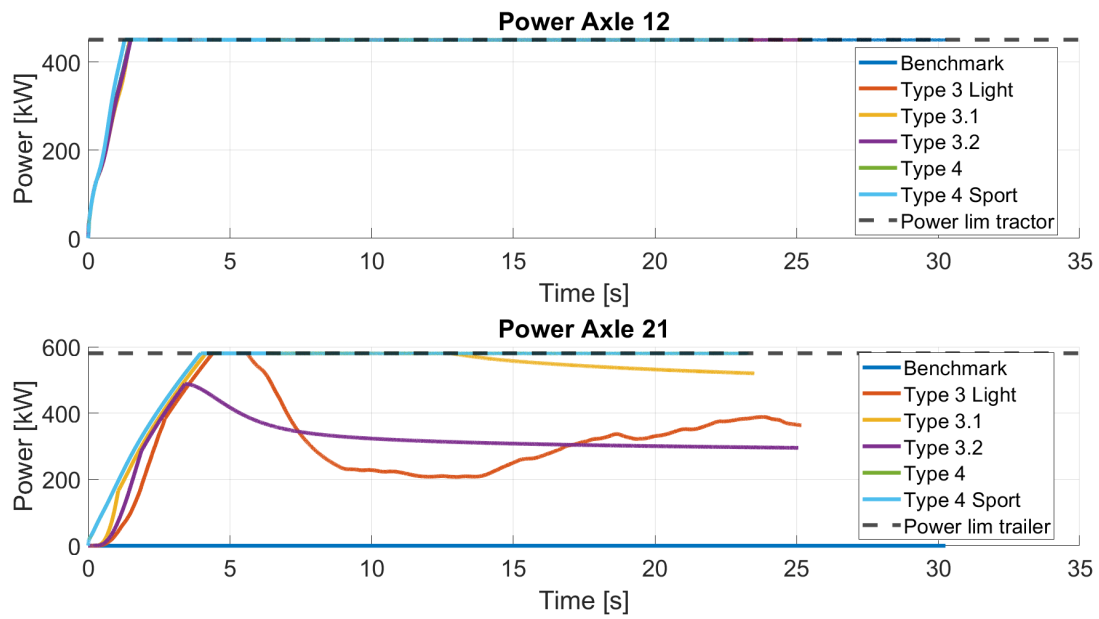


Figure 4.5: LPT - Power on driven axles, Flat road,  $\mu_{road} = 0.9$

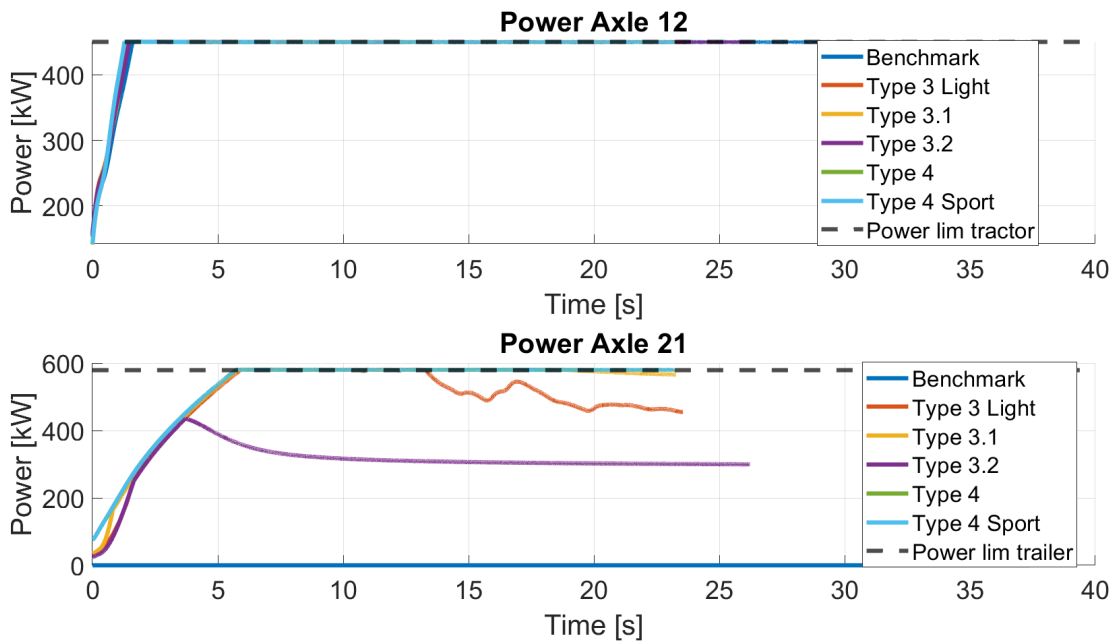


Figure 4.6: LPT - Power on driven axles, Uphill road,  $\mu_{road} = 0.9$

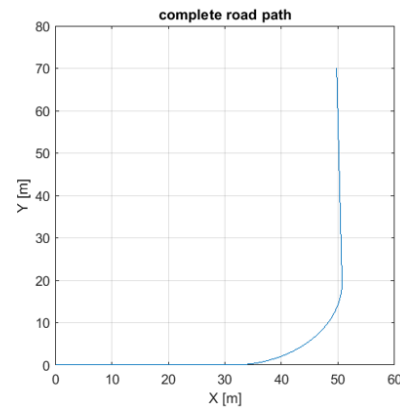
All of the graphical results from the LPT can be seen in appendix B.1.

### 4.3 Sim 2: Flat intersection

As a truck is longer than the usual road vehicle, it takes longer time for it to clear an intersection. Good acceleration from standstill or very slow speed is therefore desired to occupy the paths of other vehicles for as little time as possible. It should at the same time not be hard to control for the driver. A test of accelerating in a left turn of an intersection was therefore done. The track was inspired by the real-life intersection seen in figure 4.7a. In reality, this intersection is at the end of a highway exit where the vision to the left is bad, meaning that the vehicle will have to drive slowly or come to a complete stop before turning left.



(a) Intersection inspiration.  
Picture taken from Google Maps



(b) Intersection created in Matlab with  
approximately 19.55 m radius

**Figure 4.7:** Figures of intersection used in the flat intersection test

#### 4.3.1 Sim 2 - Setup

The vehicle approached the intersection at 5 km/h. At the start of the turn ( $X = 30.5$  in figure 4.7b) it received an acceleration request of  $0.5 \text{ m/s}^2$ . If it made it through the turn successfully, the request for the next test was increased by  $0.02 \text{ m/s}^2$ . This was done until it failed according to the unsafe scenarios in section 2.5. The simulation was also ended if the vehicle's acceleration was not increased by further increasing the requested acceleration. The criteria for ending the simulation was if the last simulation's max acceleration was within  $0.01 \text{ m/s}^2$  from the max acceleration of the simulation from 5 iterations earlier.

The test was done with all the 6 controllers mentioned in section 4.1 and with the friction coefficients  $\mu_{road} = (0.9, 0.6, 0.3)$ .

### 4.3.2 Sim 2 - Results

To compare the controllers against each other in the intersection, plots were made from numerical data collected from each simulation to visualise what happened when increasing the requested acceleration. The plots in this section shows the following:

- **Completion time versus requested acceleration**

This shows the total time from the point where the vehicle started to accelerate until it either finished the track successfully or failed, against the requested acceleration.

- **Mean acceleration versus requested acceleration**

A certain requested acceleration did not necessarily result in the same actual acceleration for all of the controllers. Therefore, the mean acceleration from the point when the vehicle started to accelerate until it either finished the test successfully or failed was plotted against the requested acceleration.

- **Cumulative SWA versus completion time**

The cumulative SWA was measured from the end of the turn when the road straightened out, until the end of the road. The focus of this metric was to see the amount of corrections the driver model needed to make to keep the vehicle stable when exiting the corner. It was plotted against completion time to see if faster times meant more steering corrections, and how the controllers compared in terms of corrections for a certain completion time.

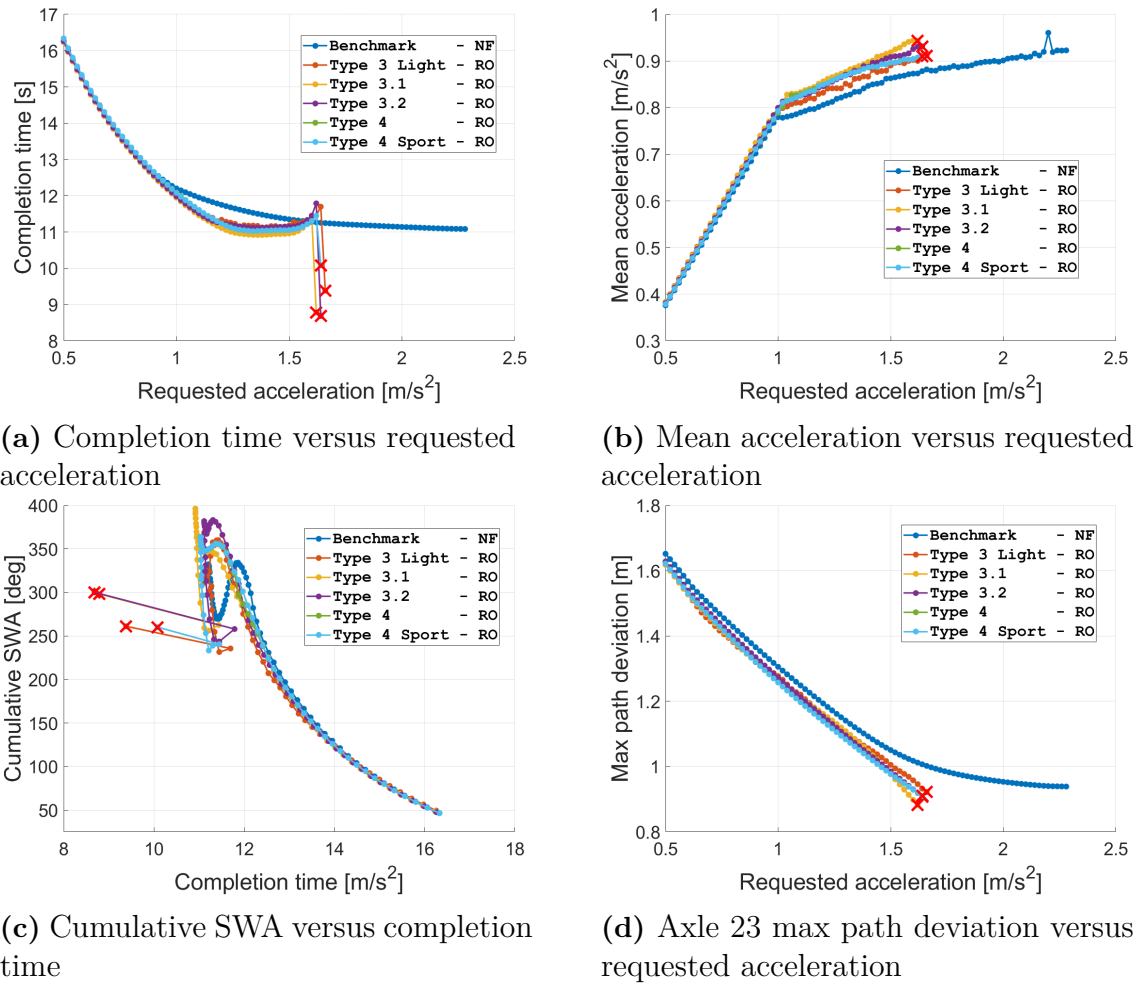
- **Semitrailer path deviation versus request acceleration**

The maximum value of the semitrailer's most rearward axle's deviation from the intended path was plotted against the requested acceleration.

The figures in this section are sorted by the road friction coefficient for the test. Except for the name of the controller in the legend, there is an abbreviation for the type of failure that the controller experienced when the requested acceleration ended in failure. The abbreviation explanation is seen in the list below:

- **NF** = No failure
- **RO** - Rollover
- **JK** - Jackknife
- **TS** - Trailer-sway
- **OT** - Off-tracking

#### 4. Final comparison of E-semitrailer controller algorithms



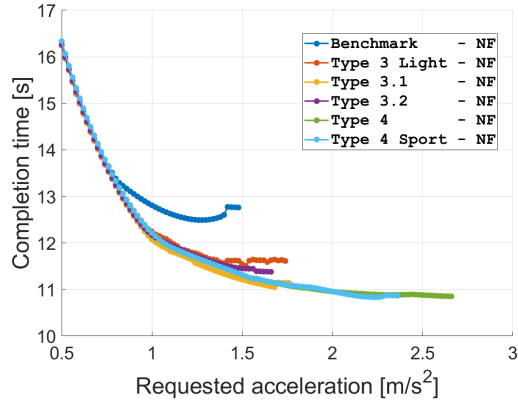
**Figure 4.8:** Flat intersection test results for  $\mu_{road} = 0.9$ . Red cross = simulation that ended in an unsafe scenario.

Figure 4.8 shows the flat intersection results for a high road friction coefficient. All controllers except the benchmark controller failed eventually due to a rollover. The benchmark never failed as it was not able to increase its velocity enough for a rollover, no matter the amount of acceleration requested. The completion time was very similar for all of the controllers, which can also be seen by the mean acceleration in figure 4.8b. Just before the point of stagnation, the benchmark controller achieved similar acceleration levels and completion times as the other controllers.

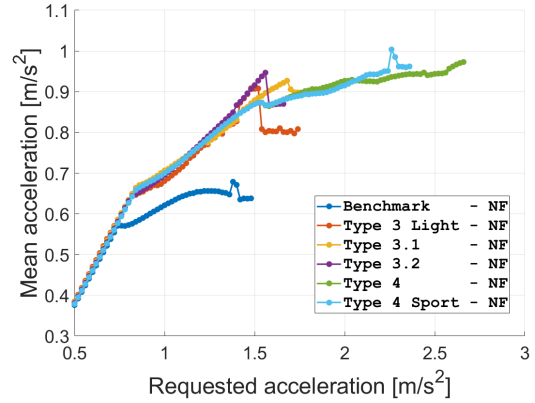
Cumulative SWA increased with decreasing completion time, basically meaning the faster the vehicle combination drove, the more corrections were needed from the driver after the corner. There was, however, not much difference between the controllers. The benchmark controller was eventually able to reach similar completion times as the other controllers but with less steering involved.

Semitrailer max path deviation decreases with increased requested acceleration. This makes sense because semitrailers generally cut corners when turning, but the centrifugal forces increase with velocity and push the semitrailer further outwards

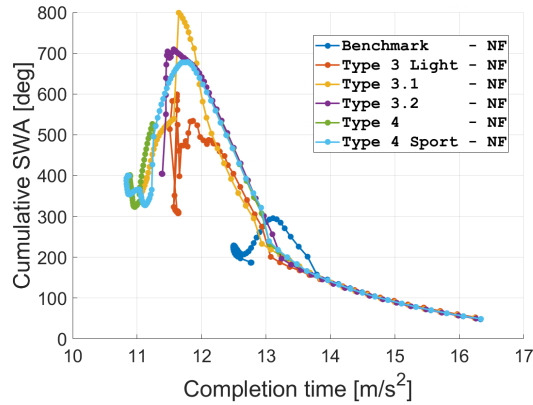
from the centre of the turning circle.



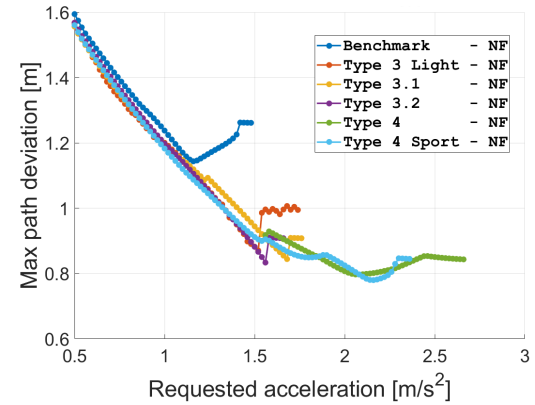
(a) Completion time versus requested acceleration



(b) Mean acceleration versus requested acceleration



(c) Cumulative SWA versus completion time



(d) Axle 23 max path deviation versus requested acceleration

**Figure 4.9:** Flat intersection test results for  $\mu_{road} = 0.6$ . Red cross = simulation that ended in an unsafe scenario.

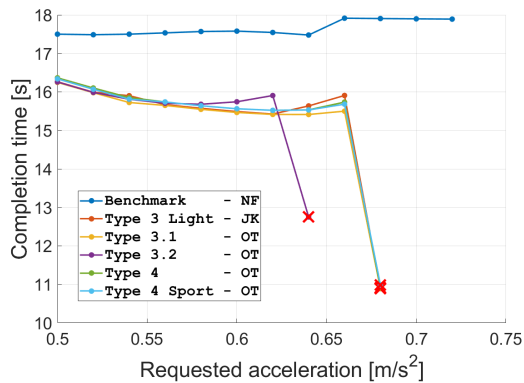
Figure 4.9 shows the flat intersection results for a medium level of road friction coefficient. None of the controllers failed. This means that the graphs for completion time, mean acceleration and semitrailer max path deviation can be assumed to continue horizontally from their endpoints if larger acceleration requests would have been simulated.

The difference in completion time between the controllers was now more prevalent compared to the results for a high road friction coefficient value. The benchmark controller was the slowest one to complete the corner. The type 4 and the type 4 sport controllers achieved the fastest completion times. The type 3.1 was not far off from them.

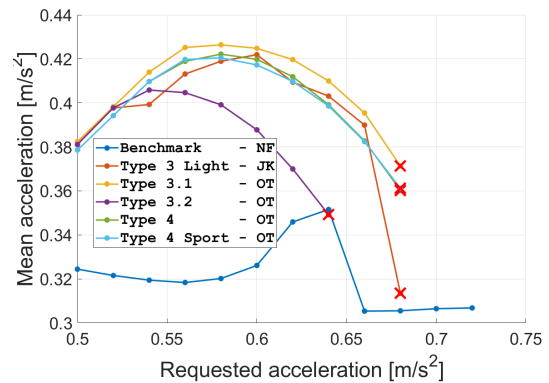
The cumulative SWA increased with decreasing completion time as before but decreased at the very fastest completion times. The semitrailer path deviation followed the same trend as for a high road friction coefficient, and there was not any controller

#### 4. Final comparison of E-semitrailer controller algorithms

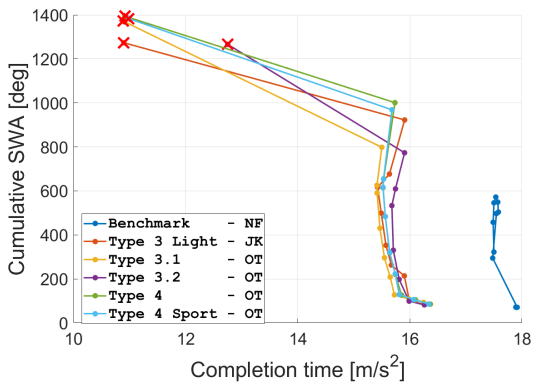
that stood out.



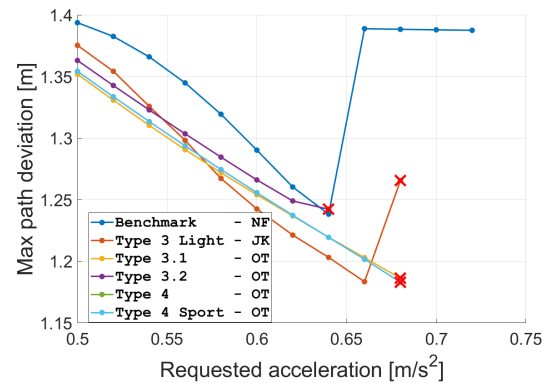
(a) Completion time versus requested acceleration



(b) Mean acceleration versus requested acceleration



(c) Cumulative SWA versus completion time



(d) Axle 23 max path deviation versus requested acceleration

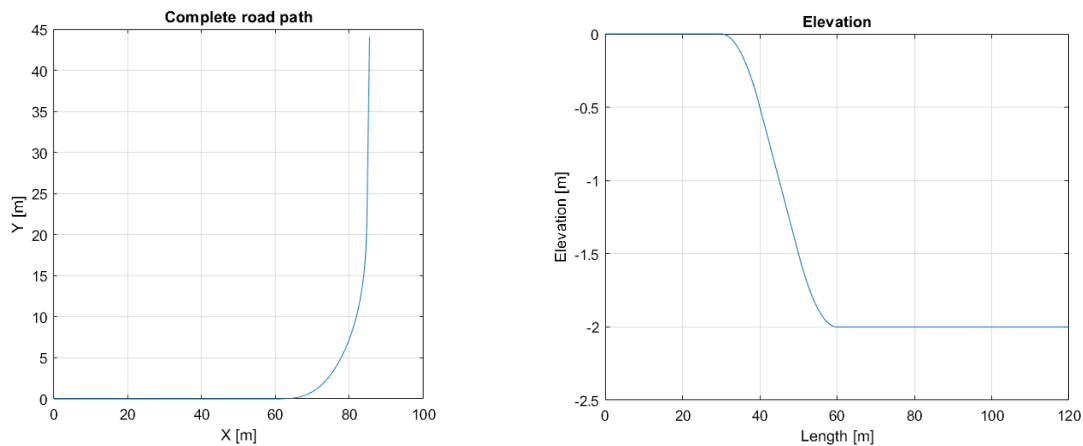
**Figure 4.10:** Flat intersection test results for  $\mu_{road} = 0.3$ . Red cross = simulation that ended in an unsafe scenario.

Figure 4.10 shows the flat intersection results for a low road friction coefficient. All controllers except the benchmark controller failed. The type 3 light controller jackknifed while all the other ones failed due to off-tracking. The completion times were very similar between the controllers except for the benchmark.

The cumulative SWA increased a lot with barely any decrease in completion time for all of the controllers. There were not any relevant differences in semitrailer path deviation between the controllers.

## 4.4 Sim 3: Downhill intersection

This test scenario also tested the trucks performance while accelerating in a turn. For this test, however, the truck was driving on a downhill slope just before reaching the intersection. The reason for this test was to understand if a difference between the pitch angles of the semitrailer and tractor would impact the results from the flat intersection test. The controllers' ability to immediately go from braking to accelerating was another reason for the test. Figure 4.11 shows the road profile in Matlab.



(a) Downhill intersection test - XY-plot

(b) Downhill intersection test - elevation-plot

**Figure 4.11:** Downhill intersection road profile

### 4.4.1 Sim 3 - Setup

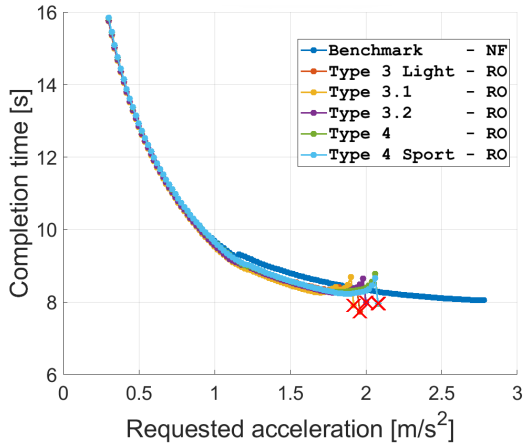
The vehicle combination drove downhill on a road with a slope gradient of -10% for 60 meters at 5 km/h. As the slope ended the road flattened out into a 90° left turn with a radius of 19.5 meters, representing an intersection. As it turned, an acceleration request was applied to the tractor's speed controller.

The simulations started with an acceleration request of  $0.3 \text{ m/s}^2$ . If the truck made it through the turn successfully, it was simulated again with a  $0.02 \text{ m/s}^2$  larger acceleration request. This iteration was continued until the truck failed by any of the defined unsafe scenarios in section 2.5, or until it could not increase its acceleration further, according to the same logic as in section 4.3.1.

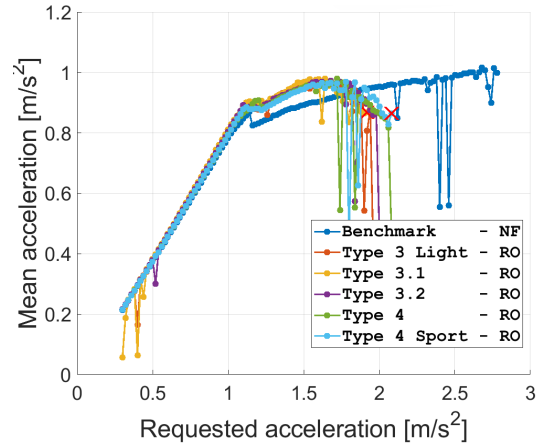
The test was done with all the 6 controllers mentioned in section 4.1 and with the friction coefficients  $\mu_{road} = (0.9, 0.6, 0.3)$ .

### 4.4.2 Sim 3 - Results

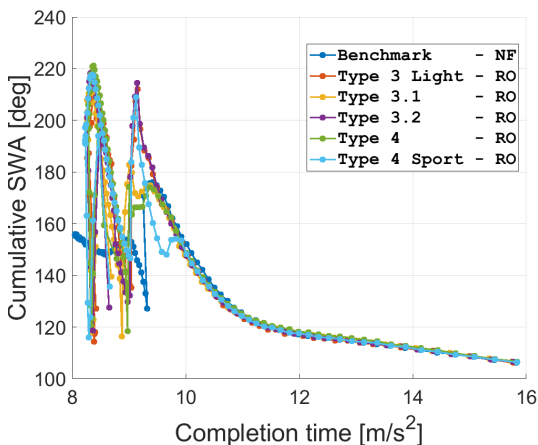
The same type of results as for the flat intersection test were plotted. Read the beginning of section 4.3.2 for an explanation of the meaning of the figures.



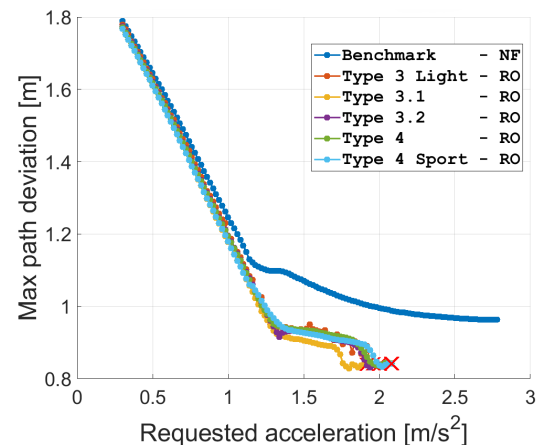
(a) Completion time versus requested acceleration



(b) Mean acceleration versus requested acceleration



(c) Cumulative SWA versus completion time



(d) Axle 23 max path deviation versus requested acceleration

**Figure 4.12:** Downhill intersection test results for  $\mu_{road} = 0.9$ .

Red cross = simulation that ended in an unsafe scenario.

Figure 4.12 shows the results for high road friction ( $\mu_{road} = 0.9$ ). Subfigure 4.12a shows that the vehicles with propelled semitrailers seem to be more prone to rollover, even when they were driving through the intersection at the same time as the benchmark truck.

This could be due to the smaller powertrain in the benchmark (only tractor propulsion) not being able to accelerate as much at the beginning of the curve. This will result in a lower speed in the steepest part of the turn, compared to the vehicles with propelled semitrailers, and thereby it will experience less lateral acceleration, which is the biggest factor for rollover accidents. The increased mean acceleration

and lower time through the curve could be the acceleration immediately after the steepest part of the turn being higher. Subfigure 4.12b shows that the mean acceleration per requested acceleration was lower on the benchmark than the rest, but it was able to continue further with larger acceleration requests.

The cumulative SWA did not significantly differ between the controllers. It increased equally with decreasing completion time for all controllers and started to fluctuate at simulation under 10 seconds (see subfigure 4.12c). Subfigure 4.12d shows that there were not any relevant differences in semitrailer path deviation between the controllers.

They were all quite equal in their performance on all the runs they could finish. The difference in communication and torque distribution strategy did not seem to impact the results.

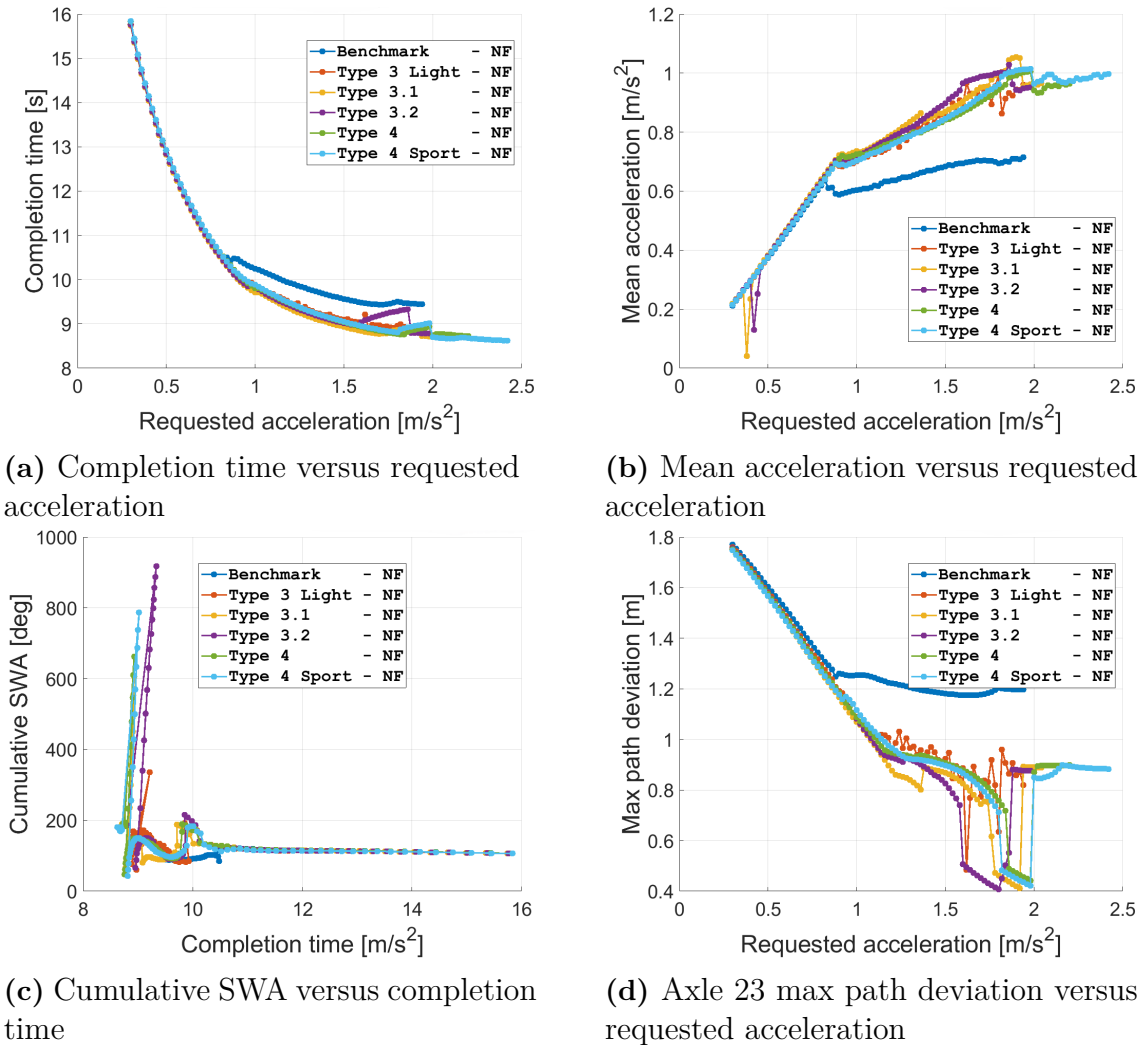


**Figure 4.13:** Downhill intersection test results for  $\mu_{road} = 0.6$ .

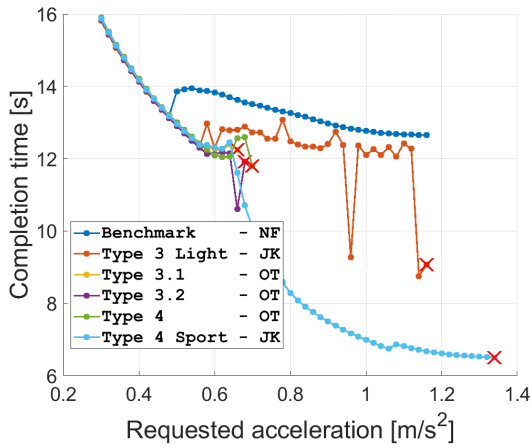
Red cross = simulation that ended in an unsafe scenario.

Figure 4.13 shows the results for medium road friction ( $\mu_{road} = 0.6$ ). The vehicles with propelled semitrailers performed better than the benchmark, going through the turn approximately 0.5 seconds faster than the benchmark (subfigure 4.13a), and reaching significantly higher mean accelerations (subfigure 4.13b).

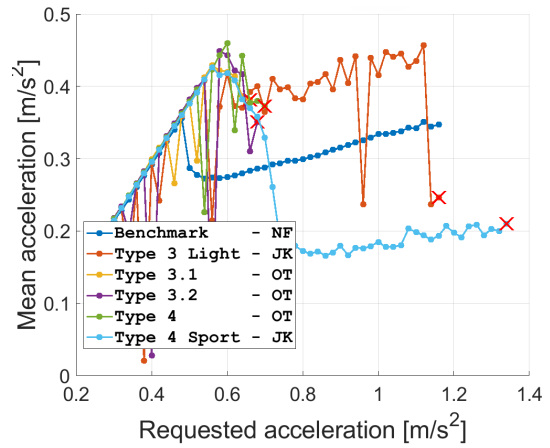
The cumulative SWA did not differ between the different controllers on lower friction either, but the behaviour with decreasing speed changed. It remained at approximately the same value between completion times of 10 to 15 seconds. At lower completion times the cumulative SWA fluctuated before it failed.

There were not any relevant differences in semitrailer path deviation between the controllers, except for huge fluctuations at higher accelerations. Some controllers suddenly reached a small max path deviation error before it increased at higher requested accelerations again.

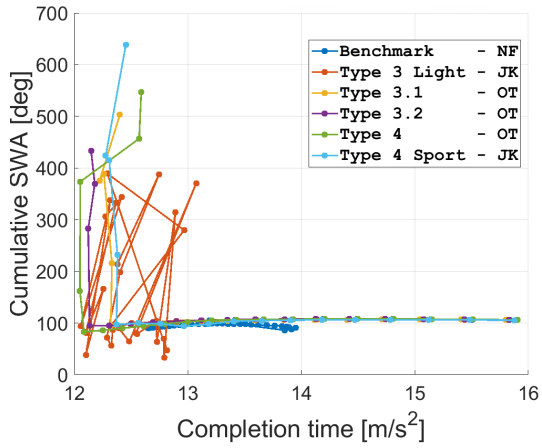
#### 4. Final comparison of E-semitrailer controller algorithms



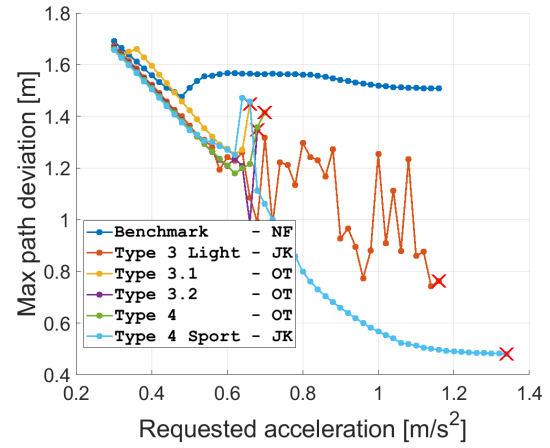
(a) Completion time versus requested acceleration



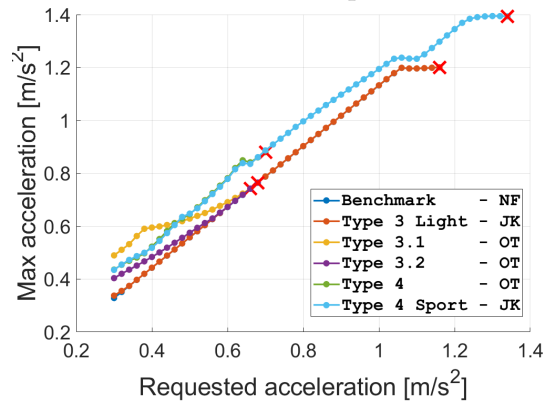
(b) Mean acceleration versus requested acceleration



(c) Cumulative SWA versus completion time



(d) Axle 23 max path deviation versus requested acceleration



(e) Max acceleration versus requested acceleration

**Figure 4.14:** Downhill intersection test results for  $\mu_{road} = 0.3$ . Red cross = simulation that ended in an unsafe scenario.

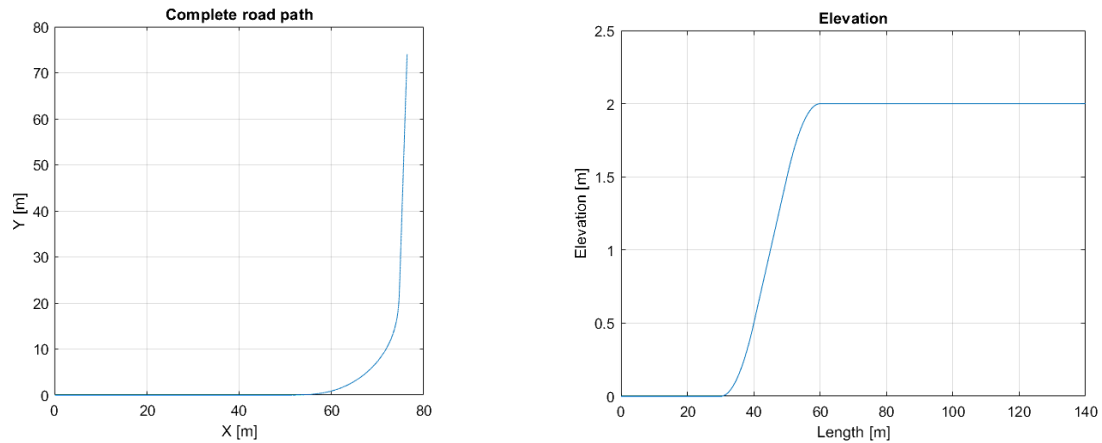
Figure 4.14 shows the results for low road friction ( $\mu_{road} = 0.3$ ). Here, many of the vehicles with a propelled semitrailer were driving really unstable, failing very

early. The type 4 sport was able to perform a lot better than the rest, managing a significantly lower time through the turn, but barely increased its mean acceleration (subfigure 4.14b), although it had a high maximum acceleration, as seen in subfigure 4.14e. The mean acceleration decreased at higher acceleration requests. This could be due to the traction control intervening, as the lateral forces increased in the turn it was forced to decrease the longitudinal force, the wheel-torque.

The cumulative SWA value remained constant with decreasing completion time. At very low completion times it fluctuated heavily. The type 4 sport controller reached a lower value of max path deviation than the other controllers, as they failed earlier.

## 4.5 Sim 4: Uphill intersection

The same kind of intersection as tested in previous chapters was also tested with an uphill slope just before it. It was tested for the same reasons as given for the downhill intersection. The vehicle's units will have a slightly different pitch angles at the start of the acceleration. In this case, the heavier semitrailer will also be "pulling" the tractor more at the beginning of the turn compared to the other type of intersections that have been tested. Figure 4.15 shows the road profile in Matlab.



(a) Uphill intersection test - XY-plot

(b) Uphill intersection test - elevation-plot

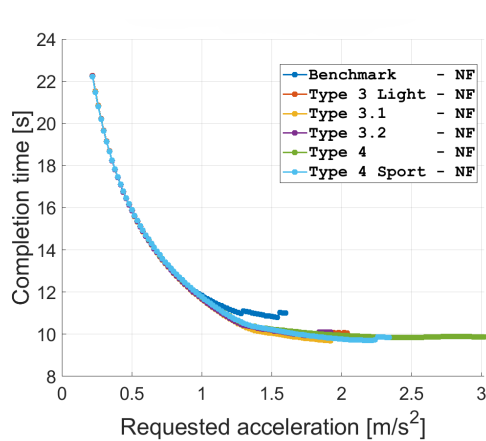
**Figure 4.15:** Uphill intersection road profile

### 4.5.1 Sim 4 - Setup

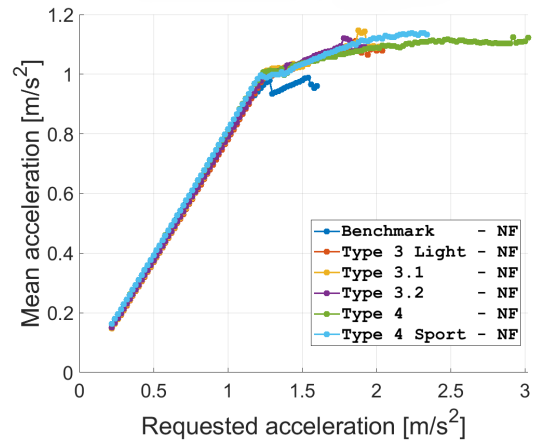
The setup of simulation 4 was almost identical to simulation 3 (4.4.1) except that the truck was driving uphill before the intersection instead. The road slope gradient was 10% and flattened out just as the intersection started. The acceleration request was given at 55 meters in this scenario.

### 4.5.2 Sim 4 - Results

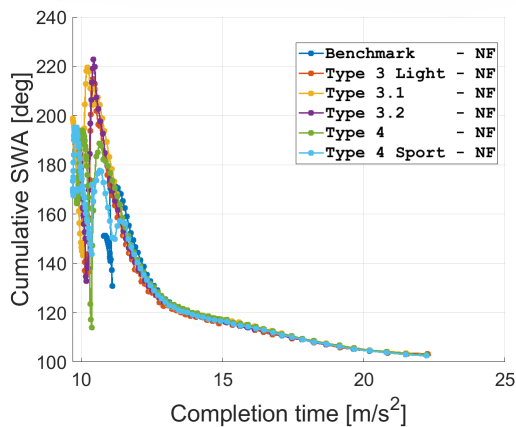
The same type of results as for the flat intersection test was plotted. Read the beginning of section 4.3.2 for an explanation of the meaning of the figures.



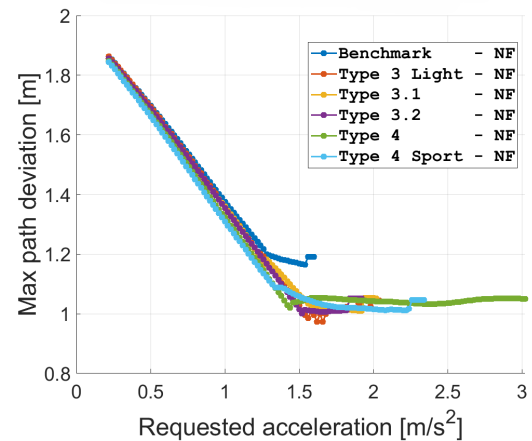
(a) Completion time versus requested acceleration



(b) Mean acceleration versus requested acceleration



(c) Cumulative SWA versus completion time

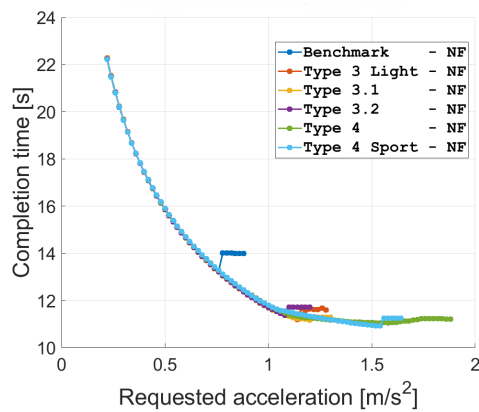


(d) Axle 23 max path deviation versus requested acceleration

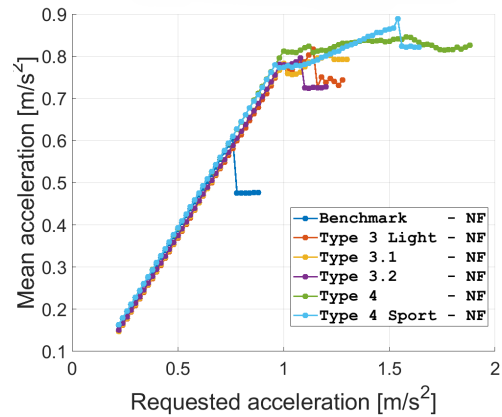
**Figure 4.16:** Uphill intersection test results for  $\mu_{road} = 0.9$ . Red cross = simulation that ended in an unsafe scenario.

Figure 4.16 shows the results for high road friction ( $\mu_{road} = 0.9$ ). All controllers performed similarly, and they all outperformed the benchmark truck. Neither of them failed due to any unsafe scenarios on high friction. The biggest difference between them was the acceleration (subfigure 4.16b). The benchmark had, as mentioned previously, an overall smaller powertrain, which was why it did not reach the same levels of acceleration. The rest of the controllers performed within such small differences that they can be assumed to perform equally.

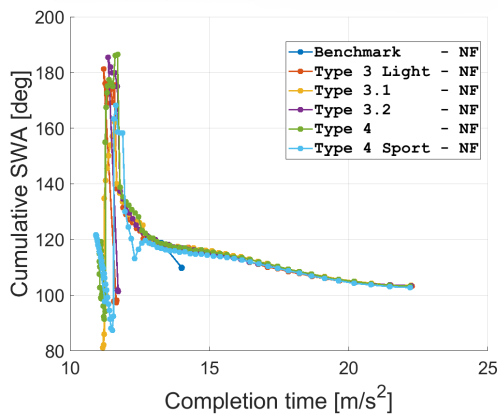
#### 4. Final comparison of E-semitrailer controller algorithms



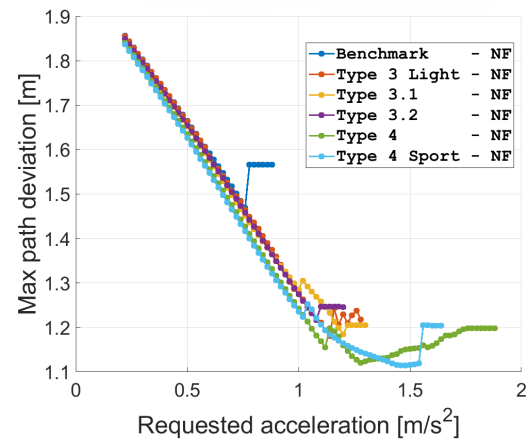
(a) Completion time versus requested acceleration



(b) Mean acceleration versus requested acceleration



(c) Cumulative SWA versus completion time



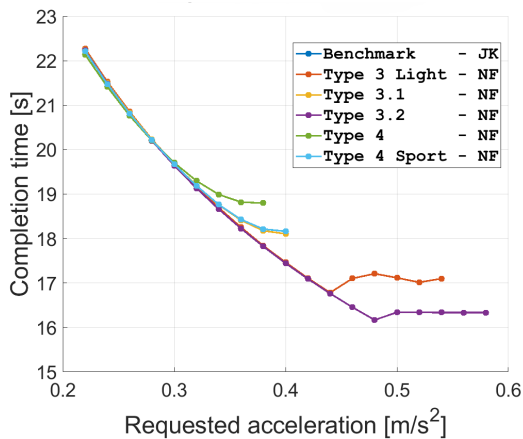
(d) Axle 23 max path deviation versus requested acceleration

**Figure 4.17:** Uphill intersection test results for  $\mu_{road} = 0.6$ . Red cross = simulation that ended in an unsafe scenario.

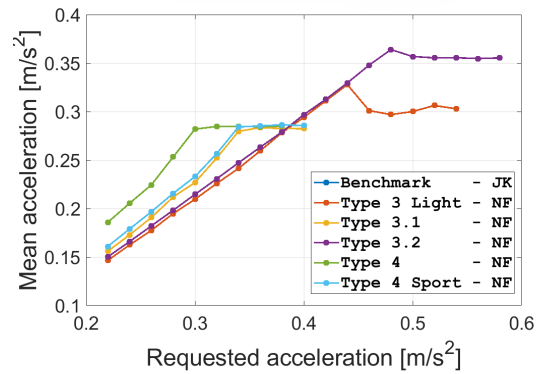
Figure 4.17 shows the results for medium road friction ( $\mu_{road} = 0.6$ ). There was a bigger difference between the type 3 and the type 4 controllers. The type 4 controllers were able to achieve a higher mean acceleration (subfigure 4.17b), and drove through the intersection at faster times (subfigure 4.17a). But still within small differences, only a few tenths of a second.

There were no relevant differences between the controllers regarding the cumulative SWA and semitrailer max path deviation results.

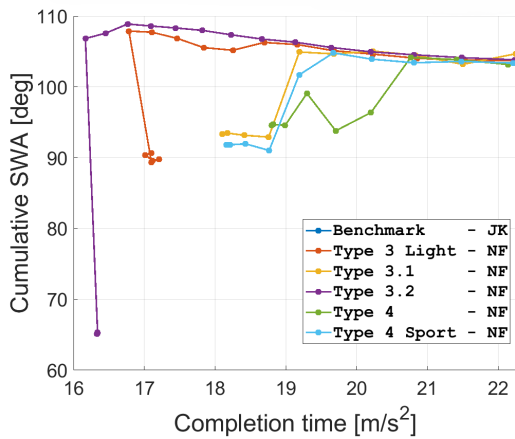
#### 4. Final comparison of E-semitrailer controller algorithms



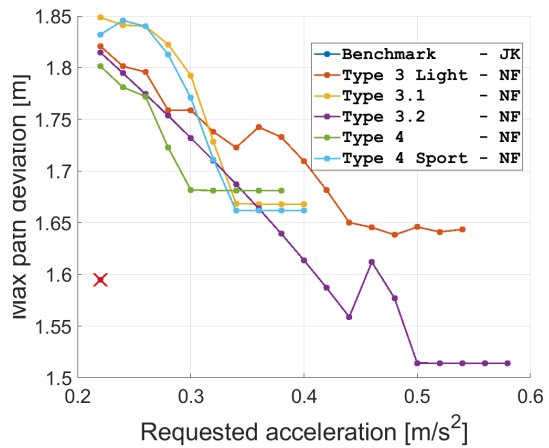
(a) Completion time versus requested acceleration



(b) Mean acceleration versus requested acceleration



(c) Cumulative SWA versus completion time



(d) Axle 23 max path deviation versus requested acceleration

**Figure 4.18:** Uphill intersection test results for  $\mu_{road} = 0.3$ . Red cross = simulation that ended in an unsafe scenario.

Figure 4.18 shows the results for low road friction ( $\mu_{road} = 0.3$ ). Type 3.2 performed the best. It was able to go through the intersection at a lower time (subfigure 4.18a), and reached a higher mean acceleration (subfigure 4.18b).

The benchmark truck was not able to drive through the intersection at all, it jackknifed immediately. The rest failed due to not being able to increase their acceleration.

The cumulative SWA actually decreased a small amount at faster completion times, but most controllers showed this behaviour. The semitrailer max path deviation results did not show any relevant differences.

# 5

## Discussion

### 5.1 Type 3 coupling force sensor

Sensor data in VTM simulation is ideal. In reality, there would be more jerking motions in the coupling, potentially from the powertrain, and from the elasticity in the coupling. This could lead to oscillations and big amplifications which can result in an unstable vehicle leading to harmful scenarios. Oscillations could also be induced by uneven roads. Since the force applied to the semitrailer is based on the vertical load, uneven roads can create big changes in the torque request on the semitrailer.

To avoid big amplifications, a limit to the increase of applied torque could be used. It could also be equipped with an observer to indicate oscillations and avoid them by decreasing the torque and smothering the changes.

There could also be an algorithm to detect gear switches from the tractor and propel a bit extra at that moment to prevent speed reduction while switching gears, especially if the vehicle is going uphill.

### 5.2 Type 3.1 vs type 4

It might feel a bit wrong that the type 3, with limited communication, in most cases performed just as well, or sometimes even better than the type 4 did. But in a simulation environment, it was not that unexpected. Since they used the same fundamental logic for propulsion, torque proportional by axle load, and the vertical force in the coupling compared to the longitudinal coupling force is almost equal to the proportion in the tractor axle load compared to its longitudinal force, they can not be that different.

In the real world, where sensor data might not be as exact (as mentioned in section 5.1), the similarities could also be due to the ideal traction control used in this project which never allowed for any slip. It was also never under one of the most difficult situations where it was believed that the type 4 almost certainly would outperform the type 3, standstill on low  $\mu$  in an uphill. Even worse could be if it is stuck in the snow. In this scenario the type 4 would almost certainly have a

big advantage over the type 3, as the type 3 requires a slight acceleration before it will apply any torque onto the tractor, whilst the type 4 can immediately send a torque request, essentially making it a four-wheel driven vehicle instantly, which will greatly increase its chance to get going. The type 3 might just burrow itself down when it is trying to accelerate from a standstill as it doesn't get any help from the E-semitrailer.

This could unfortunately not be tested in the current model, as the ideal traction control and exact sensor data would always make it able to accelerate with the power from both of the powertrains immediately.

### 5.3 Traction control and fail statistics

The ideal traction controller significantly reduced the risk of jackknifing and trailer-sway during intersection tests. It achieved this by using the friction circle to control the maximum torque output, ensuring the vehicle combination did not exceed the traction limits in both the x- and y-directions. This decreased the propulsion force when high lateral acceleration occurred during turning.

Given this, it was more relevant to assess the current state and how much the vehicles could accelerate in a turn until the point of failure, rather than analysing the cause of failure. Investigating the cause of failure might not be practical. Even in scenarios where the simulation did not result in failure or an increase in acceleration, it might have been due to the traction control interference.

### 5.4 Type 3 light speed sensor

The type 3 light is in most cases a few percent slower than the type 3.1 and type 4, this was due to the method used to find the current acceleration (described in section 3.2.4.4). It used the current wheel speeds derivative, and to compensate for high peaks and stuttering (which is common when derivating sensor data like this) a transfer function was used to smooth the sensor data. This method resulted in a measured acceleration that was lower than the actual acceleration. This is not necessarily bad since it resulted in a bigger safety margin (as lower torque on the semitrailer is safer in general), but it stopped the type 3 light from showing its full potential.

### 5.5 Result discussion

#### 5.5.1 Uphill intersection test on low $\mu$

The type 3.2 performed the best, probably because it propels with a lower torque on the semitrailer than the rest of the type 3 and type 4 controllers, but still enough to go up the hill. This makes the peak acceleration occur later in the turn, while the vehicle is in a more stable state. It has also been shown that a lower torque on

the semitrailer while turning is good for stability. This case might be an indicator that the torque factor also should depend on friction. It should probably adjust the allowed amount of articulation angle to a lower value to reduce the torque earlier, and possibly at a higher rate.

## 5.6 Torque factor

A big takeaway from the tests was that propelling only on the tractor always seems to have the lowest amount of failures. This suggests that propelling the semitrailer increases the risk of unsafe scenarios, which is typically occurring in turns. This is why the torque factor is such an important implementation to ensure a safer vehicle combination. The torque factor modelled in this project only depended on articulation angle, and the resulting function was only based on tests on a specific friction coefficient in a single turn with altering acceleration requests (explained in section 3.1.3). The torque factor could probably depend on a lot more variables, such as friction and current speed.

## 5.7 Speed controller

The design of the speed controller was not necessarily equally good for all of the different types of controllers. The speed controller determined the acceleration request which was translated to a torque request in the torque controller. The speed controller has a big effect on the request and how the specific torque controller behaves. It might be a big advantage for one of the controllers, but not the other, depending on how it is constructed. This needs to be taken into account when evaluating the different controllers and torque distribution strategies. Before making any final conclusions, a speed controller should be proven to be realistic to an actual speed controller or a more accurate driver model should be implemented. The current one should at least be evaluated on how "realistic" it is, since it can determine a lot of the results.



# 6

## Conclusion

There are clear advantages to having an electrified semitrailer compared to a regular non-driven semitrailer. The added power from the powertrain makes the vehicle combination able to conquer steep hills and lower friction, but it comes with risks. The force applied from the semitrailer to the coupling makes the vehicle combination more prone to accidents. On higher friction, the vehicle seems to have a higher risk of rollover, and on lower friction, it is more prone to jackknife and off-tracking.

This is why the vehicle combination with an electrified semitrailer needs to be driven with caution and can be improved by more in-depth research about the torque factor and how it should re-distribute torque during turns, especially while accelerating.

While driving at a constant speed, the distribution of torque does not seem to matter. This gives the type 4 an advantage over the type 3 controllers as it can be driven with the majority of the power from the semitrailer to save energy in the tractor. This could be good if the driver is going to deliver the semitrailer and immediately picks up a new, fully charged, electric semitrailer. In this case, the tractor does not have to stop and charge. In the case where it is an ICE tractor, the amount of fuel being used is reduced, and the vehicle combination can be driven on electricity only (depending on the use case).

The purpose of this thesis was to compare how the different levels of communication (type 3 versus type 4) would affect performance, stability and driveability. The simulation tests that have been done have found little to no difference between the two levels of communication. They were all able to operate at a vertical load proportional distribution, even if they do not have any ability to communicate the sensor data. This fact, together with the ideal traction control and stiff coupling (discussed in section 5.1 and 5.2), resulted in the two variants performing at an equal level on the majority of the tests.

The final conclusion is that the level of communication does not affect the performance, stability and drive-ability in a significant way for the simulation tests that have been done in this thesis. The main difference when switching from type 4 to type 3 level communication is the loss of the ability to manually choose the distribution.



# 7

## Future work

### 7.1 Traction control and tyre model

The ideal traction control used in this thesis limited the output force to always stay inside of the friction circle, which never allowed for any slip. This resulted in a very ideal simulation, but not realistic in all cases. To further see bigger differences between the different controllers, a more realistic traction control could be modelled that looks at the slip limits of the torque when the slip goes beyond a certain threshold, instead of using the friction circle.

A more advanced tyre model could also be created to get a more realistic model to simulate. The current tyre model in VTM does not allow the vehicle to go to a complete stop. A hypothesis is that the type 3 controllers would perform worse when starting from a complete stop compared to the type 4, since the type 3 requires a coupling force, or for type 3 light, an acceleration and a velocity for the rolling resistance counter force to initiate.

A test that could be made is to start from a standstill on a steep hill (possibly on low friction) where the tractor's powertrain alone isn't enough to propel the vehicle forward at all, then the type 3 vehicles wouldn't be able to get going, whilst the type 4 tractor could immediately send a torque request to the semitrailer and start to propel forward on the semitrailer as well.

### 7.2 Torque vectoring

By utilising the knowledge of the articulation angle and the ability to control the torque on each wheel on the e-semitrailer independently, torque vectoring could be implemented to possibly give better performance and stability while turning by always pushing on the coupling in the longitudinal direction of the tractor, and possible even extra in one direction if it can prove to help to stabilise the tractor, preventing it from unsafe scenarios like jackknifing.

### **7.3 Jack-knife avoidance**

To further elaborate on avoiding unsafe scenarios, one possibility to reduce the chance of jackknifing is to develop a method of recognizing the increased chance of jackknifing. When detected, the inner wheel on the semitrailer could be braked to force the vehicle combination to straighten out, resulting in a lower chance of jackknifing.

### **7.4 Energy optimisation**

The extra powertrain on the E-semitrailer could also allow energy optimisation, especially on the type 4. This can be done regarding multiple aspects. First off could be in a case with a fossil fuel tractor, where the E-semitrailer is used to hybridise the vehicle combination, and on a highway for example, the vehicle could run on pure electricity by only propelling the E-semitrailer.

If the route is planned, or at least known by the driver, the E-semitrailer could be prioritised to reach 0% State of Charge at the destination where the driver delivers the E-semitrailer. The driver could then potentially pick up a new E-semitrailer which is fully charged and immediately continue the journey without stopping and recharging.

It gives the opportunity to retard and recharge the batteries during operation while braking even more effectively than only retarding on the tractor, as it can retard according to vertical load distributed retardation torque.

# Bibliography

- [1] A. Hansson, E. Andersson, “Safe operating envelope for electric semi-trailer,” 2022.
- [2] U. Erdinc, M. Jonasson, M. Sadeghi Kati, B. Jacobson, J. Fredriksson L. Laine, “Validation of high-fidelity simulation-based safe operating envelopes for articulated heavy vehicles using real test data,” 2024.
- [3] B. J. et al, *Compendium in Vehicle Motion Engineering*. Vehicle Dynamics Group, Divison Vehicle and Autonomous Systems, Department of Mechanics and Maritime Sciences, Chalmers University of Technology, 2024.



# A

## Matlab function scripts

### A.1 Type 4 Fz proportional distribution torque allocation

```
1 function [T_11_req, T_12_req, T_21_req, T_22_req, T_23_req,  
drive_status]= fcn(m_tot, Fx_req_tot, r_1, r_2,  
T_2_powertrain_max, Fz, drive_status)  
2  
3 Fz_11 = Fz(1);  
4 Fz_12 = Fz(2);  
5 Fz_21 = Fz(3);  
6 Fz_22 = Fz(4);  
7 Fz_23 = Fz(5);  
8  
9 Fz_1 = Fz_11 + Fz_12; % Vertical axle forces tractor  
10 Fz_2 = Fz_21 + Fz_22 + Fz_23; % Vertical axle forces  
semitrailer  
11  
12 Fz_tot = Fz_1 + Fz_2; % Total vertical force  
13  
14 a_1_ret_max = -2.5; % [m/s^2] - max retardation tractor  
15  
16 Fx_1_ret_max = m_tot * a_1_ret_max; % [N] - max retardation  
force tractor  
17  
18 T_1_ret_max = Fx_1_ret_max * r_1; % [Nm] max retardation torque  
tractor  
19  
20 T_2_ret_max= -T_2_powertrain_max; % [Nm] - max retardation  
torque semitrailer  
21  
22 Fx_2_ret_max= T_2_ret_max/r_1; % [N] - max retardation force  
semitrailer  
23  
24 % Total force divided by proportional Fz for each unit  
25 Fx_1_req = Fx_req_tot * (Fz_1/Fz_tot);  
26 Fx_2_req = Fx_req_tot * (Fz_2/Fz_tot);  
27  
28 if Fx_1_req >= 1000  
29 drive_status = 1; % Propulsion  
30 elseif (Fx_1_req <= -2000) && (Fx_1_req >= Fx_1_ret_max + 1000)
```

## A. Matlab function scripts

```
31     drive_status = 2; % Retardation
32 elseif Fx_1_req <= Fx_1_ret_max
33     drive_status = 3; % Braking (service brakes)
34 end
35
36 if drive_status==1 % Propulsion
37     if Fx_req_tot < 0
38         T_11_req = 0;
39         T_12_req = 0;
40         T_21_req = 0;
41         T_22_req = 0;
42         T_23_req = 0;
43     else
44         T_11_req = 0;
45         T_12_req = (Fx_req_tot*r_1*Fz_1)/(Fz_11+Fz_12+Fz_21+
46             Fz_22+Fz_23);
47         T_21_req = (Fx_req_tot*r_2*Fz_2)/(Fz_11+Fz_12+Fz_21+
48             Fz_22+Fz_23);
49         T_22_req = 0;
50         T_23_req = 0;
51
52         % The only difference for the manual set distribution
53         % function is:
54         % T_11_req = 0;
55         % T_12_req = Fx_req_tot*r_1*(dist);
56         % T_21_req = Fx_req_tot*r_2*(1-dist);
57         % T_22_req = 0;
58         % T_23_req = 0;
59     end
60 elseif drive_status==2 % Retardation
61     if Fx_req_tot > 0
62         T_11_req = 0;
63         T_12_req = 0;
64         T_21_req = 0;
65         T_22_req = 0;
66         T_23_req = 0;
67     else
68         if Fx_2_req < Fx_2_ret_max
69
70             T_11_req = 0;
71             T_12_req = Fx_1_req*r_1;
72             T_21_req = T_2_ret_max;
73             T_22_req = ((Fx_2_req - Fx_2_ret_max)*r_2)/2;
74             T_23_req = ((Fx_2_req - Fx_2_ret_max)*r_2)/2;
75
76         else
77
78             T_11_req = 0;
79             T_12_req = Fx_1_req*r_1;
80             T_21_req = Fx_2_req*r_2;
81             T_22_req = 0;
82             T_23_req = 0;
83         end
84     end
85 end
```

```

84     else % Braking
85         if Fx_2_req < Fx_2_ret_max
86
87             T_11_req = (Fx_1_req - Fx_1_ret_max)*r_1;
88             T_12_req = T_1_ret_max;
89             T_21_req = T_2_ret_max;
90             T_22_req = ((Fx_2_req - Fx_2_ret_max)*r_2)/2;
91             T_23_req = ((Fx_2_req - Fx_2_ret_max)*r_2)/2;
92         else
93             T_11_req = (Fx_1_req - Fx_1_ret_max)*r_1;
94             T_12_req = T_1_ret_max;
95             T_21_req = Fx_2_req*r_2;
96             T_22_req = 0;
97             T_23_req = 0;
98         end
99     end
100 end

```

**Listing A.1:** Matlab Function: Type 4 Fz proportional distribution torque allocation

## A.2 Type 3 tractor torque allocator

```

1 function [T_1_req, Fx_2_req, drive_status_1] = fcn(Fx_req_tot,
2         m_tot, r_1, Fz, drive_status_1)
3
4     Fz_11 = Fz(1);
5     Fz_12 = Fz(2);
6     Fz_21 = Fz(3);
7     Fz_22 = Fz(4);
8     Fz_23 = Fz(5);
9
10    Fz_1 = Fz_11 + Fz_12; % Vertical axle forces tractor
11    Fz_2 = Fz_21 + Fz_22 + Fz_23; % Vertical axle forces
12    semitrailer
13
14    Fz_tot = Fz_1 + Fz_2; % Total vertical force
15
16    % Brake with service brakes Fz proportional if the force
17    request becomes larger than possible retardation on tractor.
18    Assume the tractor doesn't know what the trailer does.
19
20    a_1_ret_max = -2.5; % [m/s^2] - max retardation tractor
21
22    Fx_1_ret_max = m_tot * a_1_ret_max; % [N] - max retardation
23    force tractor
24
25    T_1_ret_max = Fx_1_ret_max * r_1; % [Nm] - max retardation
26    torque tractor
27
28    % Total brake force divided by proportional Fz for each unit
29    Fx_1_req = Fx_req_tot * (Fz_1/Fz_tot);
30    Fx_2_req = Fx_req_tot * (Fz_2/Fz_tot);

```

```

26     if Fx_1_req <= 0
27
28     else % No positive braking forces
29         Fx_1_req = 0;
30         Fx_2_req = 0;
31     end
32
33     if Fx_req_tot >= 1000
34         drive_status_1 = 1; % Propulsion
35     elseif (Fx_1_req <= -10000) && (Fx_1_req >= Fx_1_ret_max +
36         1000)
37         drive_status_1 = 2; % Retardation
38
39     elseif Fx_1_req < Fx_1_ret_max
40         drive_status_1 = 3; % Braking (Service Brakes)
41     end
42
43     if drive_status_1 == 1 % Propulsion
44         if Fx_req_tot > 0
45             T_1_req = r_1*[0; Fx_req_tot];
46             Fx_2_req = 0;
47         else
48             T_1_req = r_1*[0; 0];
49             Fx_2_req = 0;
50         end
51     elseif drive_status_1 == 2 % Retardation
52         if Fx_req_tot < 0
53             T_1_req = r_1*[0; Fx_1_req];
54             Fx_2_req = Fx_2_req;
55         else
56             T_1_req = r_1*[0; 0];
57             Fx_2_req = 0;
58         end
59     else % Service Brakes
60         service_brake_req = Fx_1_req - Fx_1_ret_max;
61         T_1_req = r_1*[service_brake_req; Fx_1_ret_max];
62         Fx_2_req = Fx_2_req;
63     end
end

```

Listing A.2: Matlab Function: Type 3 tractor torque allocator

### A.3 Type 3.1 semitrailer torque allocator

```

1 function [T_2_req, drive_status_2] = fcn(Fx_2_req, Fcx, Fcz, Fz_21,
2     Fz_22, Fz_23, T_2_powertrain_max, r_2, drive_status_2)
3
4     Fz_2 = Fz_21 + Fz_22 + Fz_23; % Total vertical load semitrailer
5
6     Fx_prop_req = (Fcx*Fz2)/Fcz; % Propulsive force request
7
8     Fx_2_ret_max = -T_2_powertrain_max/r_2; % [N] - max retardation
9     force semitrailer
10
11     if Fx_2_req >= 0 && Fx_prop_req >= 2000

```

```

10     drive_status_2 = 1; % Propulsion
11 elseif Fx_2_req <= -10000 && Fx_2_req >= Fx_2_ret_max + 100
12     drive_status_2 = 2; % Retardation
13 elseif Fx_2_req < Fx_2_ret_max
14     drive_status_2 = 3; % Braking (Service Brakes)
15 end
16
17 if drive_status_2 == 1 % Propulsion
18     if Fx_prop_req > 0
19         T_2_req = r_2*[Fx_prop_req; 0; 0];
20     else
21         T_2_req = [0;0;0];
22     end
23 elseif drive_status_2 == 2 % Retardation
24     if Fx_2_req < 0
25         T_2_req = r_2*[Fx_2_req; 0; 0];
26     else
27         T_2_req = [0; 0; 0];
28     end
29 else % Braking
30     service_brake_trailer = (Fx_2_req - Fx_2_ret_max) / 2;
31     T_2_req = r_2*[Fx_2_ret_max; service_brake_trailer;
32                 service_brake_trailer];
33 end
end

```

Listing A.3: Matlab Function: Type 3.1 semitrailer torque allocator

## A.4 Type 3.2 semitrailer torque allocator

```

1 function [T_2_req, drive_status_2] = fcn(Fx_2_req, Fcx_error,
2     T_2_powertrain_max, r_2, drive_status_2)
3
4     Fx_prop_req = -Fcx_error ; % Propulsive force request
5
6     Fx_2_ret_max = -T_2_powertrain_max/r_2; % [N] - max retardation
7     force semitrailer
8
9     if Fx_2_req >= 0 && Fx_prop_req>2000
10        drive_status_2 = 1; % Propulsion
11        elseif Fx_2_req <= -10000 && Fx_2_req > Fx_2_ret_max + 100
12        drive_status_2 = 2; % Retardation
13        elseif Fx_2_req < Fx_2_ret_max
14        drive_status_2 = 3; % Service Brakes
15    end
16
17    if drive_status_2 == 1 % Propulsion
18        if Fx_prop_req > 0
19            T_2_req = r_2*[Fx_prop_req; 0; 0];
20        else
21            T_2_req = [0;0;0];
22        end
23    elseif drive_status_2 == 2 % Retardation
24        if Fx_2_req < 0
25            T_2_req = r_2*[Fx_2_req; 0; 0];

```

```

24     else
25         T_2_req = [0; 0; 0];
26     end
27     else % Braking
28         service_brake_trailer = (Fx_2_req - Fx_2_ret_max) / 2;
29         T_2_req = r_2*[Fx_2_ret_max; service_brake_trailer;
30             service_brake_trailer];
31     end
end

```

Listing A.4: Matlab Function: Type 3.2 semitrailer torque allocator

## A.5 Type 3 light semitrailer torque allocator

```

1 function [T_2_req, drive_status_2] = fcn(omega_w_22_dot, v_22,
    Fx_2_req, alpha_2, Fz_21, Fz_22, Fz_23, T_2_powertrain_max, r_2,
    drive_status_2)
2
3     g = 9.82; % Gravity constant
4
5     Fz_2 = Fz_21 + Fz_22 + Fz_23; % Total vertical load semitrailer
6     RRC=0.008; % Rolling resistance coefficient
7
8     T_2_ret_max = -T_2_powertrain_max/r_2; % Max
9
10    if v_22*3.6 > 30 % If current velocity is more than 30 km/h
11        Fx_prop_req = Fz_2*((omega_w_22_dot/g) + sin(alpha_2) + RRC
12            );
13    else
14        Fx_prop_req = Fz_2*((omega_w_22_dot/g) + sin(alpha_2));
15    end
16
17    if Fx_2_req >= 0 && Fx_prop_req > 2000
18        drive_status_2 = 1; % Propulsion
19    elseif Fx_2_req <= -10000 && Fx_2_req > T_2_ret_max + 100
20        drive_status_2 = 2; % Retardation
21    elseif Fx_2_req < T_2_ret_max
22        drive_status_2 = 3; % Braking (Service Brakes)
23    end
24
25    if drive_status_2 == 1 % Propulsion
26        if Fx_prop_req > 0
27            T_2_req = r_2*[Fx_prop_req; 0; 0];
28        else
29            T_2_req = [0;0;0];
30        end
31    elseif drive_status_2 == 2 % Retardation
32        if Fx_2_req < 0
33            T_2_req = r_2*[Fx_2_req; 0; 0];
34        else
35            T_2_req = [0; 0; 0];
36        end
37    else % Braking
38        service_brake_trailer = (Fx_2_req - T_2_ret_max) / 2;

```

```
38     T_2_req = r_2*[T_2_ret_max; service_brake_trailer;  
39                 service_brake_trailer];  
40     end  
end
```

**Listing A.5:** Matlab Function: Type 3 light semitrailer torque allocator



# B

## Simulation Results

### B.1 Longitudinal Performance Test

#### B.1.1 Flat

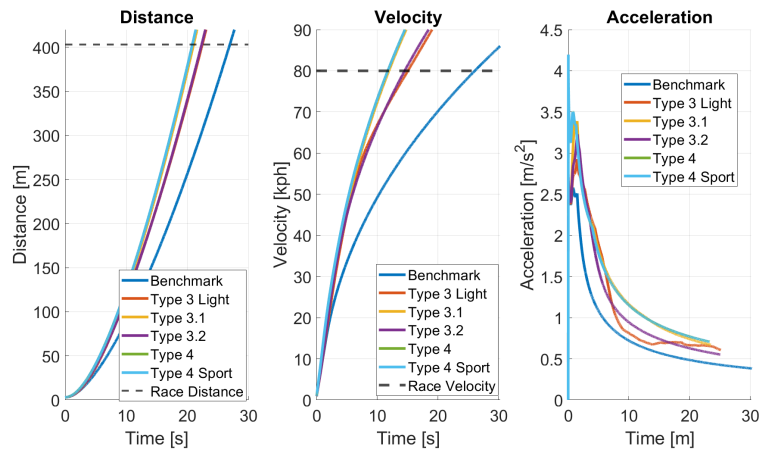


Figure B.1: LPT - Longitudinal states, Flat road,  $\mu_{road} = 0.9$

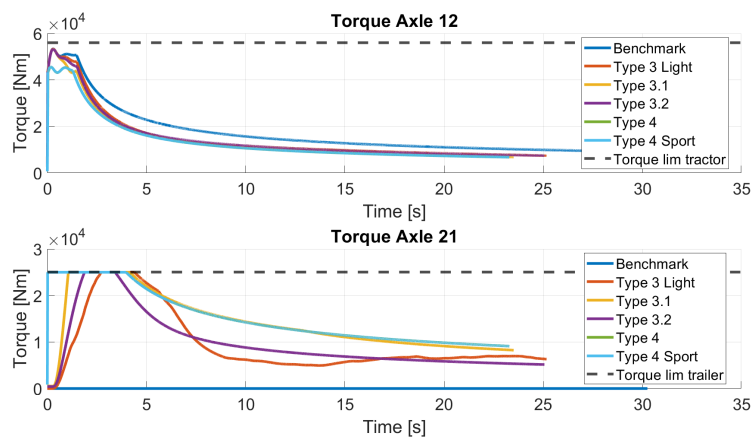


Figure B.2: LPT - Torque on driven axles, Flat road,  $\mu_{road} = 0.9$

## B. Simulation Results

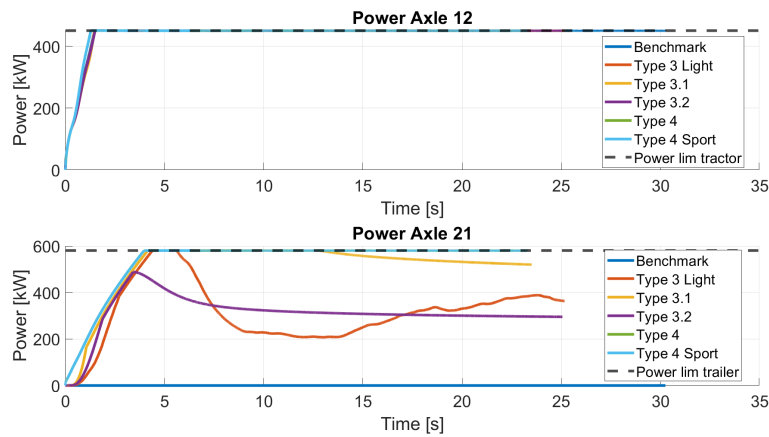


Figure B.3: LPT - Power on driven axles, Flat road,  $\mu_{road} = 0.9$

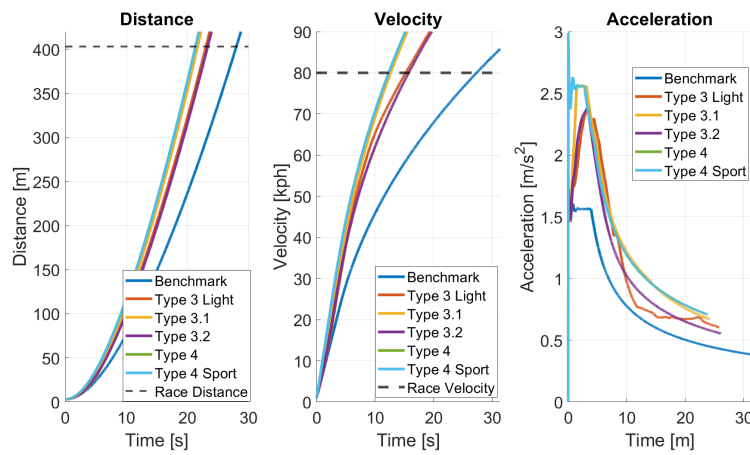


Figure B.4: LPT - Longitudinal states, Flat road,  $\mu_{road} = 0.6$

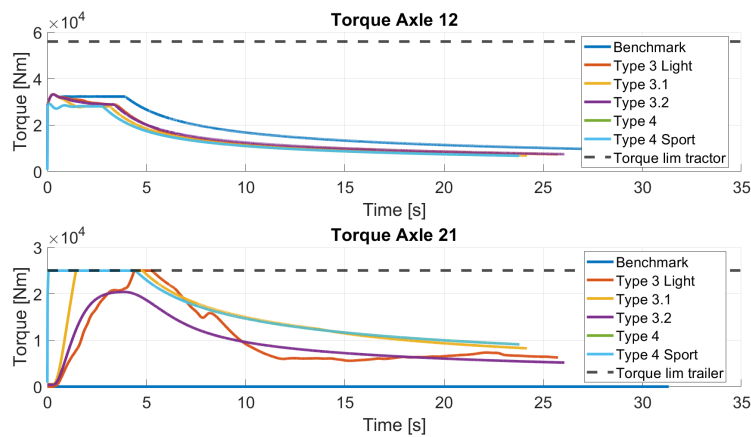


Figure B.5: LPT - Torque on driven axles, Flat road,  $\mu_{road} = 0.6$

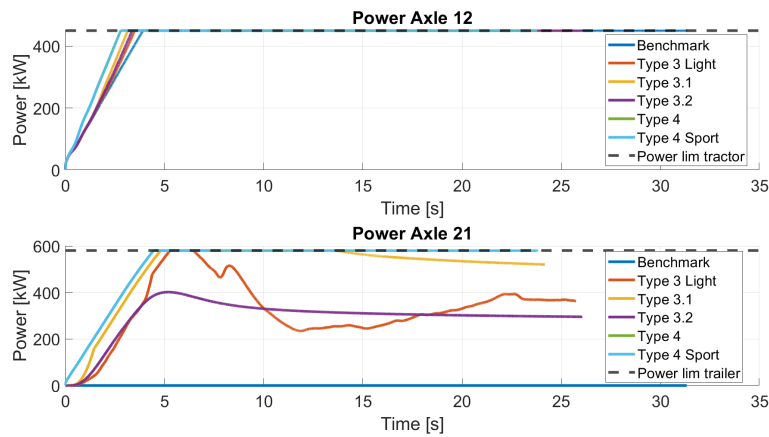


Figure B.6: LPT - Power on driven axles, Flat road,  $\mu_{road} = 0.6$

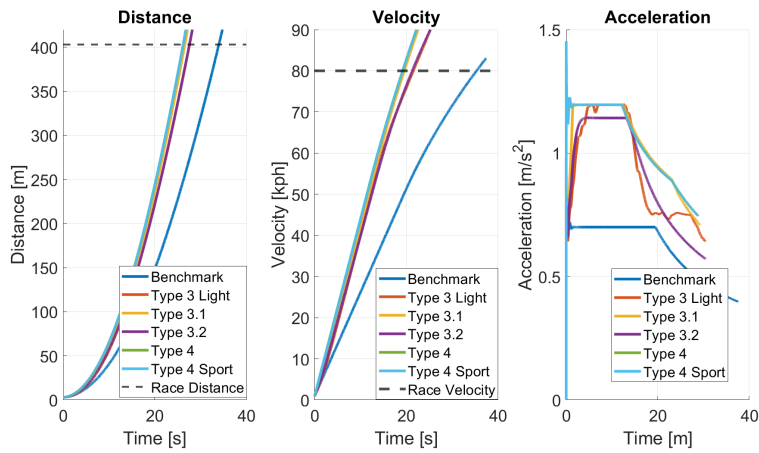


Figure B.7: LPT - Longitudinal states, Flat road,  $\mu_{road} = 0.3$

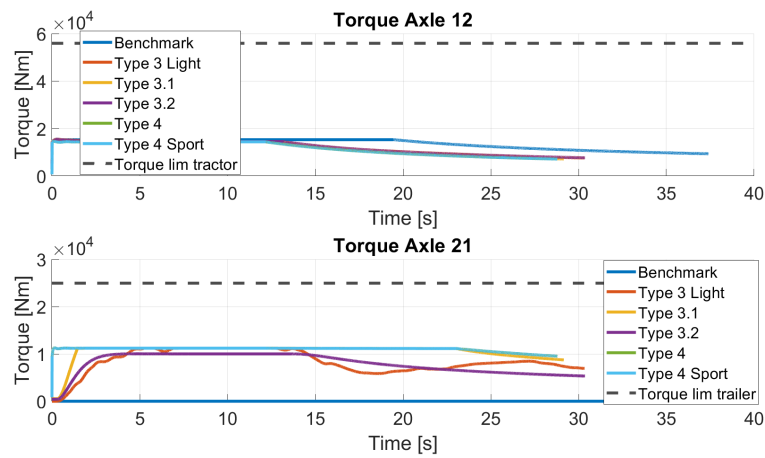


Figure B.8: LPT - Torque on driven axles, Flat road,  $\mu_{road} = 0.3$

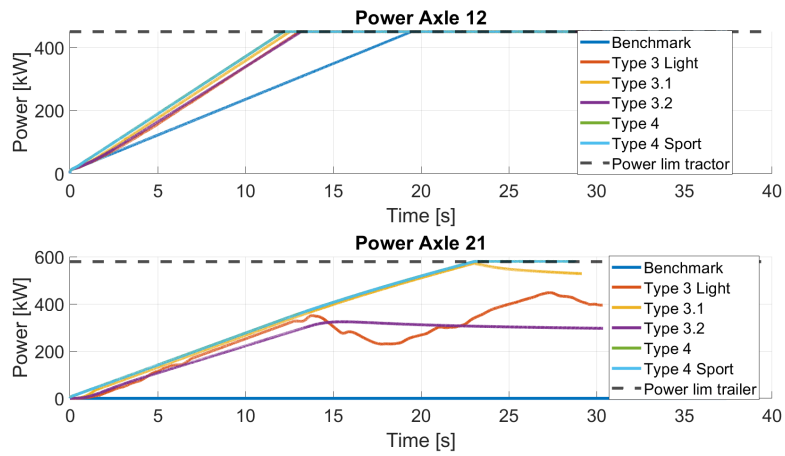


Figure B.9: LPT - Power on driven axles, Flat road,  $\mu_{road} = 0.3$

### B.1.2 Uphill

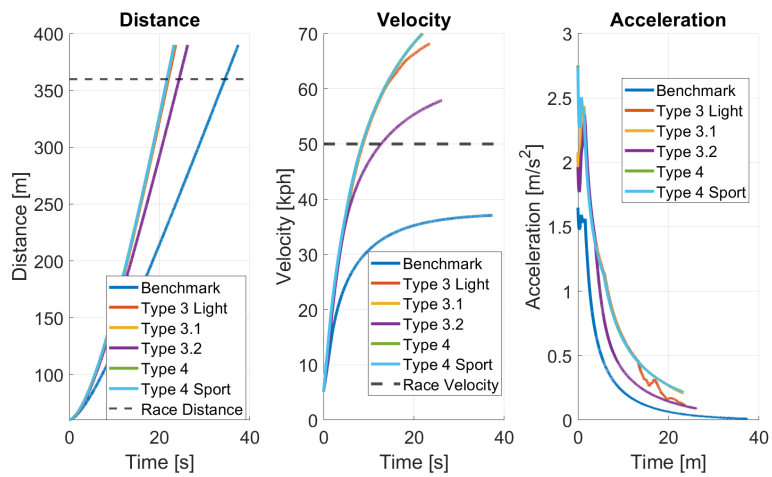


Figure B.10: LPT - Longitudinal states, Uphill road,  $\mu_{road} = 0.9$

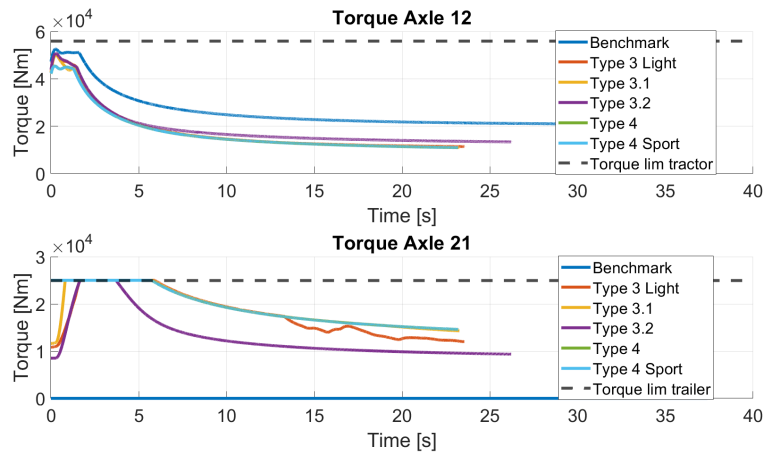


Figure B.11: LPT - Torque on driven axles, Uphill road,  $\mu_{road} = 0.9$

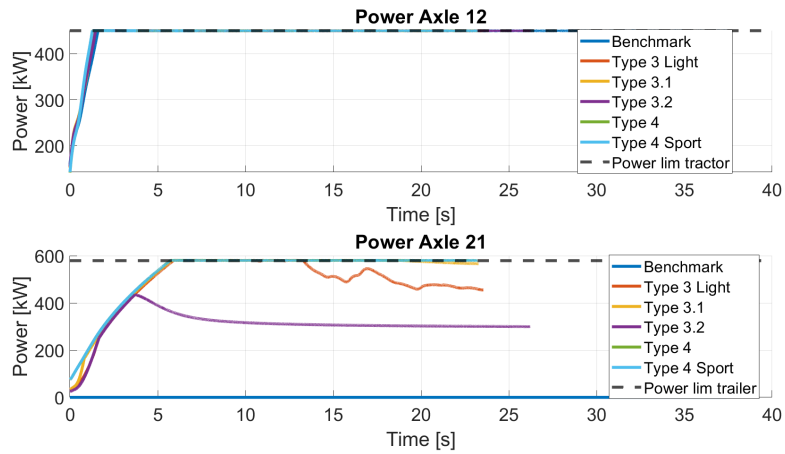


Figure B.12: LPT - Power on driven axles, Uphill road,  $\mu_{road} = 0.9$

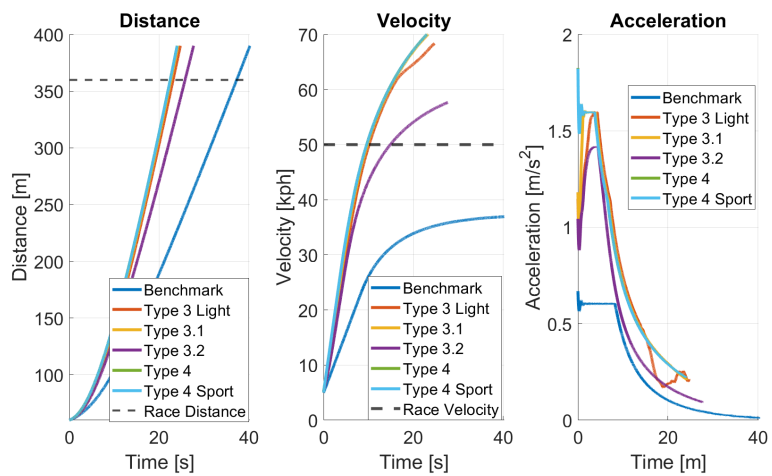


Figure B.13: LPT - Longitudinal states, Uphill road,  $\mu_{road} = 0.6$

## B. Simulation Results

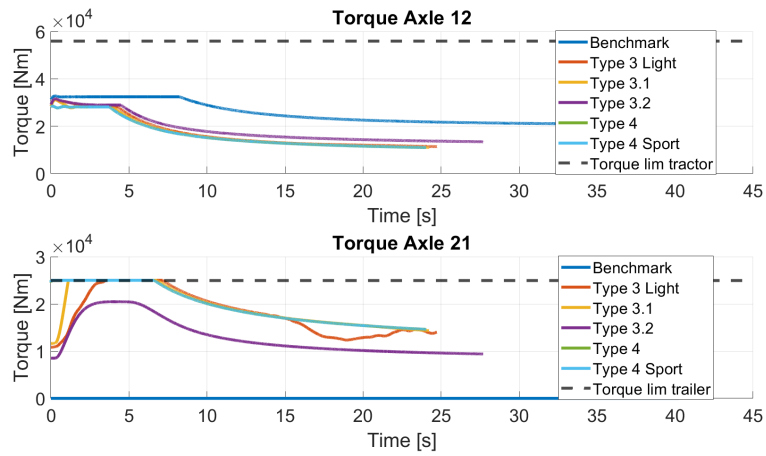


Figure B.14: LPT - Torque on driven axles, Uphill road,  $\mu_{road} = 0.6$

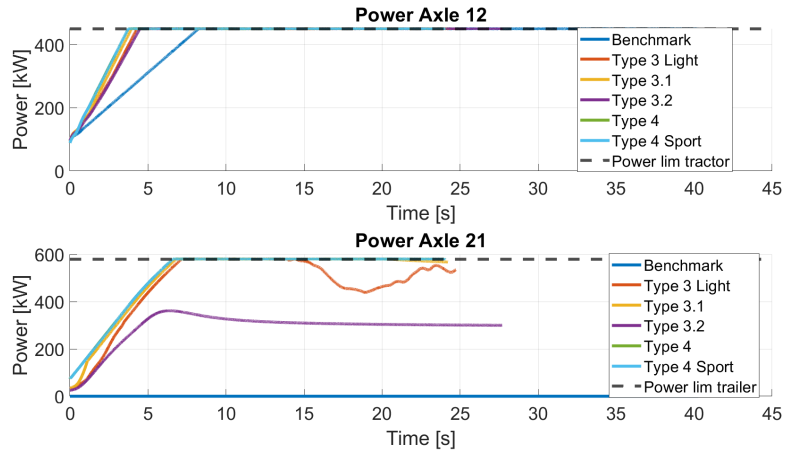


Figure B.15: LPT - Power on driven axles, Uphill road,  $\mu_{road} = 0.6$

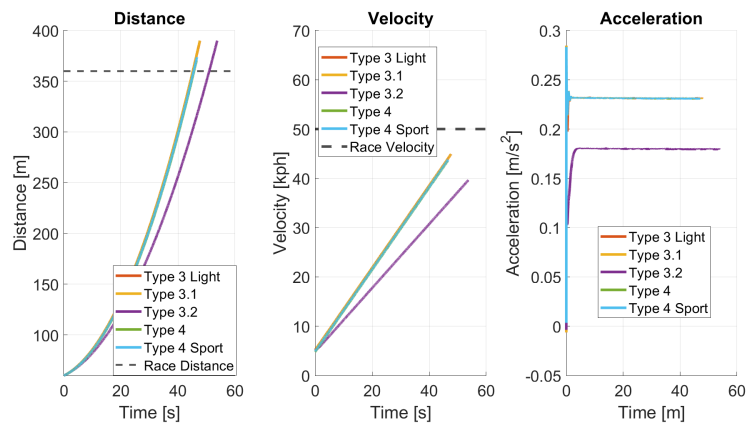


Figure B.16: LPT - Longitudinal states, Uphill road,  $\mu_{road} = 0.3$

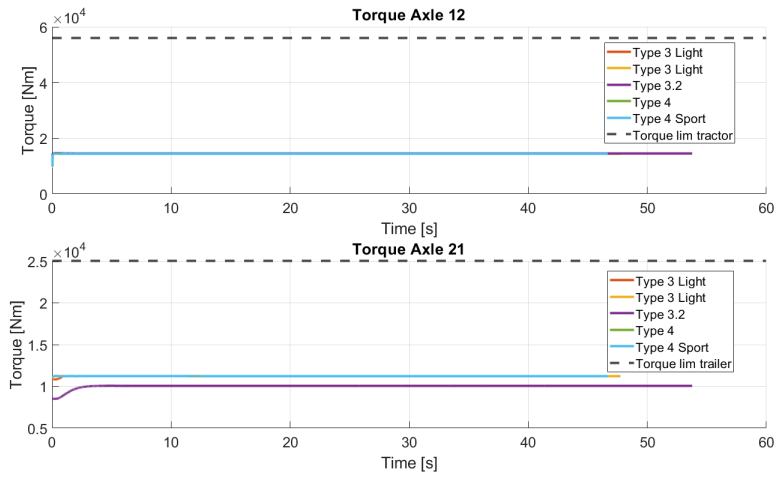


Figure B.17: LPT - Torque on driven axles, Uphill road,  $\mu_{road} = 0.3$

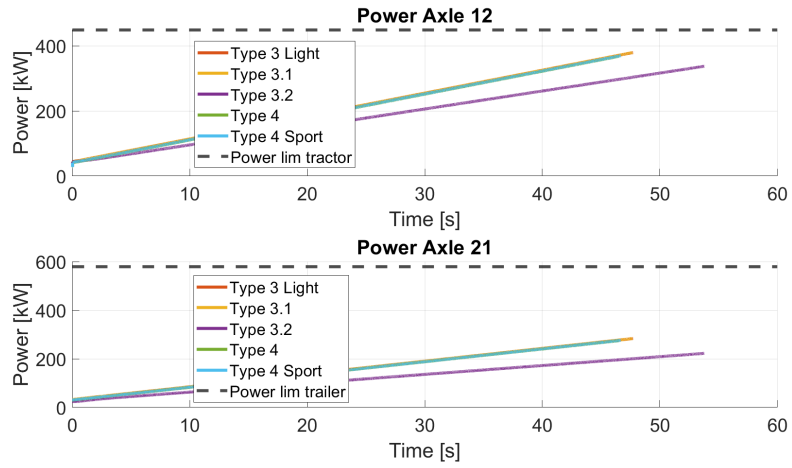


Figure B.18: LPT - Power on driven axles, Uphill road,  $\mu_{road} = 0.3$

DEPARTMENT OF MECHANICS AND MARITIME SCIENCES  
CHALMERS UNIVERSITY OF TECHNOLOGY  
Gothenburg, Sweden 2024  
[www.chalmers.se](http://www.chalmers.se)



**CHALMERS**  
UNIVERSITY OF TECHNOLOGY